USGS
science for a changing world

Geologic Map of the Katmai Volcanic Cluster, Katmai National Park, Alaska

By Wes Hildreth and Judy Fierstein

Aerial view along the main volcanic chain from the caldera lake of Mount Katmai across the craggy peaks of Trident Volcano to snow-clad Mount Mageik, a distance of about 20 km. Sea fog from Shelikof Strait invades Katmai Pass (between Trident and Mageik) and fingers into the Valley of Ten Thousand Smokes, the pale-tan ignimbrite-filled floor that lies at right center. Katmai caldera formed on June 6-7, 1912, in response to withdrawal of magma that vented at Novarupta, 10 km west, at the head of the Valley of Ten Thousand Smokes. Caldera walls rise 250-800 m above the lake, which is 250 m deep and still filling. View toward southwest from helicopter.

Pamphlet to accompany
Geologic Investigations Series I–2778

2003

U.S. Department of the Interior
U.S. Geological Survey

CONTENTS

INTRODUCTION

The Katmai volcanic cluster on the Alaska Peninsula (fig. 1) was first brought to national and international attention by the great eruption of June 1912. Although many wilderness travellers and one geological party (Spurr, 1900) had previously crossed remote Katmai Pass on foot, the National Geographic Society expeditions of 1915-19 first mapped and reconnoitered the volcanic terrain surrounding the pass in the course of investigating the effects of the 1912 eruption (Griggs, 1922; Higbie, 1975). The explosive ejection of rhyolitic, dacitic, and andesitic magma at Novarupta (fig. 1) over an interval of about 60 hr on June 6-8, 1912, (Martin, 1913; Curtis, 1968; Hildreth, 1983) was the world's most voluminous 20th century eruption. At least 17 km^3 of fall deposits and 11±3 km^3 of ash-flow tuff (ignimbrite) were produced, representing a magma volume of about 13 km^3 (Fierstein and Hildreth, 1992). This volume is larger than that erupted by Krakatau (Indonesia) in 1883 and is known to have been exceeded by only four eruptions in the last 1,000 years (Simkin and Siebert, 1994). Syneruptive caldera collapse at Mount Katmai (Hildreth, 1991), 10 km east of the eruption site, and displacements elsewhere in the magmatic plumbing system generated 14 earthquakes in the magnitude range M_S 6 to 7 (extraordinarily energetic for volcanic seismicity) and as many as 100 greater than M_S 5 (Abe, 1992; Hildreth and Fierstein, 2000).

Within 15 km of the 1912 vent at Novarupta, five andesite-dacite stratovolcanoes have erupted during the Holocene and remain fumarolically active today: Mount Katmai, Trident Volcano, Mount Mageik, Mount Martin, and Mount Griggs (fig. 1; table 1). The first four are virtually contiguous along a N.65°E. trend that defines the Quaternary volcanic front, whereas rear-arc Mount Griggs (Hildreth and others, 2002) is centered 12 km behind the front. The frontal trend additionally includes Snowy Mountain, likewise active in the Holocene, which consists of a pair of andesite-dacite cones (Hildreth and others, 2001) 10–15 km northeast of Mount Katmai; and the extinct Alagogshak Volcano, an andesite-dacite Pleistocene edifice centered 3 km southwest of Mount Martin (Hildreth and others, 1999). We have recently mapped and studied all of the volcanoes named, some of which are compound multi-vent edifices (table 1), as portrayed on the geologic map.

PHYSIOGRAPHY AND ACCESS

The Quaternary volcanic chain of Katmai National Park is the most tightly spaced line of stratovolcanoes in Alaska (fig. 1; Wood and Kienle, 1990; Miller and Richter, 1994). Along the volcanic front, crater-to-crater spacing between adjacent (commonly contiguous) edifices is typically 5 km or less. This includes the Devils Desk-Kukak-Steller-Denison alignment northeast of Snowy Mountain (fig. 1) as well as the Katmai cluster near the head of the Valley of Ten Thousand Smokes (Hildreth, 1987; Hildreth and Fierstein, 2000). The frontal volcanoes of this arc segment from Devils Desk to Alagogshak were constructed along the pre-existing rangecrest (the Pacific-Bristol Bay drainage divide), where the rugged prevolcanic basement typically reaches elevations of 1,200–1,600 m. As the volcanic summits reach 1,830–2,290 m and lie in a region of high precipitation, all the centers are heavily ice covered, as (to a lesser degree) is 2,330-m-high Mount Griggs northwest of the frontal axis.

The Katmai cluster lies entirely within the wilderness of Katmai National Park, 450 km southwest of Anchorage and 170 km west of Kodiak (fig. 1). The only convenient access is by boat or amphibious aircraft from King Salmon to Brooks Camp on Naknek Lake. Scheduled commercial air service is available during summer months, and scenic flight tours of the volcanoes can be arranged in good weather at both places. A daily commercial shuttle bus or van traverses a 37-km-long dirt road from Brooks Camp to the Overlook Cabin, a visitor center perched on a scenic knoll near the terminus of the ash-flow sheet in the Valley of Ten Thousand Smokes. The distal part of the sheet can be reached in an hour's walk by steep trail from the Overlook Cabin, but anything more than a brief visit demands camping expertise and survival equipment. We have encountered moose, caribou, foxes, wolves, wolverines, and many brown bears, as well as various smaller critters that would eat your lunch. Reaching Novarupta requires a day-long backpack trip, each way. The surrounding ice-clad stratovolcanoes should not be climbed without mountaineering skills and equipment. High winds, frequent rain and drizzle, brown bears, icy stream crossings, crevassed glaciers, and especially its remoteness make the area a true wilderness, exhilarating but risky, occasionally glorious, seldom comfortable, and never to be trifled with. Information can be obtained from the National Park Service (Box 7, King Salmon, Alaska 99613; 907-246-3305; www.nps.gov) or the King Salmon Visitor Center (907-246-4250).

Nearly all streams on the Pacific slope, southeast of the volcanic axis, drain to bays that jag the crenulate shoreline of Shelikof Strait. Streams northwest of the axis drain either directly or by way of Naknek Lake to Bristol Bay. As the map area is uninhabited, only hikers near the streams and boats in the bays would be at risk from debris flows resulting from eruption or avalanche at the volcanoes.

PREVIOUS WORK

The events, effects, and products of the 1912 eruption have been studied by Martin (1913), Griggs (1918, 1920, 1922), Fenner (1920, 1923, 1925, 1926, 1930, 1938, 1950), Bordet and others (1963), Curtis (1968), Hildreth (1983, 1987, 1991), Fierstein and Hildreth (1992, 2000), Fierstein and others (1997, 1998), Houghton and others (2003) and Hildreth and Fierstein (1987, 1992, 2000). Investigations of the "ten thousand smokes" (the fumaroles and their products

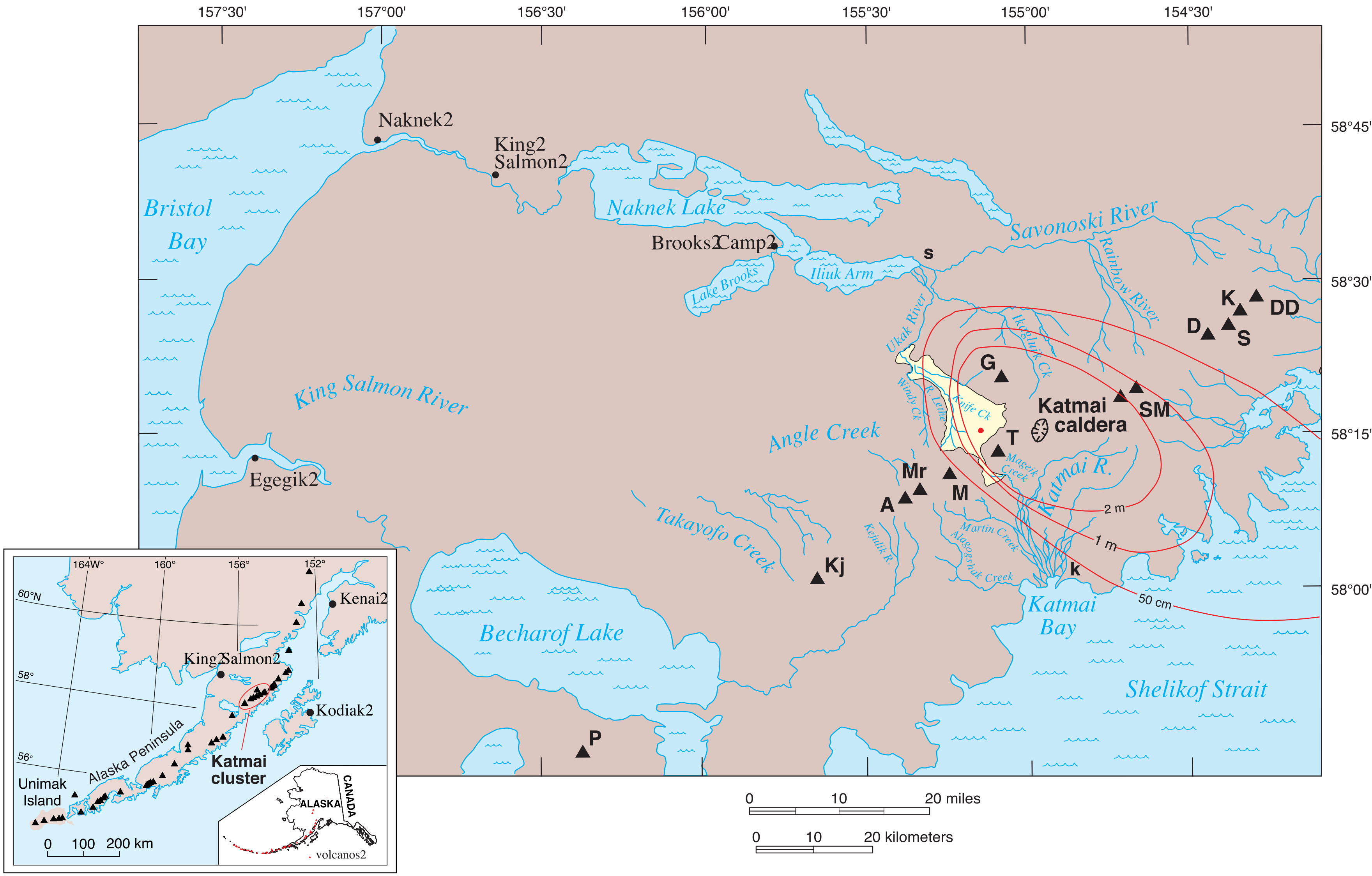

Figure 1. Regional setting of area mapped on upper Alaska Peninsula. Triangles indicate andesite-dacite stratovolcanoes, identified by letter from southwest to northeast: **P**=Peulik; **Kj**=Kejulik; **A**=Alagogshak; **Mr**=Martin; **M**=Mageik; **T**=Trident; **G**=Griggs; **SM**=Snowy Mountain (two cones); **D**=Denison; **S**=Steller; **K**=Kukak; **DD**=Devils Desk. Only Griggs volcano (formerly Knife Peak) lies significantly behind the main axial chain. Just west of Katmai caldera, yellow area is Valley of Ten Thousand Smokes ash-flow sheet, which erupted at Novarupta (red dot) in June 1912 and also poured south through Katmai Pass between Trident and Mageik volcanoes. Isopachs show thickness of cumulative 3-day plinian fallout from Novarupta. City of King Salmon and three villages indicated are the only settlements in this otherwise uninhabited wilderness. Small letters, **k** on Katmai Bay and **s** on Savonoski River, indicate sites of former villages abandoned during the 1912 eruption.

Table 1. Data for Katmai Cluster Volcanoes

Volcano	Compositional range of products[1] (wt% SiO_2)	Age of activity[2]	Elevation (m)			Present-day		Estimated volume erupted[6] (km^3)
			Summit[3]	Lowest lavas	Highest basement[4]	Area (km^2)	Volume[5] (km^3)	
NE Snowy	61.7–63.7	171 ka to Holocene	2161	610	1705	20	5	8 ± 2
SW Snowy	55.5–62.2	199 ka to 92 ka	2063	1040	1850	13	2	5 ± 2
NE Katmai	52.5–66.2	> 70 ka to <50 ka	2047(2244)	670	1370	25	10	15
SW Katmai	51.6–72.3	<50 ka to 1912	1890(2287)	150	1370	61	20	25
E Trident	58.2–65.2	143 ka	1832	915	915	8	2.3	8
Trident I[7]	53.4–63.4	>100 ka	1864	450	750	14	4	8
W Trident	54.4–64.4	40–50 ka	1709	825	750	9	2.4	3
SW Trident	56.9–64.8	1953–1974	1515	490	1175	8.5	0.65	0.7
Mageik	56.3–67.9	93 ka to Holocene	2165	305	1555	80	20	30
Martin	58.9–64.2	Holocene	1860	350	1450	33	7	8
Alagogshak	51.8–65.8	680 ka to 43 ka	1860	400	1585	20	5	14 ± 4
Griggs	53.6–63.4	292 ka to Holocene	2330	565	1340	60	25	30–35

[1] Analyses recalculated to sum to 99.6 wt % volatile-free leaving 0.4 % for trace elements and halogens.

[2] In Age column, > means older than and < means younger than.

[3] For Mount Katmai, parenthetical elevations and entries in volume column refer to edifices prior to caldera collapse in 1912.

[4] Basement refers to rugged prevolcanic topography made up of Jurassic Naknek Formation and Tertiary porphyry intrusions.

[5] Estimates of volumes may be no better than ± 20%, owing to glacial erosion and present-day ice cover. Present-day edifice volumes sum to 103 km^3. In addition, volumes of several domes (not tabulated) peripheral to Trident (including Falling Mountain and Mount Cerberus) sum to 0.7 km^3 today (or 1 km^3 erupted).

[6] Estimated volumes erupted, based on edifice reconstructions, sum to 161 km^3. To this must be added 5±2 km^3 for off-edifice dacitic pyroclastic deposits from Mount Katmai;12 ± 5 km^3 for the 22.5-ka rhyolitic plinian and ignimbrite deposits; and 13 km^3 of magma released at Novarupta in 1912 giving 70 km^3 for Mount Katmai and 191 km^3 for the whole Katmai volcanic cluster.

[7] For Trident I, in addition to range indicated, blocks in lithic pyroclastic-flow deposits are as silicic as 67.5% SiO_2.

within the 1912 ash-flow sheet and at the Novarupta vent complex) were reported by Sayre and Hagelbarger (1919), Shipley (1920), Allen and Zies (1923), Zies (1924a, 1924b, 1929), Lovering (1957), Ramdohr (1962), Kodosky (1989), Keith (1991a, 1991b), Keith and others (1992), Papike and others (1991a, 1991b), Papike (1992), and Sheppard and others (1992). Topical petrological studies of 1912 ejecta include those of Clocchiatti (1972), Hildreth (1983), Shearer and others (1991), Westrich and others (1991), Avery (1992), Lowenstern (1993), Coombs and Gardner (2001), and Hammer and others (2002).

In contrast to enduring interest in the 1912 deposits, most volcanoes of the Katmai cluster had been investigated only in reconnaissance prior to the present effort. Regional reconnaissance maps had been prepared by Keller and Reiser (1959) and Riehle and others (1993), and a tectonic overview of the arc presented by Kienle and others (1983). Stratigraphic studies emphasizing prevolcanic basement rocks had been published by Smith (1925), Martin (1926), Burk (1965), and Detterman and others (1996); and work on surficial deposits (principally glacial) had been undertaken by Muller (1952, 1953), Pinney and Beget (1991), and Riehle and Detterman (1993). Reports concerning the sequence and products of eruptions at Southwest Trident in 1953-74 include those by Snyder (1954), Muller and others (1954), Ray (1967), Ward and Matumoto (1967), Hildreth (1990), Hildreth and others (2000), and Coombs and others (2000). Kosco (1981) gave results of a petrological reconnaissance of several volcanoes in the Katmai cluster, and we have published a series of edifice studies for most of them (Hildreth and others, 1999, 2000, 2001, 2002, 2003; Hildreth and Fierstein, 2000).

Geophysical work includes regional surveys cited by Riehle and others (1993); several preliminary local studies summarized in updated reports by Ward and others (1991) and Kienle (1991); and topical investigations in and near the Valley of Ten Thousand Smokes by Goodliffe and others (1991), Kasameyer and others (1991), Ballard and others (1991), Lowell and Keith (1991), Kleinman and others (1997), Lu and others (1997), Lu and Freymuller (1998), Jolly and McNutt (1999), Power and others (2001), and Moran (2003).

METHODS

Our study of the products of the 1912 eruption began in 1976, and by 1995 we had spent parts of 12 summers, almost exclusively on foot, working in the Valley of Ten Thousand Smokes, Mageik Creek, Katmai River, and on parts of the Mageik, Trident, and Katmai edifices. In the summers of 1987 and 1988, Fierstein undertook expeditions by boat along both coasts of Shelikof Strait and on Naknek Lake to log sections of the 1912 fallout. Starting in 1996, at the request of the Alaska Volcano Observatory, we began helicopter-assisted mapping and hazards analysis of the stratovolcanoes, work that continued annually through the summer of 2001.

Work on the 1912 pyroclastic deposits demanded the most time and detailed attention, entailing the logging of hundreds of local stratigraphic sections, field sieving and pumice counting, and collection of more than 2,000 samples. Work on the stratovolcanoes amounted to a detailed reconnaissance, the best we could do in the face of the extensive cover by glacial ice and 1912 fallout, but it entailed collection of an additional 700 samples. Once we went airborne, the pace of progress on the stratovolcanoes accelerated and we reached outcrops we would not have risked on foot. Although color aerial photographs were useful, especially in the office and on the low-relief surface of the Valley of Ten Thousand Smokes, our sections, samples, and contacts were plotted on 15-minute topographic quadrangle maps at a scale of 1:63,360, the largest scale yet produced by the U.S. Geological Survey for the Alaska Peninsula. The accompanying geologic map is based on a composite of seven such quadrangles, at the same scale and retaining their contour interval of 100 ft. In the office, topography and geology were scanned and entered digitally in ARC/INFO.

As our objective was to understand and record the behavior and eruptive histories of the Quaternary volcanoes, the Jurassic and Tertiary basement rocks were largely ignored. Exceptions include (1) lithic fragments of basement rocks ejected at Novarupta during the explosive eruptions of 1912, because they provide information about concealed levels of the 1912 vent and conduit; (2) several remnants of Pliocene or early Quaternary volcanic and shallow intrusive rocks close to the Valley of Ten Thousand Smokes (units QTm, QTri, Trs); and (3) a few Tertiary granitoid intrusions (unit Ti) adjacent to the volcanoes and readily accessible. Basement geology is represented on the regional geologic map of Riehle and others (1993).

Many samples from each volcano were analyzed chemically, the main goals being to document the compositional range erupted at each vent, to establish correlations and distinctions among the products of eruptive packages and subedifices at each center, and to investigate the complex magmatic plumbing system that linked Mount Katmai and Novarupta (Hildreth and Fierstein, 2000). Major-oxide contents were determined by wavelength-dispersive X-ray fluorescence (XRF) spectroscopy in the U.S. Geological Survey laboratory at Lakewood, Colorado, principally by D.F. Siems. Rb, Sr, Y, Zr, and (for selected samples) other trace elements were determined by energy-dispersive XRF spectroscopy at Lakewood or at Menlo Park, California.

Because we wanted to know how long each volcano has been active and to establish the ages of major eruptive events and episodes of elevated eruptive output, K-Ar geochronology became an important part of the investigation. Samples were dated in the U.S. Geological Survey laboratory supervised by Marvin Lanphere at Menlo Park. Sample selection criteria and analytical methods were described by Hildreth and Lanphere (1994) and Lanphere (2000). We tried to identify and date lavas basal to each eruptive package or subedifice and, where possible, to date the youngest pre-Holocene products of each center. Numerous radiocarbon dates, principally for peat and organics-bearing aeolian silt and soil, were also measured in order to bracket eruptive ages of ash layers that resulted from postglacial explosive eruptions (Fierstein and Hildreth, in press).

GEOLOGIC SETTING

BASEMENT ROCKS

Quaternary volcanoes of the Katmai cluster have been constructed upon a rugged set of glaciated ridges carved from the subhorizontal to gently warped, marine siltstone and sandstone of the Jurassic Naknek Formation (Riehle and others, 1993; Detterman and others, 1996). These well-stratified rocks are intruded locally by several porphyritic granitoid stocks of Tertiary age. Although Quaternary lavas of the several volcanoes drape the basement to elevations as low as 600–1,800 ft (180–550 m), the Jurassic strata crop out as high as 4,400 ft (1,340 m) on Mount Griggs, 4,500 ft (1,370 m) on Mount Katmai, and 5,100 ft (1,555 m) in the saddle between Mounts Martin and Mageik (table 1). Because the axial volcanic chain straddles the basement-rock drainage divide of the Alaska Peninsula (fig. 1), eruptive products can flow either southeastward down the Pacific slope toward Shelikof Strait or northwestward toward Bristol Bay and the Naknek Lake system.

Permian to Jurassic sedimentary rocks that regionally underlie the Naknek Formation (itself more than 2 km thick) do not crop out in the Katmai area, but the stratigraphic framework of the Alaska Peninsula (Detterman and others, 1996) suggests that such rocks are as thick as 3.5 km beneath the Katmai volcanoes.

A few remnants of Pliocene or early Quaternary volcanic rocks cap peaks and ridges near Mount Griggs, but most such rocks have been eroded from the area surrounding the Valley of Ten Thousand Smokes. Much of the basement east of Mount Katmai and south of Snowy Mountain, however, includes altered volcanic rocks (Riehle and others, 1993) that have received little attention. Erupted from several ill-defined centers, these rocks are ordinary arc andesites and dacites, either undeformed or gently warped, variably altered hydrothermally, and presumed to be mostly Neogene (Shew and Lanphere, 1992) but possibly also in part early Quaternary.

CONVERGENT MARGIN

The Quaternary volcanic front trends rather linearly N.65°E. along the Katmai segment of the Aleutian arc (fig. 1). The Mesozoic basement rocks upon which the volcanic centers are built belong to a tectonostratigraphic package commonly called the Peninsular terrane, which is thought to have originated far to the south and to have been added to southern Alaska during the middle or late Mesozoic (Plafker and others, 1994), prior to oroclinal bending of southern Alaska. Since then, several additional terranes and subduction-related accretionary complexes were added along Alaska's southern margin, such that the Aleutian trench (5–6 km below sea level) now lies 350 km southeast of the volcanic front. Eocene seafloor is currently being subducted here, nearly orthogonally, at a convergence rate of about 6 cm/yr. The inclined seismic zone is well defined and 20–30 km thick (Kienle and others, 1983). It dips only about 10° NNW. for some 300 km, then steepens to about 45° beneath the present-day arc, and persists to depths as great as 200 km; its top lies about 100 km beneath the Katmai volcanic cluster. Although the arc alignment shifted modestly during the Tertiary (Wilson, 1985; Riehle and others, 1993), the Aleutian arc was well established along the Alaska Peninsula by the middle Eocene, soon after onset of northwestward motion of the Pacific plate beneath southern Alaska (Plafker and others, 1994). Crustal structure in the Katmai region is poorly known and the nature of the basement under the subhorizontal Mesozoic section remains particularly uncertain. Alaska Peninsula crust is thought to be 30–36 km thick farther to the northeast (Moore and others, 1991), as well as near the peninsula's southwest extremity (Fliedner and Klemperer, 2000). Although the forearc and the sub-arc lower crust may be especially mafic, having atypically high seismic velocities for normal continental crust (Fliedner and Klemperer, 2000), the many Tertiary granitoid plutons that have intruded the Peninsular terrane in the Katmai region indicate that the sub-arc crust has become essentially continental. Crustal earthquakes, generally shallower than 10 km, are abundant beneath the Katmai volcanoes (except Mount Griggs). As many as 1,000 local earthquakes each year have recently been recorded here by Alaska Volcano Observatory, nearly all of them smaller than magnitude 2.5 (Ward and others, 1991; Jolly and McNutt, 1999; Power and others, 2001).

THE QUATERNARY VOLCANOES

The Katmai volcanic cluster, depicted on the geologic map and elaborated in the Description of Map Units, consists of 15 stratovolcanic edifices and several lava domes. Here, we provide an overview of the morphology, structure, and composition of each volcano.

MOUNT GRIGGS

Mount Griggs, the highest peak in Katmai National Park, is a fumarolically active andesitic stratovolcano that stands alone 12 km behind the main volcanic chain of the Alaska Peninsula rangecrest. Its summit reaches an elevation of 7,650 ft (2,330 m), about 1,750 m above the nearby floor of the Valley of Ten Thousand Smokes. K-Ar ages indicate that the volcano is as old as 292±11 ka and thus predates inception of the nearby volcanic-front centers (Hildreth and others, 2002). Present-day symmetry of the apparently little dissected edifice reflects numerous and voluminous postglacial effusions of andesitic lava that have healed and concealed older scars of glacial erosion. Constructed in several episodes but exposed today in only a few windows, the middle Pleistocene edifice was glacially ravaged before reconstruction of the modern cone during the late Pleistocene and Holocene. Collapse of the southwest sector early in the Holocene left a 1.5-km-wide amphitheater at the summit and shed a 1-km^3 debris avalanche into the valley of Knife Creek. Smaller debris-avalanche deposits emplaced later to the east, north, and west are also of early Holocene age. Post-collapse andesite eruptions built an inner cone that nearly filled the amphitheater and covered the southwest slope of the volcano with a fan of leveed lava flows. The inner cone is topped by a pair of nested craters and supports two clusters of mildly superheated, sulfur-precipitating fumaroles—one cluster near the west rim of the innermost crater, the other high on the southwest slope of the cone. Outer slopes of both cones consist largely of overlapping leveed tongues of blocky andesitic lava 10–60 m thick. Many such lava flows bifurcate and thicken downslope, and others grade into distal lobes of disintegrated rubble. Two canyon-ponded lava flows to the north and east are exceptional in thickening distally to as much as 150 m. Although the northern slopes support five active glaciers, some lava flows on the south and east surfaces of the outer cone are unglaciated and only lightly degraded. Many such leveed lava flows armoring the outer cone are apparently postglacial, as is the entire inner cone. Bedded scoria falls and layers of poorly sorted phreatomagmatic ejecta are exposed on rims of the inner craters but rarely elsewhere. Holocene ash from Mount Griggs is inconspicuous beyond the edifice, and no evidence was found for exceptionally explosive ejection of its crystal-rich andesitic magmas. Future debris flows from any sector of the volcano would have a 25-km runout into Naknek Lake through uninhabited wilderness.

High-precision K-Ar geochronology (Hildreth and others, 2002) yields ages ranging from 292 to 21 ka for glacially eroded lavas from all sectors of the main outer cone. Present-day edifice volume is 20 to 25 km^3, of which about 2.2 km^3 erupted during the Holocene. Reconstruction of eroded components of the edifice yields an estimate of 30–35 km^3 for the total volume erupted. On this basis, average productivity is estimated to have been in the range 0.10 to 0.12 km^3/1,000 yr for the lifetime of the volcano and appears to have been in the range between 0.2 and 0.4 km^3/1,000 yr since about 50 ka.

Eruptive products are olivine-bearing two-pyroxene andesites rich in plagioclase that have remained especially phenocryst-rich (25–60 volume percent crystals) throughout the lifetime of the volcano. Olivine-rich andesite makes up a larger proportion of the lavas at Mount Griggs than at other volcanoes of the cluster, and dacite is rare. A total of 77 analyzed samples define a typical Ti-poor, medium-K calc-alkaline arc suite, largely in the range from 55 to 63 percent SiO_2, that shows no systematic change with time (Hildreth and others, 2002). Relative to products of the nearby volcanic-front centers, those of Mount Griggs are slightly depleted in Fe, generally enriched in Rb, Sr, Al, and P, and consistently enriched in K and Zr. Fumarolic gases at Mount Griggs are richer in He than those at other Katmai volcanoes and have $^3He/^4He$ values as high as 7.7 times the atmospheric ratio (Poreda and Craig, 1989; Sheppard and others, 1992). The magmatic plumbing system of Mount Griggs is independent of those beneath the main volcanic chain, probably all the way to mantle depths (Hildreth and others, 2002).

ALAGOGSHAK VOLCANO

Alagogshak volcano, oldest edifice in the Katmai cluster, is centered on the rangecrest 15 km southwest of Katmai Pass and only 3 km southwest of Mount Martin. Originating by 680±20 ka, the glacially dissected volcano produced 10 to 18 km^3 of andesite-dacite eruptive products during several episodes of activity in the middle and late Pleistocene (Hildreth and others, 1999). From a central vent marked by hydrothermal alteration and remnants of a cratered fragmental cone on the drainage divide, glacially incised stacks of lava flows dip radially and extend 6 to 10 km in most directions. Intracanyon flows, now largely stripped, no doubt extended much farther. Lava flows that make up four ridge-capping outliers well west of the volcano may also have erupted there, but one or more may be from an unidentified older source vent. The youngest unit recognized (unit aac) is a glassy andesitic lava flow (61 percent SiO_2) that descended steeply from the rangecrest and spread into upper Alagogshak Creek, where its 100-m-thick distal lobe now forms a glacially scoured plateau; originating at an ice-clad knob, which is probably a flank-vent dome 1 km east of the crater, the lava flow gives a K-Ar age of 43±8 ka. No evidence has been found for younger activity. The medium-K calcalkaline eruptive suite (57 to 66 percent SiO_2) at Alagogshak volcano is compositionally varied (Hildreth and others, 1999), probably reflecting independent evolution of different magma batches supplied intermittently over a lifetime of more than 600,000 yr, much longer than that of other volcanoes in the Katmai cluster.

MOUNT MARTIN

Mount Martin consists of a small fragmental cone and a staircase of 10 overlapping coulees of blocky dacite, each 75–100 m thick, that descend northwestward for 10 km. Although its summit exceeds 1,860 m in elevation, the 2-km-wide cone itself has local relief of only 500 m, owing to its construction upon a high ridge of Jurassic basement rocks. Of the 7-km^3 present-day volume we estimate for Mount Martin, the cone makes up only 5 percent and the 31-km^2

lava-flow field about 95 percent. Despite a cone-encircling collar of small active glaciers, erosion of the cone and coulees is almost insignificant, indicating that Mount Martin is a Holocene volcano in its entirety. Glaciated lavas adjacent to its west flank are chemically and stratigraphically distinguished as flows from Alagogshak volcano (Hildreth and others, 1999). The unilaterally asymmetrical distribution of lava flows with respect to the summit vent resembles the stacked array of Southwest Trident, the Holocene array from the East Summit of Mount Mageik, and the staircase of flows on the north side of Snowy Mountain (Hildreth and others, 2000, 2001). Interflow conformity within parts of such stacks and the compositional similarities of subsets of successive flows within such stacks suggest rapid sequential emplacement. At Mount Martin the whole pile is Holocene, and much or all of it could have erupted on a timescale of several years or decades. The radiocarbon age of organics-rich soil and a regional tephra layer that overlie the topmost distal coulee indicate that the main stack of lava flows was emplaced by about 6 ka (Fierstein and Hildreth, in press).

The cone of Mount Martin is marked conspicuously by a persistent steam plume that commonly extends far downwind. The plume coalesces from as many as 20 fumaroles rich in CO_2, SO_2, and H_2S that are precipitating sulfur in the talus northwest of a shallow lake on the floor of its 300-m-wide crater. Scoriaceous and massive glassy blocks of the cone are andesitic (59–61 percent SiO_2), whereas the sequence of coulees is largely dacitic (62.5–64.2 percent SiO_2). Products of Mount Martin yield a tight compositional array that is similar in most respects to the andesite-dacite suite erupted at Novarupta in 1912 but is poorer in Sr and marginally more potassic (Hildreth and Fierstein, 2000).

MOUNT MAGEIK

Mount Mageik, a 2,165-m-high andesite-dacite compound stratovolcano, rivals Mount Katmai as the areally most extensive (80 km^2) edifice in the Katmai cluster. Each of its four ice-mantled summits is a discrete eruptive vent (Hildreth and others, 2000), and each is the source of numerous lava flows (56–68 percent SiO_2), many of them 50–200 m thick distally. Three of the four overlapping centers are of late Pleistocene age, basal lavas of the Southwest Summit subedifice being the oldest at 93±8 ka; eruptive products of the Southwest, Central, and North Summit vents are severely eroded glacially. The East Summit, however, is a Holocene subedifice, from which a dozen leveed lava flows (60–64 percent SiO_2) have descended toward Katmai Pass and Mageik Creek where blocky terminal lobes are 60 to 150 m thick. One of the youngest banks against the Mount Cerberus lava dome (114±46 ka). Ice-filled craters on the North and East Summits are usually obscured by snow, but an ice-free 350-m-wide phreatic crater (Fenner, 1930; Hildreth and others, 2000) between the East and Central Summits contains an acid lake and many superheated fumarolic jets. The Central (true) Summit appears to be an ice-clad dacite dome, whereas the Southwest Summit is probably capped by a fragmental cone like those of the North and East Summits, though its crater (if present) is wholly obscured by a thick cover of ice.

Holocene debris avalanches from three different sites on the south slopes of Mount Mageik devastated the forks of Martin Creek. The oldest and largest broke loose from the fumarolically altered southwest face of the Southwest Summit, and the youngest was emplaced during the 1912 ashfall from Novarupta, presumably shaken loose by the seismicity accompanying collapse of Mount Katmai.

Mount Mageik's fumarolic plume is often conspicuous, but none of the sporadic reports of 20th century tephra eruptions (for example, Jaggar, 1927) are plausible. Configuration of the crater has not changed since it was first photographed in 1923 (Fenner, 1930; Hildreth and others, 2000), and the only tephra deposits younger than 2 ka on the flanks of Mount Mageik are the Novarupta pumice falls of 1912 and Trident ash of 1953-74.

Lavas and ejecta of all four subedifices of Mount Mageik are plagioclase-rich pyroxene-dacites and andesites that form a calcic medium-K low-Ti arc suite (Hildreth and others, 2000). The Southwest Summit subedifice is larger, longer lived, and compositionally more complex than its companions. We estimate eruptive volumes of 15–17, 6, 2, and 5–6 km^3, respectively, for the Southwest, Central, North, and East Summit subedifices, yielding a total of about 30 km^3 erupted. For a 93,000-yr lifetime, this implies a long-term average eruption rate of 0.33 km^3 per 1,000 yr, but the Holocene rate may be twice as high.

TRIDENT VOLCANO

Trident Volcano, closest of the Katmai cluster to the 1912 vent at Novarupta, is itself a group of four stratocones and several lava domes. Although more severely dissected glacially and in part older than adjacent Mageik and Katmai volcanoes, Trident nonetheless produced the area's most recent eruptive episode—from 1953 to 1974.

Oldest of the Trident group is **East Trident** (Peak 6010), a small andesite-dacite cone (58–65 percent SiO_2) almost contiguous with Mount Katmai. The rugged edifice is exposed over a 4-by-3-km area, but its lower flanks are concealed beneath glaciers. The hydrothermally altered core of East Trident is gutted by five glacial cirques, exposing on steep glacial headwalls windows of stratified ejecta in the interior of the skeletal cone. The arêtes between cirques reveal structurally simple stacks of 10–25 radially dipping lava flows and breccia sheets. Most are silicic andesites 10–30 m thick, but 100-m-thick lava flows that support the southwest ridge and cap the northeast ridge are dacites (63–65 percent SiO_2). The latter dacite, which extends nearly to the summit, yields a K-Ar age of 142±15 ka, indicating that most of East

Trident is older still. An age of 143±8 ka for a near-basal andesite lava flow on the northwest arête suggests, however, that activity at the small East Trident cone was short lived. Peak 5700+, central prong of the "trident" as viewed from the southeast (the aspect that inspired the volcano's name; Griggs, 1922, p. 98–9), is not a separate cone but simply the ruggedly eroded southwest flank of East Trident. Reconstruction suggests that the cone may once have exceeded 6,600 ft in elevation, which would probably have made it the highest of the Trident summits.

Likewise sculptured glacially, **Trident I** (Peak 6115) is a discrete andesitic cone (53–63 percent SiO_2) that forms the central and highest edifice (1,864 m) of the Trident group. Its lavas appear to bank against East Trident at their (poorly exposed) mutual saddle, but some overlap of their active lifetimes is not excluded by our present data. Buttressed by East Trident on its northeast, the Trident I edifice grew asymmetrically toward the other sectors. The core of the edifice is eviscerated by a north-face cirque, the sheer headwall of which reveals the base of the vertically jointed 150-m-thick summit lava (63 percent SiO_2), which rests on more than 200 m of crudely stratified coarse andesitic breccia. This dacite lava may be a dome remnant that overlies crater fill and dome breccia on its north side. On its southwest side, the summit dacite rests on a coherent andesitic lava flow (61.7 percent SiO_2) that yields a K-Ar age of 101±12 ka. The northwest ridge of the edifice consists mostly of a glaciated stack of thinner lava flows and breccias, but low on steep north spurs of the ridge are two massive andesitic lavas (60 percent SiO_2), each 100–200 m thick, which are probably glacially truncated coulees but, alternatively, might be older domes.

The smoother, less dissected south slope of Trident I consists largely of summit-derived andesitic lava flows (58–62 percent SiO_2) and lithic pyroclastic flows that descend to elevations as low as 450 m at Mageik Creek. In contrast, the southwest slope is made up of steeply dipping (25°–35°) sheets of scoria, agglutinate, and avalanche rubble that were widely altered to ocherous yellow brown, probably while still hot. Juvenile scoriae in these deposits are the most mafic material (53–55 percent SiO_2) known to have erupted from the Trident group. Although the edifice of Trident I is glacially ravaged and has had no Holocene eruptions, its lower southeast flank is marked at 3,600'–4,000' (1,100–1,220 m) elevation by a field of sulfur-depositing fumaroles first recorded in 1916 by Griggs (1922, p. 98) and still vigorous. Another fumarole, visible on 1951 aerial photographs as a 100-m-wide steaming pit at 3,850' (1,175 m) on the southwest ridge of Trident I, became the vent site for a new volcanic cone that began to grow in 1953 (see discussion below of Southwest Trident).

Closest to Novarupta of the Trident cones is **West Trident** (Peak 5605), smallest and youngest of the prehistoric Trident edifices. Heavily mantled by 1912 fallout, its lavas are poorly exposed except near the summit and along the west wall of Glacier 1. All lavas exposed are silicic andesite or dacite (58–64.4 percent SiO_2), and many are unusually rich in chilled enclaves (1–20 cm) of phenocryst-poor, relatively mafic andesite (54–58 percent SiO_2). The summit lava (61 percent SiO_2) is more than 125 m thick and may be a dome remnant; an associated lava flow 30–70 m thick dips 20° down the north ridgeline, and summit-derived lavas and breccia sheets dip east against Trident I at their mutual saddle. Although the contact there is obscured by 1912 pyroclastic deposits, the contrast between these silicic andesites and the steeply southwest dipping sheets of mafic agglutinate (unit tca) that make up the adjacent southwest face of Trident I supports the inference (based on physiography and attitudes of lavas) that West Trident is truly a discrete cone rather than a shoulder of Trident I isolated by erosion. A K-Ar age of 44±12 ka for a thick andesite lava flow that forms the crest of the north ridge supports our stratigraphic and morphologic inference that West Trident is the youngest of the prehistoric centers in the Trident group.

Largely ice free today, West Trident was formerly ice covered and is everywhere glacially modified. On its flanks, poorly exposed glaciated lavas form an array of seven sharp-crested ridges that descend radially from the summit. Four northerly spurs and the southwest ridge all appear to be lava flows, but the west and south-southwest ridges may include lava domes abutted by lava flows from West Trident and later jointly sculptured glacially and blanketed by 1912 pumice falls. Some of the northerly lava flows bank against Falling Mountain dome (70±8 ka), and, just east of there, the distal parts of adjacent lavas were destroyed on June 6, 1912, by collapse into the Novarupta vent, thereby providing most of the andesitic lithics among the Episode I ejecta (Fierstein and Hildreth, 1992).

At least five (and as many as eight) **peripheral lava domes** of pyroxene dacite (62–65 percent SiO_2) line the lower west and south flanks of the Trident group. Three ambiguous candidates along Katmai Pass are steep blunt-nosed buttresses of West Trident that were abutted or overrun by younger lava flows, sculptured glacially, and so heavily mantled by 1912 pyroclastic deposits that distinguishing them as domes or thick flow lobes from West Trident remains uncertain. These eight do not include the four domes (or thick proximal flows) already mentioned high on the adjacent edifices of Trident I and West Trident. All 12 lie within 7 km of each other in a compact zone that includes the site of the 1953-74 cone. The two largest domes, 425-m-high **Falling Mountain** and 365-m-high **Mount Cerberus** (each about 0.3 km^3), are similar compositionally to the smaller (unnamed) domes, the volumes of which are in the range 0.015–0.12 km^3. Like West Trident, all the domes contain relatively mafic enclaves (1–20 cm) of phenocryst-poor andesite (54–58 percent SiO_2), though they are rare in the dacite of Mount Cerberus. Most of the domes are glacially scoured and several are severely eroded. Mount Cerberus and Falling Mountain are morphologically little modified by ice and were suspected of being very young (Hildreth, 1983, 1987), but repeated search has turned up few remnants of fully glassy carapace, and K-Ar determinations have given late Pleistocene ages for both domes: Falling Mountain yields an age of 70±8 ka and Mount Cerberus an age of 114±46 ka. The superficiality of glacial erosion may reflect their compact profiles and locations close to the peninsular drainage divide.

Beginning in February 1953, a new andesitic edifice (0.7 km^3) was built at the southwest margin of the Trident group (Snyder, 1954; Ray, 1967). Although sometimes referred to informally as "New Trident", we have called it **Southwest Trident**, in anticipation of the day it ceases to be Trident's youngest component. During two decades of sporadic explosive activity (vulcanian and effusive), a new 3-km^2 composite cone was constructed of block-and-ash deposits, scoria, agglutinate, stubby lava lobes, and the intercalated proximal parts of the main lava flows that spread as an apron around the cone. The cone grew to an elevation of 1,515 m (GPS measurement reported by Coombs and others, 2000) on the former site of a 100-m-wide fumarolic pit at an elevation of about 1,175 m on the steep southwest flank of Trident I. Although relief on its south slope exceeds 700 m, the new cone thus has a central thickness of only 340 m and a volume of about 0.3 km^3 (Hildreth and others, 2000). At successive stages of cone construction, four blocky leveed lava flows effused from its central vent, in 1953, 1957, 1958, and during the winter of 1959-60. Each flow is 25-60 m thick and 2.5-4 km long, and altogether they add about 0.35 km^3 to the eruptive volume. The cone's summit is today marked by a shallow crater 350 m wide (Hildreth and others, 2000, in press) that was the site of several small ephemeral plugs, which were emplaced after the final lava flow and were repeatedly destroyed by intermittent explosive activity (1960-74).

Black ash clouds rose 6–9 km at least 10 times between 1953 and 1974 and perhaps to 12 km once or twice. Several times during the first month of activity, light ashfall dusted areas as far as 30–50 km from the vent, in all sectors. By far the most voluminous fallout appears to have resulted from the initial outburst of February 15, 1953 (Snyder, 1954). A single non-graded scoria-fall layer (5–17 cm thick) deposited during that event is preserved at a few protected sites as far away as Mount Katmai and upper Knife Creek. Sieve data for bulk samples of this layer yield median and maximum particle sizes of 6.5 mm and 10 cm in the saddle 1 km north of the vent, and 2.1 mm and 2 cm in the saddle 7 km northeast of the vent—between the twin western summits of Mount Katmai. Thin sheets of finer ash that fell during the many subsequent events have been almost entirely removed or reworked by wind and runoff. Abundant ballistic blocks, variously breadcrusted, densely vitrophyric, or scoriaceous, are scattered as far as 3 km from the vent and are products of many discrete explosive episodes (none of which were closely observed) distributed over two decades. Liberal estimates of total fallout yield no more than 0.05 km^3, contributing less than 10 percent of the total eruptive volume of 0.7±0.1 km^3.

The period of most frequent observation was from February to September 1953, principally by military reconnaissance aircraft during the early months (Snyder, 1954) and by a U.S. Geological Survey party that camped at Knife Creek during the summer (Muller and others, 1954). When the vent was first seen through the cloud layer on the fourth day of activity (February 18, 1953), an effusive lava flow (then already 250 m wide) was upwelling centrally and spreading radially (Hildreth and others, 2003). Although a fumarolic pit as deep as 40 m was conspicuous at the impending vent site on aerial photographs taken in 1951 (and had probably been further excavated by the explosive outburst of February 15), any such crater was soon filled and buried by the effusive lava, which continued to extrude and spread slowly throughout the seven months of intermittent observation in 1953. At different times, lava lobes emerged laterally through the chilled carapace at the foot of the pile, or the pile itself "expanded like a balloon" and extruded lobes by overflow from the vent, or small slumps and slide masses detached from the steep flow margins (Snyder, 1954). By June 1953, the main southerly tongue of lava, ultimately 4.2 km long, had advanced only 1,250 m from the vent. Snyder (1954) estimated the volume of fallout and lava produced by June 17, 1953, to have been between 0.23 and 0.3 km^3, roughly a third of the eventual output. During the summer, steady steaming and continued spreading of the lava was punctuated sporadically by steam bursts or occasional "smoke columns" (Muller and others, 1954) that rose 1–3 km and dusted various proximal sectors with minor additional ashfall.

Observations after September 1953 were sporadic and few. A general chronology of major events was compiled by Decker (1963) and augmented by Ray (1967), largely from intermittent National Park Service reports. The 1953 lava flow may not have attained its final dimensions until early 1954 or later. It appears that there were no observations at all during eruption and outflow of the lava flows of 1957, 1958, and 1959-60, merely aerial snapshots taken in the summer seasons following emplacement of each. Time of emplacement of the lava flow attributed to the winter of 1959-60 is the least well known, as no photographs are known to have been taken between September 1958 and August 1960. The 1958 lava flow partly overran the 1953 flow and impounded a small lake on upper Mageik Creek that soon filled in with pumiceous alluvium, becoming a mudflat (Ferruginous Flat) now marked by numerous iron-precipitating warm springs.

Growth of the fragmental cone only began after much or all of the 1953 lava flow had been emplaced. It accumulated progressively during the later 1950s, as shown by emergence of the successive lava flows at different levels of the fragmental edifice. National Park Service photographs show that the cone had attained nearly its full height by 1960, but explosive showers of blocks continued to augment the cone until 1974. In addition to the four main lava flows, cone construction included emplacement of several stubby lava lobes limited to its proximal southwest slope. The southeast side of the cone completely buried a 1-km^2 cirque glacier, producing no recognized effects on eruptive behavior or edifice structure, though it is possible that enhanced steaming could have contributed to the stronger fumarolic emission and alteration on that side of the cone. Explosive ejections of tephra, some involving blowout of plugs and at least one spine, took place from 1960 to 1974, but volumetrically significant eruptions ended by 1963. Numerous sulfurous fumaroles, superheated in the 1960s but below and at the boiling point today, persist on upper parts of the cone. Dark-gray bouldery debris flows reworked from the pyroclastic deposits have built a proximal fan and thin distal sheets (1 to 4 m thick) that cap stream terraces for 3 km downstream along Mageik Creek. Some debris flows resulted from the initial February 1953 fallout over snow, others in later years by avalanching of rubble from the steep slopes of the cone.

The lava flows and ejecta are olivine-poor, two-pyroxene andesite and dacite that span a compositional continuum from 56 to 65.5 percent SiO_2. All products are plagioclase-rich and contain 33 to 45 percent phenocrysts, many of them complexly zoned, resorbed, and overgrown (Ray, 1967; Kosco, 1981; Coombs and others, 2000). The least evolved bulk material identified is the initial scoria fall of February 1953 (56–57 percent SiO_2). Andesitic enclaves are abundant, relatively mafic (56–59 percent SiO_2), contain the same phenocryst species as the host material, and fall mostly in the size range from 1 to 30 cm (Coombs and others, 2000). No evidence of contamination by leftover 1912 magma (such as quartz phenocrysts) has been found, and small but consistent compositional differences (Hildreth and Fierstein, 2000) indicate that the andesite-dacite magmas erupted in 1912 and in 1953-74 were different batches. For the Southwest Trident batch, Coombs and others (2000) presented experimental and analytical evidence for mixing between resident dacite magma stored at 890°C at a depth of about 3 km and a newly arrived batch of 1000°C andesite magma; they interpreted diffusion profiles in phenocrysts to suggest that thorough mixing could have produced the linear compositional array within about a month before the eruption began.

MOUNT KATMAI

Mount Katmai, centered 10 km east of Novarupta, is a compound stratovolcano that consisted of two large contiguous cones, both beheaded by the caldera collapse of 1912. On the caldera walls are exposed separate foci of hydrothermal alteration and abutting stacks of lavas and ejecta that dip toward each other from discrete **Northeast Katmai** and **Southwest Katmai** centers. A coastal survey in 1908 (Griggs, 1922, p. 270–275) sketched four summits, three of which were lost in 1912. The westernmost of the four survived the collapse and forms present-day twin peaks 6128 and 6200⁺ (fig. 4 of Hildreth and Fierstein, 2000). These rise above the west edge of a remnant of the pre-1912 crater of the southwest cone. The east margin of that crater apparently included the main summit, former Peak 7500. The two other pre-1912 summits (Peaks 7360 and 7260 of Griggs, 1922, p. 270) belonged to the northeast cone and were probably high points on the rim of its summit crater, now wholly destroyed. Katmai caldera, described by Griggs (1922), Fenner (1930), and Hildreth (1983, 1991), has an area of 4 km^2 at the floor and 8.8 km^2 at the rim. Its floor lies at an elevation of 990 m, and its jagged rim has a high of 2,047 m and a low of about 1,488 m. Its internal volume is today about 4 km^3, and the foundered superstructure amounted to an additional 1.1–1.5 km^3, giving a collapsed volume of between 5.0 and 5.5 km^3. The Horseshoe Island dacite dome and numerous fumaroles on the caldera floor (Fenner, 1930) were by 1930 covered by rising lakewater, which is now deeper than 250 m and more than 1 km^3 in volume.

Products of Mount Katmai extend from basalt to rhyolite (51.6–72.3 percent SiO_2), a range wider than that of any other stratovolcano in the cluster (table 1), surpassed only by the zoned 1912 eruption itself (50.4–77.7 percent SiO_2). Our 130 analyzed samples represent most of the eruptive units exposed on the caldera rim and on the outer slopes of both cones, but none were taken from the precipitous walls below the rim. Andesitic lava flows (mostly 5–50 m thick) are the volumetrically dominant material of both Katmai cones, and products more mafic than 55 percent SiO_2 are sparse. Silicic lavas (63–72 percent SiO_2) are common, dominating the stratigraphically youngest products of both cones. No lava domes have been recognized on the caldera walls (or elsewhere on Mount Katmai), though some silicic lava flows beheaded by the walls could have issued from former summit domes that were obliterated by the 1912 collapse. Fragmental materials exposed on the caldera walls are abundant in the northeast edifice and somewhat less so in the lava-dominated southwest edifice. Commonest of these are lava-flow breccias, but bedded phreatomagmatic deposits, massive block-and-ash units, and scoria and pumice falls are also present. The most silicic materials identified in the Northeast Katmai edifice are dacite lava flows (66 percent SiO_2) as thick as 60 m that cap the north rim. The Southwest Katmai cone likewise has many dacites but additionally produced several rhyodacitic to rhyolitic lava flows (68–72 percent SiO_2) that armor its upper southern slopes and cap much of its south to southeast rim. The most evolved (unit krh) of these south-rim silicic lavas yields an $^{40}Ar/^{39}Ar$ age of 22.5±1.6 ka.

The highest point surviving on Mount Katmai, Peak 6715 on the northeast rim, is part of a thick pile of thin rubbly mafic lava flows (52–53 percent SiO_2) that dip steeply outward. An andesitic lava flow resting directly upon the mafic pile at the northeastern toe of the cone yields a K-Ar age of 70±13 ka. Although a few ridge-capping andesite-dacite lavas are younger, most of the Northeast Katmai cone is older than the dated lava flow. Caldera-wall stratigraphy shows that the two Katmai cones overlap in age, but Southwest Katmai is in part much younger. An andesite lava flow basal to the Southwest Katmai pile at Katmai River gave a K-Ar age of 39±12 ka, and a dacite lava flow (also basal or near-basal) west of the caldera gave 47±13 ka. The Southwest Katmai cone erupted at least twice postglacially, as well as producing the Horseshoe Island dacite dome on the floor of the caldera, directly below the former principal summit, after the collapse of 1912 (Griggs, 1922; Fenner, 1930, 1950).

Along and near Katmai River, several lava flows relatively low in the Mount Katmai pile are 50–150 m thick, pervasively glassy and columnar, and display entablatures of slender curving columns, many of which are subhorizontal and locally form rosettes. Such features, which occur in both silicic and mafic andesites of Southwest Katmai and even in basaltic lavas of Northeast Katmai, suggest ponding of many early Katmai lavas against ice near paleocanyon floors. Despite persistence of active glaciers on both cones, the stacks of generally thinner andesite-dacite lavas higher on the compound edifice rarely display such pervasive ice-contact features.

Off-edifice pyroclastic deposits erupted at Mount Katmai include (1) valley-floor remnants of a late Pleistocene plinian pumice-fall deposit and associated ignimbrite (unit krp), which are chemically (71–72 percent SiO_2) and mineralogically similar to the south-rim rhyolite lava flow (unit krh) dated at 22.5±1.6 ka, (2) remnants of a sintered dacitic scoria-flow deposit (unit ksf) at the south foot of Mount Griggs, and (3) the Lethe assemblage (unit kla), pumiceous debris flows and hyperconcentrated sandflow deposits exposed along the lower River Lethe and lower Windy Creek (Pinney and Beget, 1991; Hildreth and others, 2000). Each of these units is discussed below in the section entitled "Recent Eruptions."

NOVARUPTA

The novel name "Novarupta" was applied by the discoverer, R.F. Griggs, to the rhyolitic plug-dome and its surrounding ejecta ring at the vent of the 1912 eruption. The name was apt because the eruption broke out through Jurassic basement rocks at a site not previously marked by a volcano. Although Griggs (1918, 1922) and Fenner (1920, 1923) thought Novarupta to be merely one of many 1912 vents, they realized it was a major one, and Shipley (1920) unequivocally attributed the valley-filling ash flows to Novarupta. Curtis (1968) subdivided the 1912 fallout into nine units, constructed isopachs for each, and thereby demonstrated that virtually all the 1912 ejecta had vented at Novarupta. The 1912 vent and its proximal deposits and structure have been discussed by Hildreth (1983, 1987), Hildreth and Fierstein (1987, 2000), Wallmann and others (1990), Fierstein and Hildreth (1992), Fierstein and others (1997), and Houghton and others (2002). The term "Novarupta" is today variously applied to the 380-m-wide lava dome, to the 1-km-wide ejecta-ringed inner vent that was explosively active on the second and third days of the 1912 eruptive sequence, and to the 2-km-wide backfilled depression that formed during the volumetrically dominant opening-day eruptive episode (Hildreth, 1987). The great eruption at Novarupta, its episodes, and its products are described below in the section entitled "The 1912 Eruption."

SNOWY MOUNTAIN

Snowy Mountain is a small andesite-dacite volcanic center that straddles the rangecrest northeast of the main Katmai cluster, separated by about 10 km from Mount Katmai and by 15 km from Mount Griggs. Snowy Mountain was named during the National Geographic Society expedition to Katmai in 1917 (Griggs, 1922, p. 131). The name chosen evidently reflected how impressed those explorers were with its extensive mantle of snow and ice as seen from upper Katmai River, which was their closest approach to the edifice. Rising to an elevation of 7,090 ft (2,161 m), Snowy Mountain remains today the source of 10 substantial glaciers. Because glacial ice still covers nearly 90 percent of the edifice, the principal rock exposures are limited to narrow ice-bounded arêtes at higher elevations and ice-scoured lava-flow benches at lower elevations.

Activity began at about 200 ka, and infrequent eruptions have since taken place from two vents 4 km apart that built contiguous subedifices which extensively overlap in age (Hildreth and others, 2001). Only the northeast vent has been active in the Holocene. Sector collapse of the hydrothermally weakened upper part of the northeast cone in the late Holocene produced a 22-km^2 debris avalanche and left a 1.5-km^2 amphitheater that was subsequently occupied by a blocky dacite lava dome. Many products of the southwest vent are olivine-bearing andesites (55–62 percent SiO_2), whereas those of the northeast vent are largely pyroxene dacites (62–64 percent SiO_2). Estimates of eruptive volume yield 8±2 km^3 for the northeastern edifice, 5±2 km^3 for the southwestern, and 13±4 km^3 for the Snowy Mountain center as a whole. Only half to two-thirds of this material remains in place on the glacially ravaged skeletal edifices today.

RAINBOW RIVER CONE

Rainbow River cone is a modest, short-lived (conceivably monogenetic), basaltic volcano (51.8–53.1 percent SiO_2) perched on a basement ridge east of Rainbow River, 17 km north of Snowy Mountain and 15 km northwest of Mount Denison (fig. 1). The glacially sculpted cone, which is only 1 km wide and has about 330 m relief, consists of radially dipping stacks of thin lavas and breccias intercalated with brick-red and black scoria falls, all well exposed on bounding cliffs, cut by numerous dikes, and gutted by a northerly cirque. A summit crag is supported by a cliff-forming mass of lava 25 m high, probably part of a plug but capped by agglutinated spatter. Lavas and ejecta contain sparse olivine and plagioclase. Remnants of an ice-scoured lava plateau extend 1 km southeastward from the base of the cone. Dense holocrystalline lava from the plateau gave a K-Ar age of 390±39 ka.

CLUSTERED STRATOVOLCANOES

The small adjacent cones of Snowy Mountain are characteristic of late Quaternary andesite-dacite arc volcanism in the Katmai area. Along the same rangecrest (fig. 1), four discrete cones of Mount Mageik, four cones of Trident, and two of Mount Katmai, as well as Alagogshak volcano, Mount Martin, and several peripheral lava domes, form a chain only 30 km long, display eruptive volumes of 1–30 km^3 each, and have mutual spacings of only 1–8 km. The close-set array of small cones contrasts strikingly with such giant stratocones as Veniaminof and Shishaldin (each well over 100 km^3) farther down the chain, and it conflicts with the conventional myth of evenly spaced arc volcanoes 40–70 km apart. Additional, comparably close-set arrays of stratovolcanoes on the Alaska Peninsula include the Pavlof and Stepovak Bay groups (Wood and Kienle, 1990; Miller and Richter, 1994) and, just northeast of Snowy Mountain (fig. 1), the Denison-Steller-Kukak-Devils Desk chain. Although the last-named chain is poorly known, volumes of the four contiguous cones appear to fall in the range from 5 to 15 km^3 each, and the mutual spacing of their vents is 3 to 4 km. [Mount Steller is not spelled correctly on many published maps; it is named for Georg Wilhelm Steller, 1709-46, naturalist on the 1741 voyage of Vitus Bering.]

Why are so many, closely spaced, mostly small, andesite-dacite volcanoes perched directly atop the peninsular drainage divide (fig. 1) from Alagogshak to Devils Desk? It has been suggested (Keller and Reiser, 1959; Kienle and others, 1983) that the volcanic chain in the Katmai district is built on the crest of a regional anticline in the Mesozoic basement rocks. Examination of the geologic map and structural cross sections of Riehle and others (1993), however, shows that the volcanoes do not necessarily lie right along the ill-defined structural crest and that the so-called “anticline” is at best a broad regional warp defined by strata dipping only 5˚–20˚ and complicated by a variety of oblique lesser folds and by intrusion of numerous Tertiary plutons into the warped Mesozoic strata. It seems unlikely that any such upper-crustal structure controls the linear alignment of the Quaternary volcanic chain illustrated in figure 1. Alternatives to upper-crustal control include (1) a narrowly linear pattern of fluid release from the subducting slab, (2) a sharp convecting corner or some other mechanism producing a narrowly linear curtain of magma generation and ascent in the mantle wedge, or (3) some linear structure in the deep crust that traps and stores mantle-derived magma batches long enough for assimilation, fractionation, and admixture of local partial melts to re-establish buoyant ascent (Hildreth and Moorbath, 1988). The observation that Mount Griggs, a 30–35 km^3 stratovolcano 12 km behind the main volcanic chain (fig. 1), has produced an eruptive suite significantly more potassic than any of the contemporaneous centers along the chain itself generally supports the notion of deep influence. Perhaps an unusually narrow belt of magma storage in the deep crust or mantle-crust transition zone leads to some degree of mixing and modulation of any mantle-derived compositional diversity beneath the main chain. Antecedent to renewed dike transport toward the upper crust and distribution of magma into discrete eruptive centers, such deep-crustal storage and modulation might account for the grossly similar compositional trends (Hildreth and Fierstein, 2000) of Katmai volcanoes along the main volcanic line.

Although the along-arc distribution of andesite-dacite magma into many small, close-set eruptive centers, as observed in the Katmai area and in a few other stretches of the Alaska Peninsula-Aleutian arc, is not a general feature of the whole Quaternary arc, the extremely linear arrangement is. The single-file chain of volcanoes that stretches 2,500 km from Cook Inlet to Buldir Island (Miller and others, 1998) contrasts drastically with the Japanese, Cascadian, Mexican, and Andean arcs, where the Quaternary volcanic zones are typically several tens of kilometers wide and where numerous volcanoes scatter far behind the volcanic front. In the Alaska Peninsula-Aleutian arc, instead of hundreds of volcanoes behind the volcanic front, there are only a handful of Quaternary centers: for example, Ukinrek, Amak, and Bogoslof (Simkin and Siebert, 1994); or Mount Griggs and Rainbow River cone on this map. Although offsets of alignment do divide the chain into several segments, some process or deep structure imposes on this arc an extraordinarily narrow linearity that is not typical of arcs worldwide.

INFLUENCE OF ICE

Glacial ice has influenced eruptions and amplified erosion throughout the lifetime of the Katmai volcanic cluster, as attested by persistence of numerous glaciers today during one of the warmest intervals of the last million years. Successive Pleistocene glacial advances covered the Alaska Peninsula with ice from coast to coast, blanketing the entire landscape during glacial maxima and, much of the time, nourishing valley glaciers that extended far outside the peninsula’s mountainous volcanic axis (Riehle and Detterman, 1993). Extensive glacial cover and glacial erosion are directly responsible for the rarity of ashfall, pyroclastic-flow, and debris-flow deposits of pre-Holocene age in the Katmai region.

Ice-contact features such as those summarized by Lescinsky and Fink (2000) are widely retained by andesite-dacite lava flows on the Katmai volcanoes—notably, (1) ice-confined walls of glassy columnar lava; (2) elongate sets of inclined, radial, curved, or subhorizontal columns, typically more slender than basal colonnades and spatially unrelated to substrate rocks; (3) individual glassy lava flows 100–200 m thick that lack devitrified interior zones, usually ponded adjacent to or perched above paleovalleys formerly filled with ice; and (4) successively accreted glassy flow lobes or stacked sheets (some perhaps invasively subglacial), each with its own tier of columnar joints. Good examples of lava flows having such features are along the southern base of Mount Katmai, at the northwest toe of Mount Mageik, and at the northwestern limit of lavas from Alagogshak volcano. Some thick flows low on the south flank of Mount Mageik and at the east toe of Mount Griggs probably likewise abutted against valley-filling glaciers. The Angle Creek flow from Mount Mageik (unit msw) and the distal flow from Alagogshak volcano along Kejulik River (unit akc) may be examples of long lava flows emplaced along the margins of valley-filling glaciers (Lescinsky and Sisson, 1998).

ERUPTIVE HISTORY OF THE KATMAI CLUSTER

THE STRATOVOLCANOES AND LAVA DOMES

Table 1 summarizes some topographic, volumetric, compositional, and age data for the several volcanoes in the Katmai cluster. The stratovolcanoes are Mount Martin, Alagogshak volcano, the four crowded cones of Mount Mageik, the four cones of Trident Volcano, Mount Griggs, and the Southwest Katmai, Northeast Katmai, Southwest Snowy, and Northeast Snowy edifices. Lava domes include Novarupta, Phantom dome (Novarupta's destroyed dacitic predecessor), Falling Mountain, Mount Cerberus, four domes on the southwest periphery of the Trident group, three domes (or thick flow remnants) within the edifice of Trident I, three poorly exposed domes (or thick flow remnants) within or adjacent to the West Trident edifice, the Central Summit of Mount Mageik, the amphitheater-filling dome of Northeast Snowy Mountain, a small flank dome just east of Alagogshak's crater (unit aac), the Horseshoe Island dome on the floor of Katmai caldera, and, possibly, one or more precaldera summit domes (destroyed in 1912) atop the Southwest Katmai edifice at the source of the south-rim rhyodacites (unit krs). Except for the last unit listed and for rhyolitic Novarupta, all the domes consist of dacite or silicic andesite (61-66 percent SiO_2).

Alagogshak volcano is the oldest component of the Katmai cluster and also the longest lived, having erupted intermittently between 680 and 43 ka. One of its western outliers (unit aow) is even older but did not necessarily erupt at the Alagogshak center. Preserved on the skeletal edifice are glacially dissected remnants of 45–50 andesite-dacite lava flows, a stratified fragmental crater complex, and a small dome at the flank-vent source of the 43-ka Alagogshak Creek flow (unit aac). Total eruptive volume, as reconstructed, was probably in the range between 10 and 18 km^3, at least half of which has been eroded away.

Mount Martin is a small fragmental cone and a northerly apron of ten lava flows, erupted entirely during the Holocene but largely before 6 ka. Activity at this little-eroded 7-km^3 andesite-dacite center is summarized below in the section entitled "Recent Eruptions".

Mount Mageik is an ice-capped compound andesite-dacite stratovolcano younger than most other centers in the Katmai cluster. Its four crowded overlapping cones epitomize the close clustering of the Katmai volcanoes. The Central Summit (unit msc) is capped by a dacite dome and the other three by fragmental summit cones with ice-filled craters. At least 57 lava flows are exposed, of which about a dozen from the East Summit erupted in the Holocene. The Southwest Summit cone was built first, followed successively by the Central, North, and East Summit subedifices. The oldest lava flow exposed gave a K-Ar age of 93±8 ka. The total eruptive volume is estimated to be about 30 km^3, of which 5–6 km^3 is postglacial. These estimates suggest a long-term average eruption rate of 0.33 km^3/1,000 yr, but a Holocene rate greater than 0.5 km^3/1,000 yr.

Trident Volcano, like Mount Mageik, consists of four contiguous andesite-dacite cones, only one of which was constructed in the Holocene. That cone, Southwest Trident, erupted between 1953 and 1974 (as described in detail above) but was largely built in the 7-yr interval 1953-60, during which four lava flows were emplaced and most of the composite cone accumulated. The three Pleistocene edifices are progressively younger from east to west, and all three are severely eroded glacially. Several glaciated lava domes were also emplaced within and peripheral to the central and western edifices. Glacial ice and the blanket of 1912 fallout obscure so much of Pleistocene Trident that counting lava flows is an uncertain exercise; we estimate roughly 40 for the eastern edifice, 25 for the central, and 10 for the western. One of the oldest lava flows exposed gives a K-Ar age of 143±8 ka. As reconstructed, the total eruptive volume for the Trident group is about 21±4 km^3, yielding a long-term average eruption rate in the range between 0.11 and 0.18 km^3/1,000 yr.

Mount Katmai consists of two overlapping edifices, which (taken together) represent the most productive, most explosive, and compositionally most varied (basalt to rhyolite) center in the Katmai cluster. At the northeast edifice, a mafic cone was built first, then, beginning about 70 ka, capped by andesite and dacite lavas and breccias that partly interfinger with products of the generally younger southwest edifice, which began growth around 47 ka. The southwest volcano has produced several explosive silicic eruptions in the last 23,000 yr, as described in the following section entitled "Recent Eruptions". In 1912, the new vent at **Novarupta** drained 13 km^3 of magma from beneath Mount Katmai, permitting collapse of its summit into the partly evacuated reservoir. Soon afterward, the Horseshoe Island dacite dome erupted on the caldera floor, 10 km east of the

Novarupta vent. The thick mantle of 1912 ejecta makes estimates uncertain, but each component cone is likely to contain as many as 100 lava flows. Total magma volume erupted from Mount Katmai (including the 1912 ejecta and older far-flung pyroclastic units) is estimated to be 70±18 km^3 (table 1). Efforts to date the early mafic cone have been unsuccessful. If it were little older than 70 ka, the long-term eruption rate would be about 1 km^3/1,000 yr; if it were as old as 100 ka, the rate would be 0.7 km^3/1,000 yr. In any case, Mount Katmai is the most productive center in the cluster, its volumetric eruption rate being two or three times that of Mount Mageik.

Mount Griggs consists of three main parts: (1) remnants of a middle Pleistocene edifice as old as 292 ka, exposed in only a few windows, (2) a late Pleistocene cone consisting of at least 50 lava flows and well preserved except for its southwest quadrant, which underwent postglacial sector collapse, and (3) a Holocene inner edifice that filled the collapse amphitheater by building a cone with two nested inner craters, at least 20 lava flows, and a volume of about 2.2 km^3. Nearly all products are andesitic, ranging from olivine-rich mafic andesite to two-pyroxene silicic andesite and a single lava flow of pyroxene dacite. In contrast to the compound volcanic-front centers, Mount Griggs has maintained a stable central vent position throughout its three-stage history. Stratified ejecta of limited dispersal are largely restricted to near the crater rims. A reconstructed eruptive volume of 30–35 km^3 suggests a long-term eruption rate of 0.10–0.12 km^3/1,000 yr, far lower than those of Mounts Katmai and Mageik.

Snowy Mountain consists of two small contiguous edifices that were supplied from long-lived central vents only 4 km apart. The southwest cone is as old as 200 ka and the northeast cone at least as old as 171 ka. Extensive ice cover limits exposure, but each cone appears to consist of only 12–15 andesite-dacite lava flows, apparently erupted as a few packages at widely spaced intervals. The only Holocene eruption was emplacement of a dacite dome in the amphitheater of the northeast cone shortly after sector collapse about 1,000–1,500 years ago. Fumarolic emissions have been reported intermittently but at other times have been undetectable (Hildreth and others, 2001). Total eruptive volume is estimated to have been 13±4 km^3. As much as half has been removed by glacial erosion.

Rainbow River cone is a small basaltic volcano, probably monogenetic or nearly so, located about 15 km behind the volcanic front, inboard of Snowy Mountain and Mount Denison (fig. 1). The glacially sculpted cone consists of 100 or more thin, radially dipping lava flows, breccia and agglutinate sheets, intercalated scoria falls, and a central summit plug. The stratified sections are cut by numerous dikes and are well exposed by glacial erosion. The pile probably accumulated in a brief eruptive interval about 390±39 ka, the age measured for a lava-flow apron at the southeast toe of the cone.

RECENT ERUPTIONS

Katmai, Trident, Mageik, Martin, Griggs, and Snowy have each erupted at least once since the withdrawal of regionally extensive glaciers (Riehle and Detterman, 1993) at the Pleistocene-Holocene transition. As younger products of evolving magma reservoirs might bear more meaningfully on the current state of the volcanoes, we highlight here all units of the Katmai cluster that erupted in the very late Pleistocene or Holocene.

1. Youngest is the Southwest Trident cone (unit tsw), which grew between 1953 and 1974. Total volume erupted was about 0.7 km^3 of andesite-dacite, including four blocky lava flows, a 0.3-km^3 fragmental cone, and a small amount of fallout, as discussed above in the section entitled "Trident Volcano."

2. The Horseshoe Island dome on the floor of Katmai caldera (unit khi) was emplaced after the caldera collapse of June 6-8, 1912, but before the caldera interior was first seen in 1916 (Griggs, 1922; Hildreth, 1991). Its volume was less than 0.001 km^3 of dacite (66 percent SiO_2; Fenner, 1930, 1950; Hildreth, 1983).

3. The Novarupta outburst of June 1912 is summarized in the next section. The explosive eruption of 13 km^3 of magma zoned from 77.7 to 50.4 percent SiO_2 included concurrent plinian, strombolian, and ash-flow activity in several pulses that spanned about 60 hr. Emplacement of two successive plug-domes (units npd and nrd) followed the climactic eruption, probably within weeks or months.

4. A blocky dome of hornblende-bearing pyroxene-dacite lava (unit snd) was emplaced within the summit amphitheater of the Northeast Snowy Mountain edifice, probably soon after the amphitheater was formed by sector collapse about 1,000–1,500 yr ago (Hildreth and others, 2001). The 700-by-1,400-m dome has about 500 m vertical relief and two or three exogenous lobes. Despite a growing icecap that obscures most of it, the glassy dome is as yet little eroded.

5. The East Summit subedifice of Mount Mageik is the source of a dozen blocky Holocene lava flows (60–64 percent SiO_2), which were emplaced (judging by their relative degradation) in several discrete episodes (units mse, meo) that probably range in age from early postglacial to late Holocene. From the ice-filled crater at an elevation of more than 2,010 m, two of the flows extend 6 km to termini as low as 300–350 m in Martin Creek. One of the youngest flows bifurcates to the northeast, one of its lobes banking against Mount Cerberus and the other halting at Katmai Pass against the toe of an andesite lava flow from West Trident volcano. The postglacial eruptive volume is 5–6 km^3, to which dacitic fallout and a small andesitic pyroclastic-flow deposit probably contribute no more than 0.1 km^3 (Hildreth and others, 2000).

6. Following sector collapse of Mount Griggs in the early Holocene, a new central cone was constructed that

filled the amphitheater and built a 12-km^2 fan of rubbly to blocky andesite lava flows (units gyo, gyi) on the southwest slope of the volcano. Exposed on the Holocene fan are at least 20 flow lobes and leveed lava tongues (55–62 percent SiO_2) that cover a fourth of the volcano's surface (Hildreth and others, 2002). The upper part of the inner cone is marked by two nested craters and includes sheets of variably agglutinated scoria and spatter and poorly sorted phreatomagmatic ejecta. Although mantled by several meters of 1912 pumice, many lava flows on the fan retain such rugged near-primary surfaces that they are likely to have been emplaced in the middle or late Holocene.

7. Mount Martin, entirely postglacial, consists of a 7-km^3 stack of 10 overlapping lava flows of blocky dacite (unit rdl) and a small vent cone of fragmental andesite (unit rac). The stack of lavas, confined to a 75° northerly sector and all fairly similar compositionally, could represent an eruptive episode only years or decades long. Because the topmost flow distally is overlain by soil and tephra layers as old as 6 ka, the package of flows must have been emplaced in the early Holocene.

8. Southwest Katmai ejected a sheet of scoriaceous to agglutinated dacite fallout (unit kwa; 64–66 percent SiO_2) that widely caps the west rim of Katmai caldera, drapes the summit of Peak 6128, and thickens into a pre-1912 crater (largely obliterated in 1912) where it reaches a maximum preserved thickness of more than 60 m on the caldera's inner southwest wall (illustrated in Plate 9 of Curtis, 1968). Glacier-covered until 1912, this variably welded, stratified fall unit is now well exposed, still mantles steep topography, and represents one of the youngest pre-1912 eruptive units identified at Mount Katmai.

9. Southwest Katmai produced a branching set of postglacial lava flows of blocky dacite (64 percent SiO_2) that poured 4 km down the southeast slope to the floor of Katmai River canyon, apparently from a poorly exposed flank vent just outside the caldera rim. Although eroded proximally by present-day glaciers, these leveed flows are unique on Mount Katmai in retaining primary surfaces—glassy, vesicular, blocky, even craggy. They are also unique compositionally in having contents of Zr elevated relative to all other Mount Katmai lavas.

10. Exposed along the south rim of Katmai caldera are beheaded remnants of at least four rhyodacite lava lobes (unit krs; 67–69 percent SiO_2), all part of the Southwest Katmai edifice and presumably derived from its former summit vent. Westernmost of these flows includes the 40-m-high "tooth" in the south rim notch (illustrated by Griggs, 1922, pp. 100, 175; and by Curtis, 1968, plate 9). For 2 km east of that notch, rhyodacite lavas make up most of the south rim, extending nearly to the east rim notch. They contain plentiful enclaves (1–20 cm) of chilled andesite (54–59 percent SiO_2). On the caldera wall, the rhyodacites overlie a 500-m stack of thin rubbly andesitic lava flows, and on the outside (where covered by ice and 1912 fallout), they extend as far as 1 km downslope. As the rhyodacites also overlie units kzs and krh (described next), they are younger than 22.5±1.6 ka (see unit krh).

11. Beneath the rim-forming rhyodacite lavas (unit krs) just east of the south notch on the Katmai caldera rim is a 40-m-thick remnant of a coarse proximal pumice-and-scoria fall (unit kzs), incipiently welded to densely eutaxitic, that zones upward from dacite to andesite (65.4–57.8 percent SiO_2). Its dacite is compositionally similar to that in the Lethe assemblage (unit kla) in the lower Valley of Ten Thousand Smokes. Neither deposit has been dated directly, but both are stratigraphically constrained to have erupted in the latest Pleistocene or early Holocene.

12. The most evolved unit cropping out at Mount Katmai (and the only one known to contain amphibole) is a hornblende-orthopyroxene-plagioclase rhyolite lava flow (unit krh; 72 percent SiO_2) at the south rim notch. The flow-foliated lava, 30–50 m thick, crops out along the south wall of the caldera for about 250 m, directly beneath zoned fall unit kzs. The lava yields a late Pleistocene $^{40}Ar/^{39}Ar$ age of 22.5±1.6 ka.

13. Plinian pumice-fall deposits and overlying nonwelded ignimbrite as thick as 75 m (unit krp) locally preserved along Mageik and Windy Creeks (respectively, 7–9 km southwest and 21 km west of the caldera rim) are mineralogically and chemically similar (not identical) to the south-rim rhyolite lava (unit krh) just described. Together, the lava and pumice are unique among products of the Katmai cluster in containing hornblende phenocrysts and in having 72 percent SiO_2. Overlain by coarse debris flows and thin glacial deposits at both remnants, the rhyolitic pyroclastic deposits are clearly of late Pleistocene age. Organic material at the base of the plinian pumice fall in Mageik Creek yields an age of 19,240±70 ^{14}C yr B.P., equivalent to a calendar age of 22.8 ka, which is similar to the $^{40}Ar/^{39}Ar$ age of the hornblende rhyodacite lava on the south rim. As the fall remnants are, respectively, 7 m and 5 m thick and consist predominantly of pumice lapilli, the plinian eruption might well have been greater in magnitude than that of 1912.

THE 1912 ERUPTION

Explosive coeruption of high-silica rhyolitic magma and a continuum of dacitic to andesitic magma at Novarupta in June 1912 was the world's most voluminous volcanic outpouring of the 20th century. At least 17 km^3 of fall deposits and 11±3 km^3 of ash-flow tuff (ignimbrite) were emplaced in about 60 hr, representing a magma volume of about 13 km^3 (Fierstein and Hildreth, 1992). This volume is exceeded by only four eruptions in the last 1,000 years: Tambora (Indonesia) in 1815, Laki (Iceland) in 1783-4, Kuwae (Vanuatu) in 1452, and Baitoushan (Korea-China) in 1050. Caldera collapse at Mount Katmai (Hildreth, 1991), 10 km east of the eruption site, and displacements elsewhere in the magmatic plumbing system generated 14 earthquakes in the magnitude range M_S 6 to 7, as many as 100 greater than M_S 5, and about 250 times the total seismic energy released during the 1991 caldera-forming eruption of Pinatubo in the Philippines (Fenner, 1925; Abe, 1992; Hildreth and Fierstein, 2000).

The significance of the 1912 eruption, however, transcends mere magnitude. The compositional range of the 1912 ejecta (50.4 to 77.7 percent SiO_2) is extraordinary, and the high proportion of different components (10 percent andesite and 35 percent dacite versus 55 percent rhyolite) is unusual (Hildreth, 1981, 1983, 1987). Historically, this was one of the rare eruptions to include high-silica rhyolite (more than 75 percent SiO_2), or to produce an extensive subaerial ash-flow sheet (120 km^2), or to generate welded tuff and a resulting fumarole field. The high-temperature fumaroles in the Valley of Ten Thousand Smokes, many of which lasted longer than 20 yr, provoked enduring interest in vapor transport of ore metals (Shipley, 1920; Allen and Zies, 1923; Zies, 1924b, 1929; Ramdohr, 1962; Kodosky, 1989; Keith, 1991b; Papike and others, 1991a, 1991b; Papike, 1992; Lowenstern, 1993). The abundant compositionally banded pumice raised the profiles of assimilation and mixing as important magmatic processes (Fenner, 1923, 1950; Wright, 1952; McBirney, 1979). Stratospheric dispersal of the Novarupta ash plume, reported as a dust veil as far east as Greece and Algeria, led to pioneering work on atmospheric turbidity and the effect of aerosols on climate (Kimball, 1913; Volz, 1975). Recognition of the relatively sluggish emplacement of the valley-confined 1912 ash flows (Hildreth, 1983) led to regular citation of the 1912 ignimbrite as typifying the weakly emplaced end of a behavioral spectrum that culminates in violently emplaced, landscape-mantling flows that surmount distant topographic barriers. The 1912 deposits also allowed a clear demonstration that the sustained production of plinian fallout and voluminous ignimbrite can be concurrent rather than sequential (Hildreth, 1983; Fierstein and Hildreth, 1992); such synchroneity has since been proven common (Scott and others, 1996; Wilson and Hildreth, 1997).

The 3-day eruption at Novarupta consisted of three main episodes (fig. 2), as reported by Martin (1913) and worked out stratigraphically by Curtis (1968) and Hildreth (1983, 1987) and in detail by Fierstein and Hildreth (1992). **Episode I** began with plinian dispersal of purely rhyolitic, pumiceous fallout (Layer A) and synchronous emplacement of rhyolitic ignimbrite. Nowhere does any initial ash or other pre-plinian deposit occur beneath Layer A, indicating that the plinian column first witnessed at 1 p.m. (Alaskan local time) on June 6 indeed marked the onset of eruption. After ejection of about 3 km^3 of rhyolitic magma over the course of several hours, small amounts of andesitic and dacitic magma began (without any interruption) contributing to the erupting mixture, marking (by definition) the onset of plinian Layer B. The juvenile ejecta in Layer B are zoned from virtually all rhyolite at its base to only about 10 percent at its top, matching the progressive shift in (andesite/dacite/rhyolite) pumice proportions in the main sequence of zoned ignimbrite emplaced concurrently in the Valley of Ten Thousand Smokes (fig. 2; also see fig. 4 of Fierstein and Hildreth, 1992). Only a few thin andesite-rich flow units capping the Episode I deposits lack a widespread fallout equivalent, indicating that ignimbrite emplacement barely outlasted the plinian phase.

Episode II began after an eruptive lull no longer than a few hours and consisted principally of plinian dispersal of phenocryst-rich dacite pumice that deposited regional fallout Layers C and D. Intercalated within these layers proximally are minor intraplinian pyroclastic-flow and surge deposits made up predominantly of dacite and andesite. Subordinate rhyolite (identical to that of Episode I) accompanied the dacite during deposition of the lower part of Layer C but was negligibly sparse thereafter.

After another lull as long as several hours (during which fines-rich Layer E settled from lingering ash clouds of composite origin; Fierstein and Hildreth, 1992), **Episode III** took place. It was similar to Episode II in depositing plinian dacite Layers F and G regionally, along with thin, proximally intercalated, sheets of andesite-dacite ignimbrite and fallout (Fierstein and others, 1997). The main explosive sequence ended with Layer H, another post-plinian ashfall deposit, finer grained and more widespread than Layer E, that settled from ash clouds of composite origin (Fierstein and Hildreth, 1992). The dacite pumice that dominates the products of plinian Layers C, D, F, and G shows the same ranges of bulk and mineral compositions in all four layers. Eruptive styles were likewise similar, though Layers C and D were more strongly dispersed toward the southeast (Curtis, 1968; Fierstein and Hildreth, 1992).

Estimates of the volumes of fallout erupted during each episode, as refined by Fierstein and Hildreth (1992), are 8.8 km^3 for Episode I, 4.8 km^3 for Episode II, and 3.4 km^3 for Episode III, yielding 17 km^3 total fallout. Ignimbrite volume is not well known because the thickest deposits, in the upper Valley of Ten Thousand Smokes (Curtis, 1968; Hildreth, 1983; Kienle, 1991), are not deeply incised; our conservative estimate is now 11±3 km^3, more than 98 percent of it emplaced during Episode I. Equivalent magma volumes are 6.5 km^3 emplaced as fallout and 7±2 km^3 emplaced as ignimbrite, yielding a total volume of about 13 km^3 of magma erupted. We estimate that at least 55 percent of the magma released was high-silica rhyolite, 35 percent dacite, and no more than 10 percent andesite. Although the first 3 km^3 of magma erupted was strictly rhyolite, the coerupting proportions of rhyolite, dacite, and andesite fluctuated greatly from the middle of Episode I onward (see fig. 5 of Hildreth and Fierstein, 2000).

Neither the rhyolite nor the andesite-dacite magma was completely exhausted during the explosive episodes, as shown by subsequent extrusion of three lava domes. Horseshoe Island dacite dome extruded on the floor of Katmai caldera. Dacitic Phantom dome transiently plugged the vent at Novarupta but was explosively destroyed and never

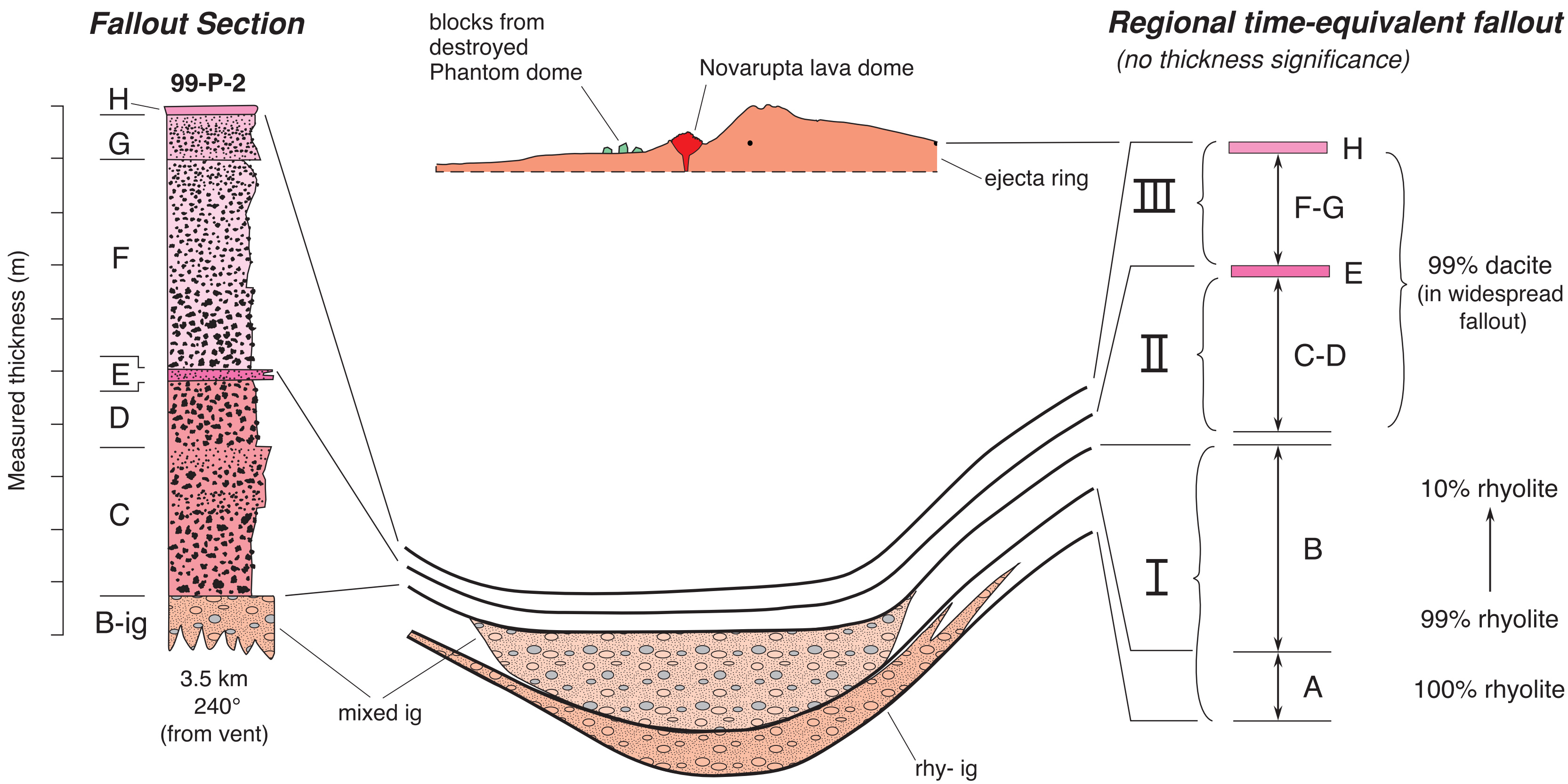

Figure 2. Eruptive sequence at Novarupta in 1912, showing schematically the concurrent emplacement during Episode I of compositionally zoned valley-filling ignimbrite (rhy ig, mixed ig) and fallout Layers A and B. These are overlain by fallout Layers C through H, emplaced during Episodes II and III on the second and third days of the eruption. Ejecta-ring material exposed close to the vent is coarser and more heterogeneous but is time-equivalent to region-wide fallout Layers G and upper F (Houghton and others, 2003). The capping dustfall, Layer H, is overlain proximally by dacitic lava blocks of transient Phantom dome, which was explosively destroyed before extrusion of rhyolitic Novarupta dome, which survived, terminating the sequence. Measured reference section 99-P-2 (Houghton and others, 2003) is at the north base of Mount Cerberus, 3.5 km southwest of the vent.

observed; its main remnants are a scattering of dacite blocks (first recognized as an integral emplacement unit by B.F. Houghton) that overlie Layer H as far as 2 km from Novarupta (Hildreth and Fierstein, 2000). The succeeding Novarupta rhyolite dome, compositionally similar to the plinian rhyolite pumice but contaminated and streaked with a few percent andesite and dacite, subsequently plugged the same vent, survived, and was first observed (by R.F. Griggs and L.G. Folsom) in July 1916 (Griggs, 1922).

The entire 3-episode explosive sequence is thought to have taken about 60 hr, based on the three intervals of downwind ashfall reported at Kodiak village 170 km to the east-southeast (Martin, 1913; Hildreth, 1983; Fierstein and Hildreth, 1992, p. 680). Essentially all the juvenile ejecta issued from the evolving vent complex at Novarupta (Curtis, 1968; fig. 2 of Hildreth, 1987). During caldera collapse, however, hydrothermal explosions expelled lithic ejecta from Mount Katmai as ballistic fragments and as thin circumcaldera sheets of muddy lithic ash intercalated within the regional Novarupta fall deposits (Hildreth, 1991; Hildreth and Fierstein, 1992). Emplacement of the first such Katmai-derived mud layer (intercalated within plinian Layer B) coincided approximately with the first large earthquake (M_S=6.5), about 11 hr into the eruption, providing the best estimate for the hour of onset of caldera collapse (Hildreth, 1991; Abe, 1992). The stratigraphic and inferred temporal positions of this and of three subsequent mud layers ejected during caldera collapse are indicated in figure 5 of Hildreth and Fierstein (2000). The remarkable seismicity that accompanied the eruption and caldera collapse was chronicled by Martin (1913) and Fenner (1925), reconstructed from seismological records by Abe (1992), and analyzed in terms of the eruptive stratigraphy by Hildreth and Fierstein (2000).

COMPOSITIONS OF THE ERUPTIVE PRODUCTS

Because our curiosity was driven by the magmatic plumbing problem and the compositionally complex eruptive sequence of 1912, one goal of our geologic mapping became an investigation of compositional affinities among the 1912 magmas and those erupted from the several edifices nearby. Accordingly, we sampled a large fraction of the lava flows exposed at each of the eruptive centers listed in table 1, as well as more than 200 pumice blocks representing all subunits of the 1912 eruption. Chemical data for more than 700 samples (collected from 1976 through 2001) are given in a series of reports on the individual volcanoes (Hildreth and others, 1999, 2000, 2001, 2002, in press; Hildreth, 1983). Selected data are illustrated in figure 3. Analyses were by X-ray fluorescence (XRF) spectroscopy in U.S. Geological Survey laboratories, wavelength dispersive for major elements and energy dispersive for trace elements. Precision and accuracy of these methods, U.S. Geological Survey rock standards used, and long-term consistency are discussed by Baedecker (1987) and Bacon and Druitt (1988).

Primitive magmas have not erupted at any of these volcanoes. Only at the Southwest Snowy and Trident I edifices have mafic products been found that contain more than 7 percent MgO. Excluding a few olivine-accumulative samples, the most magnesian products identified from Alagogshak, Northeast Katmai, Novarupta, and Griggs are in the range from 5.1 to 5.7 percent MgO. At Martin, Mageik, Northeast Snowy, Southwest Katmai, and the several other Trident cones and domes, no lavas or ejecta have been sampled that contain as much as 5 percent MgO. Low-silica rhyolite has erupted only at Mount Katmai and high-silica rhyolite only at Novarupta. At all the other volcanoes, the eruptive suites extend from mafic andesite to dacite, with rhyodacite common only at Southwest Katmai and sparse basalts present only at Northeast Katmai and Alagogshak. Alkali-lime intersections (Peacock, 1931) fall at 63–64 percent SiO_2, defining calcic suites for Novarupta and for all centers on the main volcanic line. Mount Griggs, 12 km behind the volcanic front, contrasts with the rest in having its intersection at 61 percent SiO_2, which defines a calc-alkalic suite in Peacock's original scheme.

Sample suites for all volcanoes in the Katmai cluster yield broadly similar, low-Ti, medium-K calcalkaline (non-tholeiitic) arc trends (Miyashiro, 1974; Gill, 1981) that are mutually distinguishable on variation diagrams by only a few element pairs (fig. 3). For example, the variation trends of Al, Ti, Ca, Na, Rb, Ba, Mg, and (except for Mount Griggs) Fe plotted against SiO_2 or MgO substantially overlap for all volcanoes in the cluster. A fair separation of several of the suites is provided, however, by variation patterns (fig. 3) of K_2O, Zr, and Sr against SiO_2, as shown in greater detail by Hildreth and Fierstein (figs. 8–10, 2000). Across the SiO_2 ranges identified, products of Mount Griggs consistently have higher contents of K_2O and Zr than material erupted at Katmai, Trident, and Novarupta. Along with generally greater Sr and lower Fe contents in Griggs lavas of all ages, these distinctions show that Mount Griggs has long maintained a discrete magma-storage and plumbing system, at least in the upper crust, and that its magmas have not mixed with those erupted along the nearby volcanic axis (Hildreth and others, 2002).

Figure 3 illustrates that the andesite-dacite suite released at Novarupta in 1912 is roughly collinear with the dominant trend for products of Mount Katmai. Moreover, a plot of Zr versus SiO_2 virtually separates the products of the northeast and southwest subedifices of Mount Katmai, indicating closer compositional affinity of the 1912 andesite-dacite suite with the younger Southwest Katmai center. In contrast, the 1912 suite is poorer in Sr and richer in K and Zr than most products of adjacent Trident Volcano and its peripheral domes (Hildreth and Fierstein, 2000; Hildreth and others, in press).

Eruptive products of East Trident, oldest edifice in the Trident group and the closest neighbor to Mount Katmai, are distinguishable from those of Katmai and Novarupta in having lower contents of Zr and K_2O. Trident I, West Trident, and the peripheral domes are likewise consistently deficient in Zr and K_2O relative to the Katmai-Novarupta array, and their higher Sr contents distinguish them from East Trident as well (Hildreth and Fierstein, 2000). The data thus indicate that all pre-1953 constituents of the Trident group were supplied by magma reservoirs physically separate from those that (in part concurrently) fed Mount Katmai. The compositional similarity of Falling Mountain and Mount Cerberus to West Trident and the other Trident domes likewise confirms that the magmatic affinity of those dacite domes lies with the prehistoric Trident group, not with nearby Novarupta.

Unique among the several components of Trident, the 1953-74 products of Southwest Trident are close to being compositionally collinear with those of Katmai and Novarupta in most variation diagrams. The Southwest Trident suite is nonetheless distinguishable by its slightly lower K_2O and Fe contents and slightly higher Na and Sr contents relative to the 1912 array (Hildreth and Fierstein, 2000). The most evolved 1953-74 material analysed has 65.5 percent SiO_2 (Coombs and others, 2000), and only a few samples have more than 63 percent (Ray, 1967; Kosco, 1981; Hildreth and others, in press). In contrast, the 4.5 km^3 of dacite that erupted in 1912 was zoned to 68 percent SiO_2 and most of it had more than 65 percent. No xenocrystic evidence has been found in 1953-74 material for contamination by left-over (quartz-bearing) 1912 rhyolite, and there is no hint in the 1953-74 andesite-dacite array of a mixing trend toward (Zr-deficient) 1912 rhyolite (Hildreth and Fierstein, 2000).

We conclude that the andesite-dacite magma that built Southwest Trident was similar but not identical to the 1912 andesite-dacite magma that drained from beneath Mount Katmai to the Novarupta vent at the toe of West Trident. The 1953-74 dacite probably occupied a shallow reservoir near Katmai Pass, physically remote from that of 1912. The dacite reservoir may have been disturbed by andesitic replenishment during the decade or so preceding 1951, the year when fumaroles were first observed on the subsequent site of Southwest Trident (Hildreth and others, in press). Major andesitic replenishment may not have stimulated thorough convective mixing with the resident dacite magma until a month or so before eruption began in February 1953, as suggested by the mixing and diffusion-profile data of Coombs and others (2000). Compositional similarities are consistent, however, with the possibility that the andesite batches involved in the 1912 and 1953 eruptions were ultimately supplied by the same deep-crustal reservoir.

Products of Mount Martin yield tight compositional arrays (fig. 3; Hildreth and others, 1999, 2000; Hildreth and Fierstein, 2000) that are poorer in Sr than the 1912 andesite-dacite suite and marginally more potassic but otherwise rather similar. In contrast, products of the long-lived compound Mount Mageik edifice (Hildreth and others, 2000) are far more heterogeneous than those of the other active centers, scattering above and below the arrays for Katmai and Novarupta (fig. 3). The strictly Holocene products of Mount Mageik, however, are so similar to the 1912 arrays that participation of Mageik magma in the 1912 eruption is not ruled out on chemical grounds alone (Hildreth and Fierstein, 2000). Compositional arrays for the extinct Alagogshak center (Hildreth and others, 1999) are even broader than for the whole Mount Mageik edifice, probably reflecting the evolution of several independent magma batches over its 600,000-yr lifetime. Snowy Mountain lavas are compositionally similar to those of Mount Martin or slightly more potassic (Hildreth and others, 2001). The Snowy Mountain andesite-dacite arrays are thus marginally more potassic than those of Mount Katmai and Novarupta but not as potassic as those of Mount Griggs (fig. 3).

The 7–8 km^3 of phenocryst-poor high-silica rhyolite magma released at Novarupta in 1912 was restricted to a compositional range of only 76.5–77.7 percent SiO_2, whether emplaced as pumiceous fallout or as ignimbrite. Although the rhyolitic pumice is generally xenocryst free, most of the Novarupta dome lava is slightly contaminated (Curtis, 1968; Hildreth, 1983; Coombs and Gardner, 2001). In addition to obvious bands, lenses, and enclaves of 1912 andesite and dacite, the dome rhyolite contains dispersed xenocrysts introduced from the coerupted intermediate magma and from Jurassic sandstone, volcanic xenoliths, and vent-filling fallback material as well. High-silica rhyolite is otherwise absent among Quaternary products of the Katmai cluster and is rare on the Alaska Peninsula (Miller and others, 1998). No uncontaminated 1912 pumice in the range from 69 to 76 percent SiO_2 has been recognized, and even the few pumice samples having from 66.5 to 68.6 percent SiO_2 are suspected of slight contamination by coerupted rhyolite.

VOLCANO HAZARDS

The principal volcano hazards in this uninhabited wilderness are to aviation, fish and wildlife resources, backcountry travellers, and observers attracted by precursory activity. The volcanoes are so remote that an ordinary eruption is unlikely to have much impact on ground-based people or property. Most of the 1953-74 activity at Trident was not only unobserved but went completely unnoticed. Even the great eruption of 1912, the world's largest of the 20th century, killed no one directly. In 1912, of course, there were no aircraft in Alaska and the region was sparsely populated. The ash cloud and downwind fallout from a comparably great eruption today would threaten many aircraft, discomfort thousands, and devastate the economy of southern Alaska (Fierstein and others, 1998). Any volcanic-ash plume, associated even with minor eruptions, now poses a potential hazard to aircraft (Casadevall, 1994), and local sightseeing flights and scheduled commercial flights (King Salmon to Kodiak) commonly pass directly over the Katmai cluster.

The main danger is from phreatomagmatic and magmatic eruptions that can reasonably be anticipated to produce ash clouds that typically rise to altitudes of 5–12 km (as high as 40,000 ft), endangering any aircraft overhead or downwind. As for the effects of ash clouds driven downwind, the Holocene tephra record suggests that only a handful of postglacial eruptions in the Katmai cluster have been of sufficient magnitude to produce more than a light dusting at Kodiak Island or Cook Inlet settlements (Fierstein and Hildreth, 2000, in press). Judging on the basis of past eruptive behavior, it might be anticipated that ash dispersal from Trident or Griggs would be local, from Martin or Snowy probably modest, from Mageik possibly troublesome, and from Mount Katmai potentially severe. Such inferences need to be tempered by acknowledgment that, owing to regional glaciation, the tephra record generally goes back only 8,000 yr, and that Novarupta did not even exist before its catastrophic eruption in 1912. Moreover, small outbursts of ash lasting only minutes commonly produce short-lived plumes that can endanger aircraft but leave no lasting stratigraphic record.

Each of the steep stratovolcanoes has been weakened by fumarolic alteration near its summit, and each has water and ice in its crater and glaciers on its flanks. Any new eruptive episode would therefore be likely to generate debris flows or, as in the past at Mount Mageik, Mount Griggs, Mount Katmai, and Snowy Mountain, to trigger debris avalanches. Fortunately, the runout distance is 25 km to Naknek Lake or Shelikof Strait (fig. 1), so even a large debris avalanche might merely muddy the waters in a coastal harbor or downstream on various rivers and lakes for a season or two.

In all probability, renewed eruptive activity at any of the Katmai volcanoes would be preceded by days to months of increased seismicity. Persistent clusters of shallow earthquakes beneath the volcanic axis from Mount Martin to Mount Katmai, and diffuse seismicity northwest of Snowy Mountain, have been recognized since at least 1965 (Ward and others, 1991). Most of the roughly 1,000 earthquakes

Figure 3. K_2O, Zr, and Sr versus SiO_2 contents for products of Katmai cluster volcanoes. Symbols identified in inset. LPFI=late Pleistocene rhyodacite plinian pumice fall and ignimbrite (map unit krp) erupted at Mount Katmai. Horseshoe Island dacite dome (map unit khi) was emplaced on floor of Katmai caldera after 1912 collapse; it was sampled and analysed by Fenner (1950) for major elements but not for trace elements. For clarity, field outlines alone are plotted for Alagogshak (n=44) and Mageik (n=56) volcanoes; see Hildreth and others (1999, 2000) for plots of those data. Major elements are normalized to volatile-free totals of 99.6 wt % (leaving 0.4 wt % for trace elements and halogens). High-Zr cluster for Southwest Katmai at 64% SiO_2 represents unit kds.

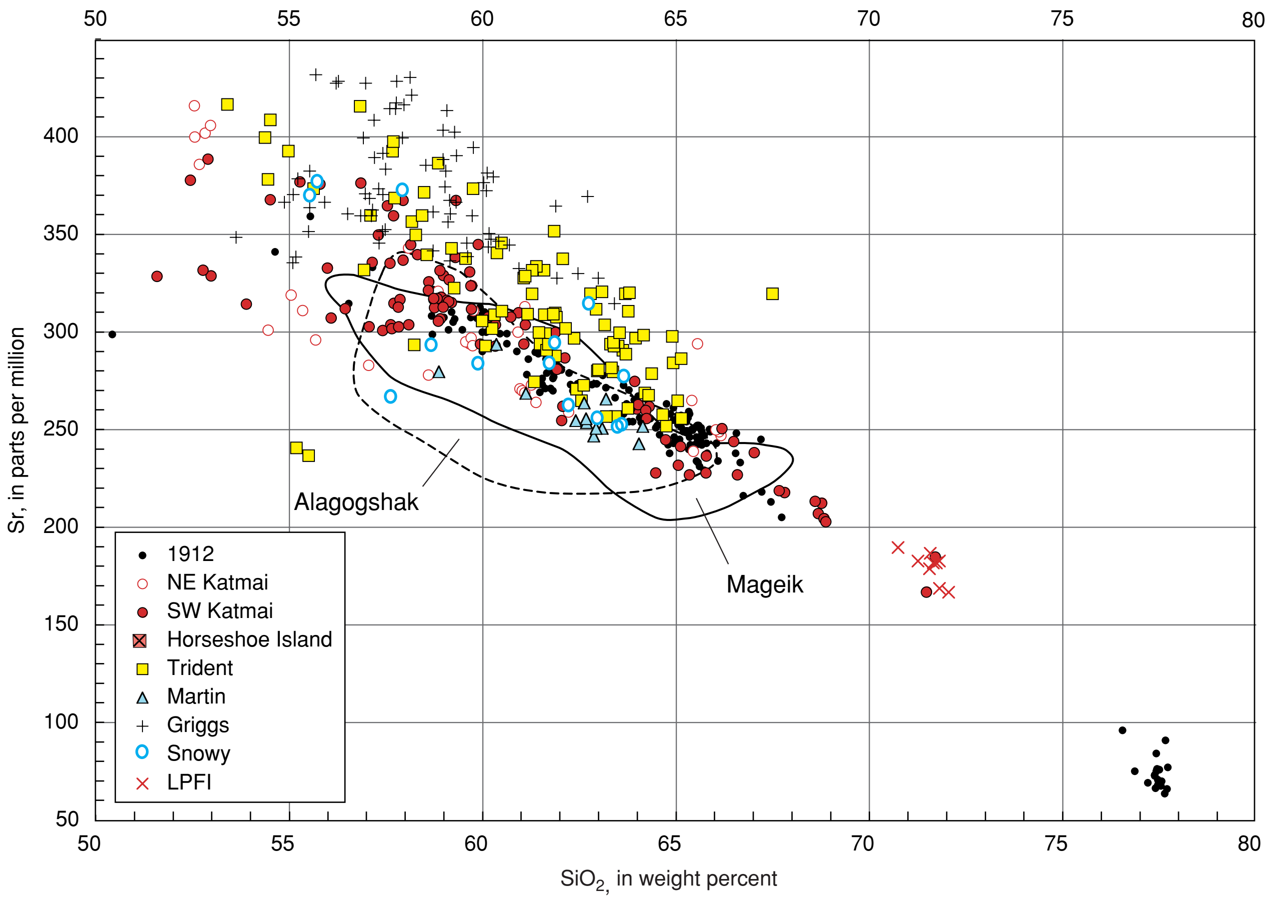

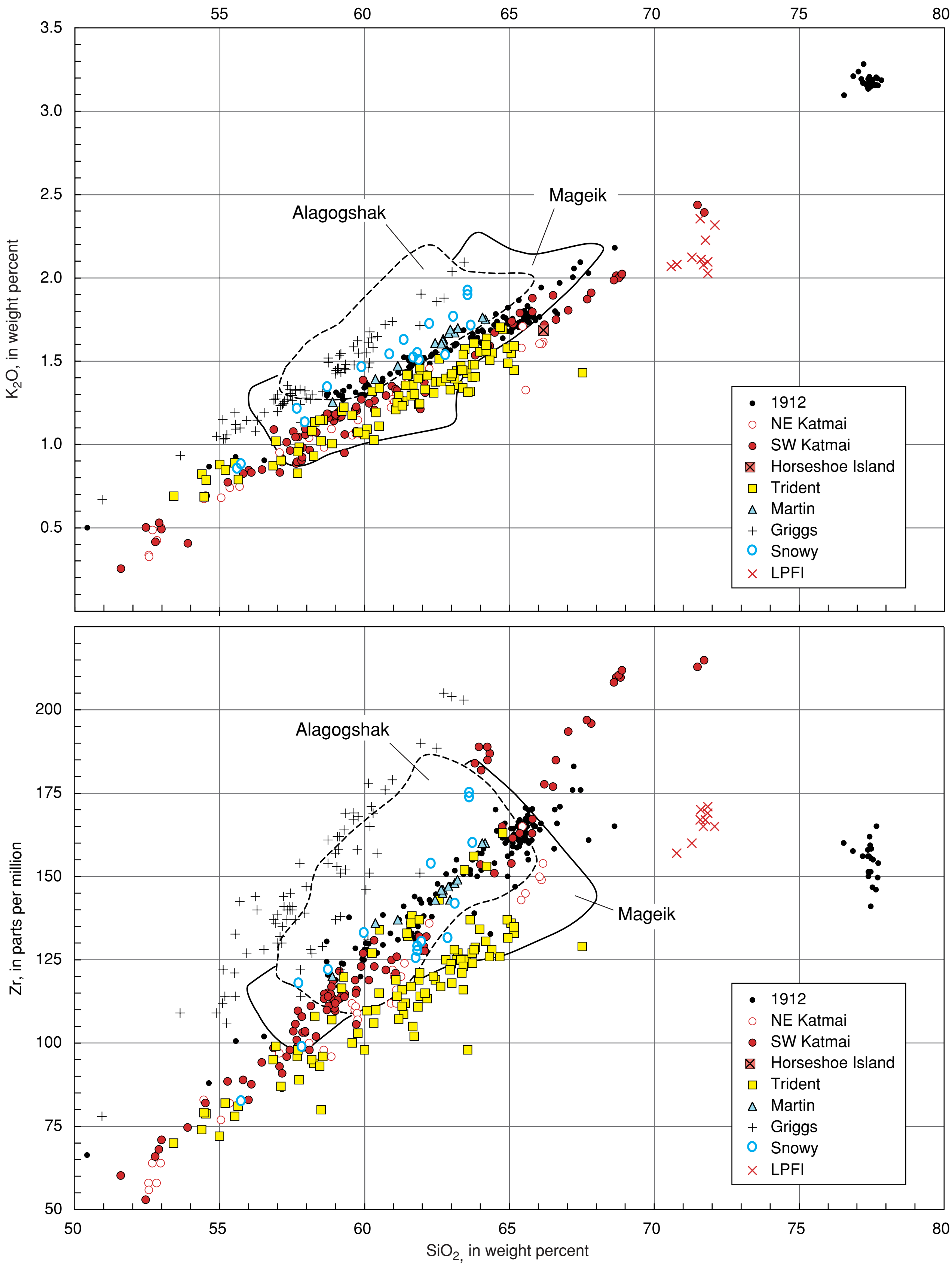

Figure 3.—*continued*

recorded each year occur at depths of 1–10 km, and all but a few are smaller than magnitude 2.5 (Jolly and McNutt, 1999; Power and others, 2001; Moran, 2003). In contrast to the chain of volcanic-front centers, the area beneath nearby Mount Griggs is virtually aseismic. Alaska Volcano Observatory (AVO) has installed a network of seismometers throughout the Katmai cluster, permitting precise location of small earthquakes and improving the ability to detect seismic activity potentially precursory to eruptions. Were signs of unrest to be detected, AVO would implement additional instrumental and observational monitoring and would notify land-management authorities, the media, and the aviation community of the impending hazard.

ACKNOWLEDGMENTS

Terry Keith, then at the helm of Alaska Volcano Observatory, proposed that we extend our Katmai work to include mapping the whole stratovolcano cluster. John Paskievitch arranged the helicopter logistics that made it possible. Helpful reviews by Tom Sisson, Tom Miller, and Scott Starratt improved the map and this accompanying text. Geochronology by Marvin Lanphere, abstracted here and published in detail elsewhere, was essential to focussing our investigations and calibrating our stratigraphy. Confronting the elements and the 1912 deposits alongside Colin Wilson and Bruce Houghton was its own reward. During helicopter-borne field seasons, we were assisted by Michelle Coombs, Dave Tucker, and Tracy Felger. In the old days on foot, substantial field contributions were made by companions Larry Jager, Dan Kosco, Anita Grunder, Dave Johnston, and Maura Hanning. Dave Siems provided high-quality, internally consistent, chemical data for samples taken year after year. National Park Service personnel, from Gil Blinn in 1976 to John Bundy in 2001, gave us permits, advice, and logistical support; those who helped make our job easier, more interesting, or more agreeable included Bud Rice, Lynn Fuller, Jim Gavin, Ralph Furbush, Dave Morris, Bruce Kaye, Janis Meldrum, Ron Squib, Rick Potts, and Karen Gustin. Brooks Lodge personnel who likewise contributed include Eric Schmidt, Perry Mollan, and Dan McDonough. Personnel of Becharof National Wildlife Refuge, especially Susan Savage and Donna Dewhurst, provided the support and facilities in King Salmon that made flying back to town worth the trouble. In successive years, pilots Tom Husted, Jim Acher, Glen Gulick, Paul Walters, Bill Springer, Jim Sink, and Sam Egli got us to some pretty breathtaking places, enabling this investigation to be more thorough than we had any right to expect. Walter Metrokin, Lucius Folsom, Jasper Sayre, Clarence Maynard, and Clarence Fenner, whose names are attached to volcanic units here, were important but under-recognized contributors to the Griggs expeditions to Katmai in 1915-19. Accompanying Griggs, Folsom was co-discoverer of the Valley of Ten Thousand Smokes. Maynard, assisted principally by Sayre, accomplished on foot the triangulation survey that led to the wonderful topographic map of the area published by Griggs (1922). Fenner is the only volcanologist known to have reached the Valley of Ten Thousand Smokes on horseback.

DESCRIPTION OF MAP UNITS

Described here are the eruptive products of 15 stratovolcanoes and several lava domes. Only six of the stratovolcanoes and three of the domes were recognized and well enough known to have been assigned geographic names prior to this investigation. These were Mounts Martin, Mageik, Katmai, and Griggs (formerly Knife Peak), Trident Volcano, and Snowy Mountain and the lava domes Novarupta, Falling Mountain, and Mount Cerberus. Four of the named volcanoes (Mageik, Trident, Katmai, and Snowy) are compound, in the sense that each consists of two to four discrete but contiguous cones. Mount Griggs maintained a single central vent during episodic cone growth, but it is also compound in the sense that it was rebuilt twice, following glacial erosion and postglacial sector collapse. Alagogshak volcano, relatively simple but long-lived, was recognized and named during this project. Among the stratocones, only Mount Martin is relatively simple and short-lived. To avoid confusion, we retain the historical volcano names as our primary descriptive framework and we describe each of their component cones as subdivisions of those edifices. Because the eruptive lifetimes of the named volcanoes overlapped extensively, we treat each volcano sequentially in the Description of Map Units, listing the component cones and discrete map units of each in (reverse) eruptive sequence, youngest unit first. The approximate time equivalence of units from the several volcanoes is portrayed in the Correlation of Map Units on the map sheet.

Novarupta demands special treatment. Its great 1912 eruption took place at a new vent that broke out through Jurassic basement rocks where no volcano had been before. It thus needs to be treated as a discrete volcano, despite its proximity to Trident and the likelihood that all or much of the 1912 magma had been stored beneath Mount Katmai (Hildreth and Fierstein, 2000). The Description of Map Units begins with Novarupta, proceeds then to Surficial Deposits (most of which are older than the Novarupta deposits), then to the other Quaternary volcanoes, and finally to pre-Quaternary basement rocks (which were given little attention during this project).

Each (volcanic) map unit is given a letter code (for example, unit nrd), the first letter indicating its primary volcanic center. Except for little-studied basement rocks, all units are Quaternary. Conventional age boundaries adopted for the Pleistocene are 2.6 Ma (Morrison and Kukla, 1998) and 10 ka, and the boundaries between early, middle, and late Pleistocene (following Richmond and Fullerton, 1986) are taken to be about 788 ka and 132–128 ka.

Compositions are given for each primary eruptive unit. Rock names are based simply on their SiO_2 contents, as follows: basalt has less than 53 percent, andesite 53–63 percent, dacite 63–68 percent, rhyodacite 68–72 percent, and rhyolite more than 72 percent. Most volcanic rocks in the Katmai cluster are plagioclase-rich two-pyroxene andesite and dacite. Olivine is also common in those having less than 58 percent SiO_2 and is sparsely present in some more silicic andesites. In the Quaternary volcanic rocks, sanidine and biotite are absent; phenocrystic quartz is present only in 1912 Novarupta rhyolite; and hornblende occurs very sparsely in a few silicic rocks (as indicated in the unit descriptions).

NOVARUPTA DOME AND PYROCLASTIC DEPOSITS OF 1912

[See Hildreth, 1983, 1987; Fierstein and Hildreth, 1992]

ndf **Pumice-rich debris-flow deposits derived from 1912 ejecta**—Deposits of 1912 fallout and pyroclastic-flow material that were remobilized from snowclad slopes as pumiceous mudflows, during and after the eruption; widespread but generally too thin and patchy to show at the scale of this map. Syneruptive mudflows intercalated in the 3-day sequence of stratified fall deposits are notably abundant in upper Knife Creek and on the slopes of Mount Griggs, Mount Katmai, and Trident. The main deposit shown, west of Ukak River in distal Valley of Ten Thousand Smokes, is as thick as 6 m, overlaps and extends beyond margin of ignimbrite, and encloses uncharred trees, some still rooted. Many thin remnants (not shown) on surface of valley-filling ignimbrite record downvalley passage of such pumiceous mudflows; some fraction of that material was transported in response to breakout of a temporary lake impounded in the Griggs Fork of Knife Creek (Hildreth, 1983). Remnants of deposits downstream from snout of Noisy Glacier (east of Mount Katmai) were once far more extensive. Compositional proportions of the pumice assemblages in these deposits varies with sector and depends in part on when they were remobilized during the zoned fallout sequence

nsl **Lake and mudflat deposits**—Plane-parallel bedded sedimentary deposits consisting largely of 1912 pyroclastic material reworked into shallow temporary lakes and mudflats, principally in three areas. At the north foot of Mount Mageik, Fissure Lake (Griggs, 1922, pp. 212, 244) extended 600 m east-northeast of present-day West Mageik Lake along a narrow cleft that had been explosively excavated by a chain of coalescent phreatic craters along the fissured hingeline of the valley-fringing compactional bench in the ignimbrite (Hildreth, 1983; Hildreth and Fierstein, 1987). After lake level dropped during the 1920s as the River Lethe outlet deepened, more than 10 m of ashy lacustrine and alluvial fill were incised by a stream flowing back into the modern lake. Along the Griggs Fork of Knife Creek, more than 12 m of plane-stratified sand and silt with intercalated pumice-rich debris flows and alluvium are inset against phreatic deposits, overlie disrupted 1912 ignimbrite, and are overlain by wavy bedded terrace gravels (Hildreth, 1983). Another lake was impounded by the 1912 ignimbrite in lower Windy Creek and had grown to 1 km long by 1919, but (after later breaching) its deposits were obliterated by action of the braided stream

npe **Phreatic explosion deposits**—Poorly sorted crossbedded deposits of remobilized 1912 pyroclastic debris (Hildreth, 1983), 1–20 m thick along upper Knife Creek, ejected from more than 60 phreatic craters rooted in the 1912 ignimbrite, which had buried snowfields and several streams. Many layers contain blocks of sintered to partially welded ignimbrite denser than any exposed at the surface. A few such craters and deposits are also present along the River Lethe and in the lower Valley of Ten Thousand Smokes where defeated tributary streams poured out onto the hot tuff, inducing explosions. Similar deposits are present at the snouts of the Knife Creek and Mageik glaciers where hot ignimbrite banked against the ice. On the map, most of the small source craters rooted in the ignimbrite (unit nig) are designated by circles and crescents within the areas of the phreatic deposits. Comparable diamictic deposits that flank the confluence of Windy Creek with the 1912 ignimbrite sheet are 1–4 m thick, extend as high as 45 m above the ignimbrite surface, contain a few rounded cobbles of basement rocks, and consist predominantly of remobilized 1912 ignimbrite material. Resting on intact Episode III fallout (two days younger than the ignimbrite), the diamictic deposits may have been emplaced explosively when a temporary lake along lower Windy Creek began to cut an outlet channel through the dam of still-hot ignimbrite

nrd **Novarupta rhyolite lava dome**—Small lava dome (77% SiO_2), 60 m high, circular in plan, emplaced within the vent for the preceding explosive eruptions of Episodes II and III. Its blocky exterior is glassy, vesicular, flow foliated, and phenocryst poor and contains common streaks of andesite and dacite viscously entrained as well as sparser angular fragments of their chilled equivalents and of basement rocks. Predominant rhyolite component has 1–2% phenocrysts of plagioclase, quartz, hypersthene, FeTi oxides, and a trace of xenocrystic amphibole (probably derived from co-eruptive dacite)

npd **Phantom dome block layer**—Strewnfield of scattered blocks of glassy dacite (62–66% SiO_2), dense to pumiceous, that overlie Layer H (the regional dustfall that completed the main fallout sequence) on the present-day surface. Distribution limited to an oval area around and as far as 2 km south of Novarupta. As the deposit does not form a physically continuous layer and has no well-defined boundary, the limit depicted by the magenta dashed line on the map is approximate. Interpreted as shattered remains of a small transient dacitic plug dome that was destroyed explosively at the same vent where rhyolitic Novarupta dome later extruded. (Dacite lava blocks should not be confused with coexisting near-vent blocks of eutaxitic pyroclastic vitrophyre, welded fallback material that backfilled the vent funnel and was recurrently shattered and re-ejected during and after explosive Episodes II and III)

ndk **Katmai River pumice-rich debris-flow deposit**—Remnant (0.6 km^2) of a secondary deposit as thick as 18 m of Novarupta ejecta remobilized from snow-covered southern slopes of Mount Katmai. Multi-flow deposit overlies complete Novarupta pumice-fall section (Episodes I, II, III) but is overlain by slower-settling regional dustfall (Layer H); emplaced, therefore, within hours or days after eruption ceased (Hildreth, 1983, 1991). Encloses uncharred trees, some still rooted. Dacitic pumice exceeds rhyolitic; andesitic pumice rare; generally lithic-poor

npp **Proximal 1912 pumice-fall deposits of Episodes II and III**—Thick fallout of Layers C through G (with minor pyroclastic-flow sheets intercalated), predominantly dacitic, deposited June 7-8, 1912 (Fierstein and Hildreth, 1992). Indicated on map only by 5-m and 10-m isopachs, inside which these fall deposits almost wholly conceal proximal parts of the subjacent main ignimbrite (unit nig) of Episode I, except in cutbanks and a few deep gullies. (The 1-m and 2-m isopachs additionally include Episode I fallout, which is trivial inside the 5-m isopach.) Within the near-vent area, pumice blocks 20–40 cm across and lithic clasts larger than 10 cm are abundant in the fallout. Equivalent medial to distal fallout, progressively thinner and finer with distance, extends more than 50 km in all directions. Owing to the influence of near-vent topography on eruption dynamics, ultraproximal fallout accumulation was greatest in the northeast sector of the ejecta ring (crest indicated by magenta dotted line) surrounding the Novarupta vent. Exposed thickness of Episode II-III deposits on the inner face of the ejecta ring just northeast of the dome is about 225 m; their total thickness (atop ultraproximal Episode I deposits) is greater still but unknown. Distensional faulting reflects compaction, welding, and gravitational spreading within this extraordinarily thick proximal pile (first called "The Turtle" by Howel Williams in 1953) on the northeast side of the vent (Hildreth, 1983, 1987; Wallmann and others, 1990; Fierstein and Hildreth, 1992; Fierstein and others, 1997; Houghton and others, 2003)

nig **Valley-filling ignimbrite of June 6-7, 1912 (Episode I)**—Principal pumice-rich ash-flow deposits of the Valley of Ten Thousand Smokes, Katmai Pass, and Mageik Creek. Numerous flow units were emplaced synchronously with ejection of regional plinian fallout Layers A and B (not separately indicated on Geologic Map; see Fierstein and Hildreth, 1992). Predominantly nonwelded, though commonly sintered in upper Valley of Ten Thousand Smokes, especially where flows were andesite rich late in eruptive sequence. Some exposures are welded and eutaxitic near Knife Creek Glacier 1, as are many phreatically ejected blocks derived from deep levels of the sheet not yet exposed by erosion. Valley-filling ignimbrite covers about 120 km^2, not including veneers on topography high above valley floors. Thickness probably exceeds 150 m in upper Valley of Ten Thousand Smokes (Curtis, 1968; Hildreth, 1983;

Kienle, 1991), thinning to less than 10 m near eroded distal termini. Correlative high-energy proximal veneers blanket near-vent ridges. Feather-edges (not shown on map) of main valley-filling sheet thin to less than a few meters where they extend up lower slopes of the Buttress Range, of Mounts Griggs, Katmai, and Mageik, and into saddles between peaks of Trident. Composition of early ash flows was strictly rhyolitic (77% SiO_2); successive ash flows contained progressively greater fractions of andesite, dacite, and banded pumice (fig. 2; Hildreth, 1983; Fierstein and Hildreth, 1992)

SURFICIAL DEPOSITS

ap **Pumiceous alluvium of 1912 Novarupta pyroclastic debris (1912 and younger)**— Principally fans of pumiceous scree and pumice-dominated alluvium of intermittent streams. Only major accumulations are shown on map, mainly in and near the Valley of Ten Thousand Smokes. Similar pumice-fan deposits (not mapped) are common within the 1912 downwind fallout sector to the east and southeast, especially at the foot of canyon walls along Ikagluik Creek, Katmai River, and Soluka Creek. Terrace remnants of hyperconcentrated sandflow deposits (not shown separately) along West Fork of Rainbow River consist of coarse rhyolitic ash remobilized from Layer A fallout

al **Alluvium (Holocene)**—Heterolithologic terrace gravels, active stream gravels, and tributary alluvial fans; water-transported, unconsolidated. Much material reworked from glacial deposits. Pumice of 1912 a subordinate but conspicuous component along Ukak River, Windy Creek, Ikagluik Creek, Soluka Creek, and Katmai River and its great braided plain

ls **Landslide deposits (Holocene)**—Unconsolidated slide and slump deposits, typically having hummocky medial-to-distal surfaces and headwall scarps exposing bedrock. For a few slumps on Observation Mountain, debris veneers are omitted, as the material is lithologically same as undisturbed bedrock (Naknek Formation, unit bu). Most landslides and debris-avalanche deposits from volcanic edifices are designated individually as map units for each volcano

rg **Rock glaciers (Holocene)**—Tongues of coarse blocky debris with interstitial or buried ice, undergoing slow downslope movement. All are adjacent to sources of abundant coarse debris, mostly steep north-facing slopes and cirques cut in basement rocks. Transverse arcuate furrows, convex downflow, characterize surfaces

gh **Glacial deposits (Holocene)**—Mostly unconsolidated till adjacent or near active glaciers but also including early Holocene moraines in the lower Valley of Ten Thousand Smokes (Fierstein and Hildreth, in press). On northwest rim of Katmai caldera, till as thick as 40 m (mixed with a mantle of 1912 caldera-collapse rubble) has been chaotically let down onto rim lavas by wasting of beheaded glaciers

ice **Glacial ice (Holocene)**—Present-day glaciers, including pockets of stagnant ice. Contacts with ice-cored moraine and with perennial snowbanks concealing bedrock are approximate. Many glaciers within 10 km east of Novarupta are still mantled by thick primary and remobilized 1912 pumice-fall and ash-flow deposits. Knife Creek Glaciers are conventionally numbered 1 through 5, from west to east

s **Surficial deposits, undivided (Holocene and late Pleistocene)**—Includes talus, scree, colluvium, colluvially disturbed till, swamp deposits, and alluvium—commonly associated intimately and not mapped separately at this scale. Minor occurrences generally omitted. Major aprons of such composite debris are present on both sides of Margot and Windy Creeks where postglacial sloughing of shaly slopes has been prodigious. In Alagogshak Creek, unit includes till, hummocky avalanche deposits, stream alluvium, and numerous swamps. At northeast foot of Falling Mountain, unit includes post-1912 talus marked by shallow craters ringed with crossbedded phreatic-explosion deposits as thick as 4 m, as well as rockfall debris of Falling Mountain dacite, some of it in shattered disintegrating piles as high as 12 m. Along arroyo between lava flows of Southwest Trident, unit includes minor pyroclastic flows and fallout emplaced during cone construction (1953-74), mostly reworked as scoria-dominated debris flows and alluvium preserved in terrace remnants 1–4 m thick as far downstream as the gorge of Mageik Creek. Along West Fork of Rainbow River, unit includes till, terrace gravels, and inset remnants as thick as 3 m of hyperconcentrated sandflow deposits consisting of 1912 rhyolitic fallout (Layer A) remobilized by the river. At Katmai Bay, unit includes beach deposits and sandbars. At lower end of Valley of Ten Thousand Smokes, unit includes aeolian dune deposits concentrated by winnowing of 1912 pyroclastic material

gp **Glacial deposits (late Pleistocene)**—Mostly unconsolidated till. Contacts approximate. Many discontinuous deposits and veneers are omitted. Patches of till cropping out complexly together with talus and thick colluvium are lumped in surficial unit s, above. (For speculative subdivision of glacial deposits, based largely on interpretation of aerial photographs, see Riehle and Detterman (1993))

MOUNT GRIGGS

[Stratovolcano 12 km behind main volcanic line; see Hildreth and others, 2002]

gyi **Andesite of innermost crater (late or middle Holocene)**—Ejecta cone rimming the inner of two craters nested inside the summit amphitheater, and a derivative multilobate lava-flow tongue (57–60% SiO_2) that overlies the more extensive lava-flow apron of unit gyo on the southwest slope of the volcano. Lava flows as thick as 30 m distally, much thinner proximally. Exposed crater-rim ejecta (black stipple) at least 10 m thick, possibly much thicker; scoria falls subordinate to agglutinated spatter and thin spatter-fed flows. Near-vent products are extensively oxidized. Several active fumarole clusters have solfatarically altered parts of the crater and proximal parts of the lava apron

gyo **Andesite of inner cone (late or middle Holocene)**—Postglacial andesitic lava flows (55–62% SiO_2) that issued at a reactivated central vent within summit amphitheater, now marked by an ejecta cone (black stipple) rimming the outer of two nested craters inside the amphitheater. Ejecta are largely agglutinated spatter but include scoria falls and poorly sorted ashy deposits rich in angular blocks of glassy andesite, some prismatically jointed. At least 20 lava flows, many with levees, refilled much of the collapsed southwest sector of the cone, some reaching the floor of Knife Creek. Although heavily mantled by Novarupta fallout of 1912, unit gyo lavas are scarcely eroded, except locally by an active glacier that spills out of the amphitheater moat and down the south-southwest flank

gda **Younger debris-avalanche deposits (early Holocene)**—Two separate valley-confined debris-avalanche deposits derived from glacially oversteepened headwalls high on north side of main cone. Each descended 2 km over glacial ice before entering stream valleys north and west of the cone. Both deposits locally overlie till of late Pleistocene or early Holocene age. Deposit to **north** is 10 to 30 m thick on both sides of a tributary of Ikagluik Creek. Consists of abundant blocks of fresh and acid-altered andesite in an orange-brown or varicolored, poorly sorted clay-bearing matrix. Levees survive medially, and distal expanse is marked by hummocks of shattered andesite as high as 3 m. Overlain by 10–40 cm of aeolian silty soil, which contains ash layers as old as 6.5 ka (Fierstein and Hildreth, in press). Probably emplaced about 7 ka (Hildreth and others, 2002). Deposit to **west** is as thick as 50 m along Juhle Fork of Knife Creek; it consists of contrasting domains of orange-brown, yellow-ochre, and brick-red, poorly sorted matrix rich in blocks as large as 8 m of shattered andesite, both fresh and acid altered. Hummocks are few but as high as 10 m medially. Flowing mass overspilled its left bank distally, where the deposit thus overlaps unit gdo. Probably emplaced about 8.5 ka (Hildreth and others, 2002)

gde **Debris-flow deposit of northeast flank (early Holocene or latest Pleistocene)**—Diamict, 4–12 m thick, that crops out for 400 m along rim of gorge tributary to Ikagluik Creek canyon at northeast toe of the volcano; sandwiched between basement rocks and 12 m of gray till. Poorly sorted, clay-bearing, orange-brown to cream-yellow matrix encloses blocks of fresh and acid-altered andesite as big as 1.5 m. Older (by at least one modest advance of local glaciers) than nearby unit gda, which probably shares a similar altered source area high on northeast side of cone

gdo **Knife Peak debris-avalanche deposit (early Holocene or latest Pleistocene)**—Major debris-avalanche deposit of west flank of Mount Griggs, derived by sector collapse that formed the summit amphitheater. Apparently deposited while a valley glacier still occupied adjacent Knife Creek.

Valley-floor deposits have largely been removed, but remnants survive on Broken Mountain, the northern nose of Baked Mountain, and at several places (too small to show) downvalley near Three Forks. Main surviving mass, as thick as 200 m, forms the 5-km^2 unglaciated western planèze of Mount Griggs, where it overlies both unit gmd and a lava flow of unit gma dated at 21±11 ka. Consists of a chaotic matrix-rich blocky assemblage of varicolored, hydrothermally altered domains and relatively fresh domains, including some 100-m-scale slabs of disrupted sets of andesitic lava flows. Deposit is overlapped by adjacent debris-avalanche unit gda (8.5 ka) along the lower Juhle Fork of Knife Creek and by postglacial lavas of unit gyo

gmd **Dacite of west flank (early Holocene or latest Pleistocene)**—Convolutely flow-foliated dacitic lava flow (63.0–63.4% SiO_2) exposed along canyon draining west flank of Mount Griggs. Phenocryst-rich glassy lava is at least 50 m thick, though much of it is concealed by screes of 1912 pumice. Unit is apparently inset against nearby window of andesitic lava flows (unit gma) dated at 21±11 ka; farther down canyon, it overlies a ledge of similar andesitic lava. Surface of the gray-weathering dacite lava flow is moderately scoured, either by ice or by passage of the adjacent debris avalanche (unit gdo), part of which overlies the upper end of the dacite exposure. Apparently one of the last eruptive units of the outer cone before sector collapse, this dacite also represents the most evolved material known to have erupted at Mount Griggs. (Attempts to date the young dacite by K-Ar repeatedly failed)

gds **Diamict of Griggs Fork (late Pleistocene)**—Massive coarse diamict 25–70 m thick at southern base of Mount Griggs. Gray-brown, sandy-gravelly matrix is fines-poor; encloses abundant angular to subangular blocks (as big as 3 m) of varied andesite, only a trivial fraction of them acid-altered. Although it rests on heterolithologic till rich in clasts of basement rocks, the glacially scoured diamict itself virtually lacks such clasts and consists almost entirely of andesitic material. There being no evidence for hot emplacement, hydrothermally altered source material, a source-area scar, or basement-rock clasts, the rubbly unstratified deposit is likely to have originated by abrupt failure of an older set of lava flows high on the edifice and dipslope emplacement as a single chaotic avalanche sheet (Hildreth and others, 2002). Unit is overlain by sintered valley-filling scoria-flow deposit erupted at Mount Katmai (unit ksf)

gma **Andesite of the outer cone (late Pleistocene)**—Andesitic lava flows (55–63% SiO_2) of main cone of Mount Griggs that predate formation of summit amphitheater by collapse of the western sector. Dozens of lava flows built a smooth late Pleistocene stratocone that concealed most remnants of the glacially ravaged middle Pleistocene edifice (unit goa). Glacial erosion of unit gma lava flows is light or nil on steep upper slopes of cone, increases downslope, and is severe in canyons around the base. Intracanyon dacite lava tongue 150 m thick at east base of cone yields an age of 90±7 ka. Lowest flow at northeast base yields 54±8 ka. Top lava flow of west-southwest window (elevation 3,400 ft) yields 21±11 ka. Lowest flow exposed where glacially eroded lavas overlap Tertiary intrusive rocks 4-5 km north-northwest of summit yields 15±18 ka

goa **Andesite windows of early edifice (middle Pleistocene)**—Older andesitic lava flows (55–62% SiO_2) of severely dissected middle Pleistocene edifice, draped by present-day stratovolcano. Exposed in only three areas, at northern and southern toes of the volcano and high on its west shoulder. Basal lava flow at northern extremity yields age of 292±11 ka. Craggy lava-flow remnant that caps west buttress yields 160±8 ka. Top flow of southern window yields 133±25 ka. Exposures are insufficient to determine whether these three episodes represent discrete growth intervals or merely partial glimpses of an eruptive history more continuous

ALAGOGSHAK VOLCANO

[Severely eroded stratovolcano; see Hildreth and others, 1999]

aac **Alagogshak Creek flow (late Pleistocene)**—Single andesite lava flow (60–61% SiO_2) that extends 6 km southeastward from 50-m-high knob (probable remnant of a flank-vent dome) 1 km east of summit. Broadens downslope into plateau-forming lobe and thickens to 100 m at eroded terminus in headwaters of Alagogshak Creek. Lava yields K-Ar age of 43±8 ka acr **Proximal andesitic ejecta (late or middle Pleistocene)**—Radially dipping layers of coarse scoria (57–58% SiO_2), agglutinate, and poorly sorted phreatomagmatic breccia that form remains of rim and walls of central crater. Variably altered hydrothermally

aef **Andesite of east fork of Kejulik River (late and middle Pleistocene)**—Stack of at least seven lava flows (57–63% SiO_2), each 5 to 25 m thick, that dip south into headwaters of east fork of Kejulik River. Platy internal zones and thin flow breccias dominate exposures; columnar jointing is uncommon. Glaciated remnants downstream show that sequence was far more extensive and as thick as 250 m. Top flow in stack yields K-Ar age of 104±10 ka

ady **Dacite east of middle fork of Angle Creek (late and middle Pleistocene)**—Package of at least six dacite and andesite lava flows (58–64.5% SiO_2) that extend from crater rim northward to east wall of middle fork of Angle Creek. Base of stack is 90 m lower than older set of flows (unit aan) facing it on west wall. Some glassy columnar flows as thick as 200 m were probably erupted englacially. Still extensively covered by ice and till

akc **Andesite of Kejulik Cleaver (middle Pleistocene)**—Stack of about 20 andesite-dacite lava flows (58–66% SiO_2), each 8 to 40 m thick, that dip gently south along divide east of main fork of Kejulik River and its source glacier. Three of the lavas extend south into a sinuous tongue of interfluve-capping flows, two of which yielded K-Ar ages of 394±46 ka and 389±71 ka. Distal one kilometer of this tongue is a single lava flow, as thick as 100 m, possibly emplaced along a glacier margin (Lescinsky and Sisson, 1998)

aan **Andesite of Angle Creek (middle Pleistocene)**—Stack of at least four north-dipping andesite lava flows (59–63% SiO_2), each 50–125 m thick, that cap ridge between west and middle forks of Angle Creek. Slender glassy columns in sets of highly varied orientation pervade some flows, suggesting ice-contact emplacement. Basal flow in gorge of middle fork yields K-Ar age of 680±20 ka

aon **Andesite of northern outliers (middle Pleistocene)**—Three shingled andesite lava flows (57–61% SiO_2), each more than 100 m thick, that cap ridge west of the west fork of Angle Creek; and a single 100-m-thick flow (58% SiO_2) that overlies basalts of unit aob on Crag 4281 of the middle outlier. All four flows dip gently northwest and are compositionally similar to typical Alagogshak lavas. Thick flow-breccia and glassy columnar zones suggest ice-contact emplacement

aob **Basalt of middle outlier (middle Pleistocene)**—Three mafic lava flows and a thick breccia zone (51–53% SiO_2) that cap much of the middle outlier, on divide between Angle and Takayofo Creeks. Rich in clinopyroxene and plagioclase phenocrysts, each commonly as big as 3 mm

aos **Andesite of southern outlier (middle or early Pleistocene)**—Single andesite lava remnant (62–63% SiO_2) as thick as 200 m that caps Peak 4647 on divide between Takayofo Creek and Kejulik River. Poorer in K_2O than typical Alagogshak lavas; source uncertain

aow **Andesite of westernmost outlier (early Pleistocene)**—Remnants of a single phenocryst-rich, 200-m-thick lava flow (61–62% SiO_2) capping the west-trending ridge separating forks of Takayofo Creek. Poorer in K_2O than typical Alagogshak lavas. K-Ar age 954±109 ka

MOUNT MARTIN

[Small Holocene composite cone; see Hildreth and others, 1999, 2000]

rac **Proximal andesitic ejecta (Holocene)**—Scoria, agglutinate, and phreatomagmatic breccia (59–61% SiO_2) that form rim, outer slopes, and part of inner walls of a small composite cone that overlies and interfingers with effusive lava flows (unit rdl) at their source. Cone ejecta are variably altered, in part by active fumaroles on floor and walls of 300-m-wide crater

rdl **Dacite and andesite lava flows (Holocene)**—Stairstep apron of at least 10 superimposed flow lobes (60–64% SiO_2), each 70-100 m thick, extending 10 km north and northwest of the crater toward Angle Creek. Topmost flow distally is overlain by soil and tephra layers as old as 6 ka. Modest erosion by existing glaciers is limited to cone and upper apron. Glaciated lava flows adjacent to west side of Mount Martin are distinguished stratigraphically and chemically as having erupted at Alagogshak volcano

MOUNT MAGEIK

[Four overlapping stratocones of different ages; see Hildreth and others, 2000]

mda1, mda2, mda3 **Debris-avalanche deposits (Holocene)**—Three hummocky valley-filling deposits of different ages, derived from the south and southeast sides of Mount Mageik. The westernmost (unit mda1) is oldest, largest, and (alone of the three) clay-rich, having originated by failure of hydrothermally altered rocks of Southwest Summit subedifice on steep headwall of Martin Creek. As thick as 70 m proximally and extending at least 16 km downvalley, the deposit covered an area greater than 15 km^2 and had a volume of about 0.35 km^3. Base of organics-bearing soil atop the deposit gives a limiting radiocarbon age of 3,130±170 ^{14}C yr B.P. The easternmost deposit (unit mda2, in the Observation Mountain fork of Martin Creek) consists of fresh andesitic rubble, apparently monolithologic, that may have broken loose from a lava flow emplaced on steep ice, probably in the middle Holocene. Abutting older unit mda1, the hummocky deposit is 15–25 m thick distally, covers 2.7 km^2, and has a volume of roughly 0.025 km^3. The central deposit (unit mda3), called the "Mageik Landslide" by Griggs (1920, 1922), consists mostly of angular blocks of fresh dacite that broke loose from a stack of lava flows low on the flank of the Southwest Summit subedifice on June 6-7, 1912, evidently triggered by seismicity accompanying caldera collapse at Mount Katmai. Leaving behind a scarp 120 m high, the deposit extends 6 km downvalley, is 5–30 m thick, covers 6 km^2, supports hummocks as high as 20 m, and represents a volume in the range 0.05 to 0.1 km^3

mse **Andesite-dacite lava flows and proximal ejecta of East Summit (Holocene)**—Eruptive products (60–64% SiO_2) that make up East Summit subedifice and eastern slopes of the mountain. Coarse scoriae and densely glassy phreatomagmatic ejecta that ring the 250-m-wide ice-filled crater are largely unaltered. At least 12 postglacial lava flows descend toward Katmai Pass and Mageik Creek, forming leveed tongues, stairstep benches, and piedmont lava lobes, each 50–150 m thick distally. An andesitic block-and-ash flow deposit (not shown on map) less than 3 m thick is exposed locally atop the northern lobe of unit meo. Surfaces of distal lava lobes (below existing glacier fronts) are blocky, glassy, and scarcely eroded. Although none are directly dated, differences in accumulation of aeolian silt, soil development, gully incision, and retention of primary surface roughness suggest that the dozen flows represent at least three periods of activity

meo **Older andesite-dacite lava flows of East Summit (Holocene or latest Pleistocene)**—Two easterly flows that form sprawling piedmont lava lobes (60–64% SiO_2) adjacent to Mageik Creek, each more than 100 m thick. Oldest lava flows from the East Summit vent; although not obviously ice-scoured, their surfaces are more degraded than those of overlying lava flows. Base of organics-bearing aeolian silt accumulation atop south lobe gives limiting radiocarbon age of 3,900±170 ^{14}C yr B.P.

msn **Andesite-dacite lava flows of North Summit (Holocene and late Pleistocene)**—Eruptive products (60–64% SiO_2) that make up North Summit subedifice (Peak 6600) and much of north slope of the mountain. About ten lava flows, each 25 to 75 m thick medially, dip northward, and a few thicken downslope to 100 or even 200 m, where some were probably impounded by thick glacial ice. Eroded termini at the north foot of Mount Mageik support high cliffs, precipitous waterfalls, and some of the most spectacular scenery in the district. Most of the lava flows were glacially eroded in the late Pleistocene, but the ejecta ring of the ice-filled summit crater and an adjacent stubby lava lobe are little modified and may be early Holocene. Crater-rim ejecta are intensely altered fumarolically. Basal lava flow resting on Jurassic basement rocks (unit bu) near West Mageik Lake yields a K-Ar age of 59±11 ka

msc **Andesite-dacite lava flows and vent dome of Central Summit (late Pleistocene)**—Eruptive products (58–66% SiO_2) that make up the Central Summit subedifice including the true summit (Peak 7100) and parts of the northwestern and southeastern sectors of the mountain. Several lava flows are exposed in windows through ice and on cleavers and benches on the southeastern slope, where the basal lava flow gave a K-Ar age of 71±11 ka. A phreatic crater, fumarolically active and floored by an acid lake 125 m wide (Hildreth and others, 2000), was reamed through the northeast margin of the ice-mantled summit dome by a nonmagmatic explosive event in the late Holocene, exposing a 100-m-high wall of massive dacite. Excavation of the crater may have been related thermally to the plumbing system beneath the younger East Summit crater nearby

msw **Andesite-dacite lava flows of the Southwest Summit (late Pleistocene)**—Eruptive products (57–68% SiO_2) that make up the Southwest Summit subedifice, including much of the western and southern parts of the mountain. Oldest and most voluminous component of Mount Mageik, it is also compositionally different in having lavas richer in K and Zr than other subedifices (Hildreth and others, 2000). The vent area is an ice-covered mound (Peak 6900), which limited marginal exposure suggests is a fragmental cone rather than a dome. The cirque headwall on the southwest margin of the mound provides the largest exposure of hydrothermally altered rock on Mount Mageik, source of the clay-rich debris-avalanche deposit, unit mda1, in Martin Creek. Stacks of 6-8 lava flows exposed through the ice in several sectors are 300-600 m thick and include individual flows as thick as 200 m, almost certainly erupted against ice. Remnants of an ice-marginal flow, one of the least silicic lavas at Mount Mageik (57% SiO_2), extend northwestward toward Angle Creek, where the eroded terminus is 150 m thick. Basal lava flows in two southerly sectors gave K-Ar ages of 93±8 ka and 89±8 ka (Hildreth and others, 2000)

TRIDENT VOLCANO

[Cluster of four stratocones and several lava domes; see Hildreth and others, in press]

tsw **Andesite-dacite lava flows and cratered ejecta cone of Southwest Trident (1953-1974)**—Eruptive products (57–65% SiO_2) emplaced sporadically between 1953 and 1974, building the Southwest Trident edifice from scratch. Four blocky lava flows, each 25–60 m thick, effused in 1953, 1957, 1958, and 1959-60, as indicated on map. The coarsely fragmental vent cone (black stipple) is topped by a shallow crater 350 m wide and consists of block-and-ash deposits, scoria, agglutinate, stubby lava lobes, and the intercalated proximal parts of the main lava flows. Patchy remnants of an eruption-opening (February 1953) layer of coarse andesitic ashfall (Snyder, 1954) are preserved only locally, as far as 10 km northeast of the vent. A scattering of ballistic blocks (breadcrusted, densely vitrophyric, or pumiceous), extends radially as far as 3 km from vent; many were expelled during repeated plug blowouts during waning activity after 1960. Dark-gray bouldery debris flows reworked from pyroclastic deposits on and below the rubbly cone form a proximal fan and medial sheets (1–4 m thick) that cap stream terraces along northern fork of Mageik Creek (see surficial unit s); lesser veneers (not shown) cap the interfluve of 1912 ignimbrite (unit nig) between forks and extend as terrace remnants as far as 2 km down the southern (main) fork of Mageik Creek

tig **Dacite ignimbrite of Mageik Creek (late Pleistocene)**—Nonwelded dacitic ignimbrite remnant on south wall of upper end of Mageik Creek gorge, due south of Trident I (Peak 6115). Single greenish-gray massive outcrop, 7 m thick and 35 m long, rests on Jurassic basement rocks a few meters above stream level. Lithic-poor tuff is rich in small pumice clasts 1–5 cm, has median grainsize of 1.3 mm, and its sandy matrix is relatively poor in fine ash. Predominant greenish-gray to black pumice is dacitic (63–64% SiO_2) but subordinate white pumice is rhyodacitic (70–71% SiO_2). Compositional affinity of all pumice types is clearly with the Trident group (low K, Zr), not with Mount Mageik or Mount Katmai, but composition fails to distinguish among Trident I, West Trident, or Trident domes (unit tdd) as likely source of these pumiceous pyroclastic flows. Overlain directly by a few meters of till, which is in turn capped only by 1912 deposits, from which we infer that the ignimbrite was emplaced very late in the Pleistocene. Because the ash flows were funnelled along the gorge at a level 30 m lower than the base of pyroclastic-flow unit tpf, unit tig is probably younger

tpf **Lithic pyroclastic-flow deposit of Mageik Creek (late Pleistocene)**—Block-and-ash flow deposit preserved as inset remnants in four alcoves high on north wall of Mageik Creek gorge at toe of Trident I (Peak 6115). Gray sandy matrix encloses black to medium-gray, dense glassy juvenile clasts as big as 50 cm (but mostly 1–10 cm), as well as abundant nonjuvenile (lithologically varied) andesitic clasts. Disregarding clasts coarser than 16 mm, sieve analysis shows the matrix to have a median grainsize of 5 mm and to have only 1.5 wt % finer than 63 microns.

Four main remnants are 10–30 m thick but eroded away between alcoves. Deposit in alcove farthest downstream is coarsest, thickest, consists of several flow units, and may represent more than one eruptive event. All four are overlain by fluvial gravel and till, probably of the Last Glacial Maximum; all rest on Jurassic basement rocks or on fluvial sediments that overlie the basement rocks. Deposit is cut by several clastic dikes, possibly induced by the stress of overriding ice. Twelve glassy clasts analyzed extend from 57.6–71.8% SiO_2, a strikingly wide range of composition that constitutes a notable anomaly, as no other sample from the Trident group has given more than 65.5% SiO_2. Nonetheless, the compositional affinity of all blocks analyzed is clearly with the Trident group (low K, Zr), not with Mount Mageik or Mount Katmai, but composition does not distinguish among Trident I, West Trident, or Trident domes as the source of the pyroclastic flows. Another block-and-ash flow deposit (not shown on map) minimally exposed 1.5 km north, in a gulch cut through thick 1912 fallout, is andesitic (61.4% SiO_2) and probably derived from a summit eruption of Trident I (Hildreth and others, in press)

twt **Andesite-dacite lava flows of West Trident (late Pleistocene)**—Eruptive products (58–65% SiO_2) of West Trident volcano (Peak 5605), youngest prehistoric edifice of the Trident group. Several radial ridges are glacially sharpened coulees or sets of a few lava flows, some of which bank against Trident I and Falling Mountain. A thick silicic andesite lava flow that caps the north ridge yields an age of 44±10 ka. A younger andesite more than 125 m thick that caps the summit (and may be a dome remnant) failed to yield measurable radiogenic argon. Most lavas are rich in enclaves (1–20 cm) of phenocryst-poor mafic andesite (54–58% SiO_2). All lavas are mantled and largely concealed by Novarupta pyroclastic deposits of 1912; on north apron, the most heavily covered lava flows are outlined by dotted form lines. North ends of some lava flows of West Trident were destroyed during the explosive eruption at Novarupta, providing some of the accidental lithic fragments in 1912 deposits

tfc **Dacite domes of Falling Mountain and Mount Cerberus (late Pleistocene)**—Two large lava domes that flank the entrance to Katmai Pass at the northwest toe of West Trident. Both pyroxene-dacite domes (63–65% SiO_2) have clear compositional affinity (low K, Zr) with the Trident group, not with Novarupta or Mount Mageik. A lava flow from the East Summit subedifice of Mount Mageik banks against Mount Cerberus, and lava flows from the West Trident cone bank against Falling Mountain. The stout massive domes, respectively 425 m and 365 m high, are morphologically little modified by glacial erosion (perhaps owing to their location on the peninsular drainage divide), but each has been stripped of its glassy carapace. Falling Mountain yields a K-Ar age of 70±8 ka and Mount Cerberus 114±46 ka. Northeast face of Falling Mountain was destroyed during the great eruption at Novarupta, providing some of the accidental lithic clasts in 1912 pyroclastic deposits

tdd **Dacite domes at west and south periphery of Trident group (late and middle Pleistocene)**—At least four domes of pyroxene dacite (62–66% SiO_2) around western and southern base of the Trident group. Southwesterly spurs of West Trident may include additional domes, glacially eroded and blanketed with 1912 Novarupta fallout. All domes have clear compositional affinity (low K, Zr) with the Trident group and are lithologically similar to summit domes and thick coulees on West Trident and Trident I. Like West Trident, all domes contain enclaves (1–20 cm) of phenocryst-poor andesite (54–58% SiO_2). None of the domes has been dated, but all are glacially eroded and older than some adjacent lava flows from West Trident and Trident I; their extrusive sequence was probably in part contemporaneous with growth of those composite volcanoes

tca **Mafic pyroclastic complex of Trident I (late and middle Pleistocene)**—Agglutinated spatter and scoria (53–55% SiO_2) forming the southwest flank of Trident I edifice. Steeply dipping sheets of mafic fallout, 0.1 to 3 m thick and rich in accidental lithic fragments, along with subordinate thin pyroclastic-flow deposits, and associated avalanche rubble; derived from central vent of Trident I. Gray-brown to brick-red, widely altered ocherous yellow brown, probably while still warm. Thicker than 100 m, but base not exposed except where it overlaps dome 3900⁺ of unit tdd. Consisting of olivine-rich mafic andesite, the least evolved eruptive product of the whole Trident group, the unit also contains abundant accidental clasts of the pyroxene andesite that makes up most of the edifice

tcs **Andesite-dacite lava flows of Trident I (late and middle Pleistocene)**—Eruptive products (53–63% SiO_2) of central summit edifice (Trident I; Peak 6115). Core of volcano is eviscerated by north-face glacial cirque, on headwall of which about 200 m of coarse andesitic breccia is overlain by a summit-capping dacite lava (150 m thick), which may be a dome remnant. On its southwest side, the summit dacite rests on a coherent andesitic lava flow (61.7% SiO_2) that yields a K-Ar age of 101±12 ka, constraining most of the edifice to be older. Lower on westerly spurs of north face, two comparably massive andesitic lavas (coulees or domes; 60% SiO_2), each 100–200 m thick, are exposed among stacks of thinner lava flows and breccias. South apron of edifice consists of stack of andesitic lava flows (58–62% SiO_2) and subordinate andesitic pyroclastic-flow deposits Severely eroded glacially, the edifice has no postglacial eruptive units, but a vigorous sulfur-depositing fumarole field (illustrated by Griggs, 1922, p. 98) is active on lower southeast flank

teo **Andesite-dacite lava flows and ejecta of East Trident (middle Pleistocene)**—Eruptive products (58–65% SiO_2) of East Trident edifice (Peak 6010), oldest stratocone of the Trident group. Acid-altered core is gutted by five glacial cirques. Radially dipping stacks of 10–25 andesitic lava flows (mostly 8 to 30 m thick), together with flow breccias and stratified ejecta, are exposed on glacier headwalls and on four arêtes. The northeast and southwest ridges are capped by 100-m-thick dacite lava flows (63–65% SiO_2). An andesite lava flow low on the northwest ridge yielded a K-Ar age of 143±8 ka; the dacite capping the northeast ridge gave 142±15 ka. Virtual identity of these ages suggests that activity at this small cone was short-lived, late in the middle Pleistocene. Peak 5700+, central prong of the "trident" as viewed from the southeast (the aspect that inspired the volcano's name; Griggs, 1922, p. 98–99) is not a separate cone but simply the ruggedly eroded southwest flank of the East Trident edifice. Reconstruction suggests that the gutted cone may originally have been 200 m higher, which would probably have made it highest of the Trident summits (Hildreth and others, in press)

MOUNT KATMAI

[Two overlapping stratocones, both cut by caldera of 1912; see Hildreth and Fierstein, 2000]

khi **Dacite lava of Horseshoe Island (1912)**—Crescent-shaped remnant of a small lava dome (66% SiO_2) emplaced (and partly destroyed explosively) on the western floor of Katmai caldera after caldera collapse of June 1912 but before caldera interior was first seen in 1916 (Griggs, 1922; Fenner, 1930, 1950; Hildreth, 1983, 1991). Now wholly concealed by 250 m of lakewater

kls **Katmai Canyon landslide deposit (1912)**—Chaotic slide mass of andesitic blocks and rubble derived from stack of lava flows that form south slope of Mount Katmai and north wall of Katmai Canyon. Slide took place on the night of June 6/7, 1912 during accumulation of Novarupta fallout Layer B, triggered by seismicity accompanying collapse of Katmai caldera (Hildreth, 1991; Abe, 1992). The slide mass impounded a large lake, which was interpreted by Griggs (1922, chapter IX) to have breached catastrophically in 1915

khb **Hydrothermal explosion breccia of Katmai caldera rim (1912)**—Sheet of poorly sorted rubble emplaced on low-relief shelf adjacent to northwest rim of Katmai caldera during caldera collapse. Breccia sheet is as thick as 12 m near the rim but thins to less than 1 m within 250 m outboard. Clasts are angular to subrounded, as big as 1 m, and are mostly hydrothermally altered lavas and tuffs that contain disseminated and veinlet sulfides. Deposit is unconsolidated, poorly sorted, unstratified, and largely clast supported, but its top 2 m grades up through matrix-supported breccia to a capping of blue-gray mud. A widespread correlative mud layer is 20–25 cm thick on the south rim and extends radially as far as 8 km, thinning to a few centimeters at distal remnants. Scattered blocks and correlative muddy diamicts likewise related to collapse are also found on rim shelves in other sectors (see unit kwa), but only the large northwest shelf retains a mappable deposit; most slopes outside the rim are too steep and ice-covered.

Depressurization of the active hydrothermal system inside the Katmai edifice, when displaced along caldera faults, caused explosive ejection of a small fraction of the collapsing mass. Several acid-altered domains are conspicuous on the caldera walls. The breccia (and correlative mud layer) is intercalated within Novarupta fallout Layer B, which accumulated on the night of June 6/7, 1912 (Hildreth, 1991; Hildreth and Fierstein, 1992). Both the Katmai-derived breccia and Novarupta-derived fallout were emplaced atop glaciers beheaded by caldera subsidence; subsequent partial wastage of the ice near the rim has disrupted all but a few intact sections

kds **Dacite lava flows of southeast slope (Holocene)**—Branching set of leveed blocky lava flows (64% SiO_2) that extend downslope as far as 4 km, from a high ice-mantled flank vent to rim of Katmai River canyon. Although overlapped and eroded proximally by present-day glaciers, most of flow surfaces are ruggedly primary, never overrun by ice. High Zr content distinguishes these lavas from all other products of Mount Katmai (Hildreth and Fierstein, 2000)

kwa **Dacite agglutinate of west rim (early Holocene or late Pleistocene)**—Stratified scoria and spatter fall deposit (64–66% SiO_2), with thin scoria flows intercalated locally, that drapes summit of Peak 6128 and the west to southwest rim of Katmai caldera. Deposit is generally 10–25 m thick, but it thickens inward to more than 60 m near top of inner southwest wall of caldera (illustrated by Curtis, 1968, plate 9), where it is evidently a remnant of formerly extensive fill of a precaldera crater obliterated in 1912. Reflecting its origin as pulsatory near-vent welded fallout, sheet is crudely layered. Internal layers are mostly 10–50 cm thick and consist predominantly of scoria lumps, 1–40 cm across, which exhibit highly varied flattening ratios from layer to layer. Layers accordingly range from lightly to densely agglutinated, though basal few meters are unconsolidated on west rim. Bulk deposit is typically dark gray and glassy with black scoriae or fiamme, but is commonly oxidized red brown and partly devitrified. Content of lithic fragments ranges from about 1% to more than 10%, predominantly lithologically varied andesites as big as 25 cm; lithic-rich layers tend to weather out as notches 10–30 cm thick. Major notch along southwest rim (about 8 m below top) that separates unit into two cliffs, however, reflects lithic-poor zone of minimum welding, 2–3 m thick, that consists of glassy scoria lumps, only tack-welded and little deformed. Layering drapes higher topography but on rim is subhorizontal or dips 10° inboard, probably owing to greater differential compaction in former crater-filling accumulation. On southwest wall of caldera, unit overlies stack of lava flows and breccia sheets that dip outboard about 25°W. Along southwest rim, unit is overlain by glacial ablation debris as thick as 7 m, which is being let down on the agglutinate ledge as the beheaded glacier has retreated 50–100 m from rim since the 1912 collapse; muddy matrix of the ablation sheet encloses mixture of pre-1912 glacial rubble, 1912 pumice blocks, and lithic blocks expelled explosively from Mount Katmai during caldera collapse (see unit khb)

ksf **Dacite scoria flow deposit of Knife Creek (early Holocene or late Pleistocene)**—Three glacially eroded remnants of a once-extensive pyroclastic-flow deposit banked against southern foot of Mount Griggs in upper Knife Creek. Dark-gray, lithic-poor, crystal-rich, coarse-ash matrix encloses abundant black scoria lapilli, mostly 1–2 cm, rarely as big as 6 cm; matrix sintered but scoriae not flattened. Several vague flow units, 0.2 to 1 m thick, are defined by slight variations in clast concentration. Deposit is as thick as 10 m but generally 4–6 m; it pinches out upslope atop subjacent diamict (unit gds) at base of Mount Griggs. Overlain by bouldery andesitic rubble, 1–8 m thick, probably deflated till. Compositional affinity is with Mount Katmai, not Mount Griggs; predominant dacite scoria clasts (64–65% SiO_2; one gave 59.5% SiO_2) are compositionally similar to those in unit kwa

krs **Pyroxene-rhyodacite lava flows capping south rim (early Holocene or late Pleistocene)**—Plagioclase-rich glassy lava flows (68–69% SiO_2), black or locally brick red, including extensive breccia zones and abundant andesitic enclaves (54–59% SiO_2). At least four flows, each 25–60 m thick, form south and southeast rim of caldera. Erosional outlier west of south rim notch forms 40-m-high crag illustrated by Griggs (1922, p. 100, 175) and Curtis (1968, plate 9). Vents were on foundered superstructure destroyed by caldera collapse of 1912, which beheaded the flows, leaving their remnants as inward-facing cliffs. Outboard, the flows extend only about 1 km downslope, eroded by present-day glaciers; their limited extent may nonetheless have been a primary feature, as they probably originated as stubby coulees or lobes of summit domes. Undated but stratigraphically higher than nearby unit krh (22.5±1.6 ka)

kzs **Zoned scoria-fall deposit on south rim (early Holocene or late Pleistocene)**—Stratified remnant of proximal scoria fall (57–66% SiO_2), at least 40 m thick, on south rim of caldera; contains pumice and scoria bombs as big as 40 cm. Lower 30 m is lightly to densely agglutinated dacite fallout (largely oxidized orange but having an 8-m-thick gray eutaxite in the middle). Upper 10 m is stratified andesitic scoria fall, partly unconsolidated and partly agglutinated, that grades upward from black to brick red. Dacite-andesite transition is abrupt but conformable. Deposit contains abundant lithic clasts, including blocks as large as 25 cm of the subjacent rhyolite lava (unit krh). Fall unit is sandwiched between rhyodacitic breccia associated with lavas of unit krs, above, and rhyolitic lava unit krh (22.5±1.6 ka), below. Dacite pumice is compositionally similar to that in Lethe assemblage (unit kla)

kla **Lethe assemblage (early Holocene or late Pleistocene)**—Fines-poor pumiceous debris flows and hyperconcentrated sandflow deposits exposed in lower River Lethe, lower Windy Creek, and nearby marshy basin south of Overlook Knoll (Pinney and Beget, 1991; Hildreth and others, 2000). About 10 debris-flow units 0.1–4 m thick are rich in dacite (63–66.5% SiO_2) pumice clasts as big as 40 cm. Their sandy matrix is continuous with interstratified massive beds of coarse (phenocryst) sand as thick as 10 m. Sand beds are predominantly plagioclase, pyroxene, and magnetite crystals identical to phenocrysts in the pumice; they display ubiquitous water-escape (dish) structures. Pumice-rich flow units are broadly lenticular, but there is no significant unconformity or intercalation of normal alluvial gravel within the assemblage, suggesting rapid emplacement in the aftermath of a single eruptive event. The assemblage is as thick as 25 to 30 m on gorge walls where the base is not exposed. Compositional data suggest a source at Mount Katmai and, in particular, a close similarity to dacite fallout of unit kzs. Ejecta were probably remobilized syneruptively by snowmelt on ice-covered slopes of source edifice, emplaced over a valley glacier, and ponded in an ice-marginal lowland depression. Assemblage is widely overlain by a few meters of early Holocene till (Fierstein and Hildreth, in press) and, where its base is exposed, it rests on latest Pleistocene till. Reger and others (1996) suggest correlation with an ashfall layer in the Kenai Lowland (350 km northeast; fig. 1, inset) for which they infer an age younger than 16,000 ^{14}C yr B.P.

krh **Hornblende-bearing rhyolite lava flow of south rim notch (late Pleistocene)**—Pale-gray to pinkish-gray, strongly flow foliated lava flow (72% SiO_2), 30–50 m thick and rich in plagioclase and orthopyroxene. Mafic enclaves are rare (in contrast to silicic lavas of nearby unit krs); but unit does contain sparse andesitic blebs as big as 1 cm. The most silicic unit at Mount Katmai, and the only lava there known to contain amphibole. May be related to compositionally similar plinian pumice-fall and ignimbrite deposits (unit krp) along Windy and Mageik Creeks. Lava overlies stack of thin andesite lava flows with prominent breccia zones that make up much of south wall of caldera. Overlain by agglutinated fall unit kzs. Rhyolite lava yields $^{40}Ar/^{39}Ar$ age of 22.5±1.6 ka

krp **Plinian pumice-fall and ignimbrite deposits of hornblende-bearing rhyodacite (late Pleistocene)**—Lithic-rich stratified pumice-fall deposits 7 m and 5 m thick along Mageik and Windy Creeks are overlain directly by nonwelded ignimbrite at least 75 m and 8 m thick, respectively. Pumice clasts, mostly white but some medium gray, have 72% SiO_2, irrespective of color, in all emplacement units. Lithic clasts range from basalt to rhyodacite. Pumice contains 8–12% phenocrysts of plagioclase, orthopyroxene, hornblende, and FeTi oxides. Organic material at base in Mageik Creek gave an age of 19,240±70 ^{14}C yr B.P., equivalent to a calibrated calendar age of 22.8 ka, which is comparable to the $^{40}Ar/^{39}Ar$ age (22.5±1.6 ka) of the compositionally similar hornblende-bearing lava (unit krh) on south rim of Katmai caldera. Survival of so few remnants of thick deposits of an unequivocally great eruption suggests that emplacement was largely over ice. Overlies fluvial gravel and laminated mud in Mageik Creek; in Windy Creek, base is below stream level, thus not exposed. At both locations, the pyroclastic deposits are cut by clastic dikes, possibly induced by the stress of overriding ice, and are overlain by till and fluvial gravel

ks **Andesite-to-rhyodacite lavas and pyroclastic deposits of Southwest Katmai (late Pleistocene)**—Eruptive products that make up the Southwest Katmai subedifice (51–72% SiO_2). Radially dipping stacks of andesite-dacite lava flows dominate caldera walls and outside slopes. Lava-flow breccia zones are an important component of the inner south wall, and thick chaotic breccia (possibly old crater fill) of the inner west wall. Lavas and breccias of the west wall are mostly hydrothermally altered; difficult of access and not sampled, they could include material of mafic composition. Mafic products (51–55% SiO_2) were actually sampled on this subedifice only as enclaves in more silicic host lavas and as blocks explosively emplaced on caldera rim during collapse. Younger dacitic and rhyodacitic units accessible on west and south rims (mapped separately and described above) extend activity of this subedifice into the Holocene. Dacite agglutinate sheet (unit kwa) drapes west rim and forms 60-m-high cliff on inner southwest rim, apparently thickening into an older crater destroyed in 1912.

Just west of caldera, a dacite lava flow at base of 350-m stack of flows exposed on north face of Peak 6128 yields K-Ar age of 47±13 ka. At south foot of Mount Katmai near mouth of Katmai River canyon, an andesite lava flow resting on Jurassic basement (unit bu) yields 39±12 ka. South-rim rhyolite (unit krh) yields $^{40}Ar/^{39}Ar$ age of 22.5±1.6 ka. Latest eruption was dacite lava of Horseshoe Island (unit khi) on floor of 1912 caldera, directly below former summit. Although Southwest Katmai cone is thus largely younger than adjacent Northeast Katmai, exposures on inner northwest wall show that its earliest products underlie some later products (unit kn) of the companion cone. Cream-white layer 25–40 m thick just below rim of northwest salient of caldera wall is acid-altered (pyrite-bearing) lava flow, perhaps originally silicic, overlain by 30 m of plane-stratified ashy sediment that accumulated in a paleodepression. Sediment marks transition between lava sequence from Southwest Katmai on lower wall and thick andesite lava flows from Northeast Katmai that make up till-mantled benches and buttresses on northwest rim of caldera

kn **Andesite-dacite lava flows and pyroclastic deposits of Northeast Katmai (late Pleistocene)**—Eruptive products (57–66% SiO_2) that make up younger, glacially sculptured parts of Northeast Katmai subedifice that unconformably drape the older mafic cone (unit kbn). North Ridge is great north-dipping set of dacite lava flows (65–66% SiO_2), several thicker than 30 m. Just west, Horn 6250 and crags and buttresses along northwest caldera rim are capped by a north-northwest-dipping stack of andesite-dacite lava flows (58–66% SiO_2), thick and thin (5–50 m), with intercalated breccia sheets. Discrete package of andesite lava flows (59–61% SiO_2) east of caldera is banked steeply along paleocanyon against the mafic cone. On northeast spur, lowest andesite lava flow (59.7% SiO_2), which directly overlies products of the mafic cone, yields K-Ar age of 70±13 ka. As no evidence exists for postglacial activity of the Northeast Katmai subedifice, the andesite-dacite sequence is probably entirely late Pleistocene; in part contemporaneous with early activity of adjacent Southwest Katmai subedifice

kbn **Basaltic and andesitic lava flows and pyroclastic deposits of Northeast Katmai (late Pleistocene)**—Predominantly mafic (52–56% SiO_2) composite cone exposed on inner east and north walls of caldera and forming true summit (Peak 6715) as well as steep outer northeast slope of cone and east planèze. Oldest exposed component of Mount Katmai. Summit crags and eastern slopes consist of outward-dipping stacks of thin mafic lavas, agglutinate, and scoria, emplaced in many shallowly unconformable packages and cut by numerous near-vertical dikes (some shown in magenta) presumed radial to a summit vent complex destroyed in 1912. Packages include intercalated oxidized scoria falls as thick as 10 m, well exposed on the outer northeast slope. Sheets of very coarse, crudely stratified phreatomagmatic breccia and chaotic block-and-ash deposits, widely altered palagonitically (golden orange) or hydrothermally (buff to cream white), interfinger with the lavas on the east caldera wall and near the east rim notch. Lower parts of the mafic section exposed on the inner north and east walls appear quite altered hydrothermally. South-dipping strata of the mafic cone are overlain by southeast-dipping lavas of Southwest Katmai subedifice (unit ks) on the southeast wall of the caldera. Products of the mafic cone are overlain unconformably on the north wall, north ridge, east planèze, and northeast spur by radially dipping andesite-dacite lava flows of unit kn. Oldest andesite overlying the toe of unit kbn lavas low on northeast spur gave K-Ar age of 70±13 ka, showing that the mafic cone is older still

SNOWY MOUNTAIN

[Two contiguous cones; see Hildreth and others, 2001]

snd **Dacite lava dome (late Holocene)**—Fresh glassy dome (63% SiO_2), 700-by-1,400 m across, extruded within summit amphitheater of Northeast Snowy Mountain edifice subsequent to sector collapse. Blocky vitrophyric dome has two or three stubby exogenous lobes, 250–500 m relief, and (though it is scarcely eroded) a small icecap. Consists of plagioclase-rich pyroxene dacite that, uniquely among products of Snowy Mountain, also has a trace of hornblende

sdr **Rainbow River debris-avalanche deposit (late Holocene)**—Hummocky orange-brown sheet consists of poorly sorted, matrix-rich andesitic rubble, much of it hydrothermally altered, emplaced by sector collapse of the Northeast Snowy Mountain edifice. Deposit is preserved for 14 km north of the resulting amphitheater and still covers 17 km^2, despite vigorous erosion by Rainbow River; overran glaciers and bedrock ridges in its path and originally covered at least 30 km^2. As thick as 40-50 m at numerous large hummocks and ridges, sheet generally thins from 40 m medially to 20 m distally. Proximal part (subunit sdr′) was overrun, then re-exposed, by advance and retreat of glaciers during the Little Ice Age. Radiocarbon ages for overlying material suggest emplacement less than 1,500 years ago (Hildreth and others, 2001)

sne **Andesite and dacite of Northeast Snowy Mountain (late and middle Pleistocene)**—Eruptive products (61–64% SiO_2) that built the Northeast Snowy Mountain edifice, prior to late Holocene sector collapse that produced the 1.5-km^2 amphitheater. Steeply dipping radial stacks of proximal lavas marked by thick flow-breccia zones are altered hydrothermally where exposed on walls of the amphitheater. Glacial erosion on the flanks has been severe. Surviving lavas downslope to the north thicken distally into a set of bench-forming flows, each 100–200 m thick. Second flow of northern stack yields an age of 171±8 ka. Near-summit fumaroles were reported during 1980s but not found in 1998-99. Edifice has been active only sporadically, from later part of middle Pleistocene to Holocene

ssw **Andesite of Southwest Snowy Mountain (late and middle Pleistocene)**—Eruptive products (55–62% SiO_2) that make up the Southwest Snowy Mountain edifice. Glacial cover and erosion are more severe than on the companion edifice. Stacks of three to six lava flows are exposed on and northwest of the summit (Peak 6770), a few of them thickening downslope to more than 100 m. On the south slope, windows through the ice reveal only one or two flows. Vent complex exposed on cliff-bounded ridge just south of summit is chaotic breccia rich in scoriaceous and dense blocks, cut by dikes and a steeply jointed intrusion 300 m wide. Top lava flow on summit gave a K-Ar age of 196±8 ka, and basal lava flow 3.3 km northwest of summit yielded 199±9 ka. Another basal lava flow, 5.2 km southeast of summit gave 92±10 ka. Southwest Snowy Mountain edifice was active from late in middle Pleistocene well into late Pleistocene, in part concurrent with the adjacent northeastern edifice, but (unlike its companion) it has long been inactive

MOUNT DENISON

dda **Andesite-dacite lavas of Mount Denison (late and middle? Pleistocene)**-Stack of 12 to 15 lava flows (59–65% SiO_2) at northeast edge of map that make up west toe of Mount Denison volcano, which largely lies east of map area. Includes intercalated agglutinate and scoria falls, a few flows as thick as 100 m, a columnar jointed basal flow that rests on Jurassic basement (unit bu), and an erosional outlier (64.5% SiO_2) west of lower

Serpent Tongue Glacier. Volcanic center remains largely unmapped

RAINBOW RIVER CONE

brr **Basalt of Rainbow River cone (middle Pleistocene)**—Eruptive products of a small basaltic volcano (51.8–53% SiO_2) perched on a basement ridge east of Rainbow River, at northeast edge of map, 17 km north of Snowy Mountain. Glacially sculpted cone, which is 1 km wide and has 330 m relief, consists of radially dipping stacks of thin lavas and breccias intercalated with brick-red and black scoria falls, all well exposed on bounding cliffs, cut by numerous dikes, and gutted by a northerly cirque. Summit crag is supported by a 25-m lava cliff, probably part of a plug capped by agglutinated spatter. An ice-scoured lava-flow plateau extends 1 km southeast from the base of the cone; its dense holocrystalline lava gave an age of 390±39 ka. Lavas and ejecta all contain sparse olivine and plagioclase

PRE-QUATERNARY ROCKS

[Investigated only in reconnaissance or not at all in this study]

QTm **Miscellaneous volcanic rocks (early Quaternary and Pliocene)**—Widely scattered erosional remnants of volcanic rocks, undeformed and relatively fresh, unrelated to the present-day Katmai volcanic cluster. Several andesite-dacite lava-flow remnants (62–63% SiO_2) mapped northeast of Snowy Mountain rest directly on Jurassic basement (unit bu), as do several remnants (60–65% SiO_2) mapped on nunataks in Noisy Glacier east of Mount Katmai; for none of these is a vent recognized. Tertiary volcanic rocks, more extensively altered, probably mostly Miocene but some potentially younger, are also widespread north and south of upper Katmai River (Riehle and others, 1993), but, unmapped and unstudied by us, they are lumped with other basement rocks in unit bu.

Five volcanic remnants northwest of Mount Griggs, all severely glaciated, were given more attention, owing to their locations well behind (northwest of) the main volcanic chain. **(1) Mount Juhle** consists principally of basement granitoid, but its summit is capped by a platy, pale-gray, phenocryst-poor, dacite lava-flow remnant (63% SiO_2), 30–80 m thick, which gives an age of 2.97±0.03 Ma. Its vent has not been found but is likely to be nearby, reduced by glaciation to a dike or conduit fill. **(2) Maynard Crag**, a shallow basaltic intrusion (51.9% SiO_2) standing high on a ridgecrest 2.5 km west of Mount Juhle is a 600-m-wide cylindrical mass with 300 m relief and striking vertical and inclined jointing in several tiers. Rich in coarse olivine and clinopyroxene, the rock lacks plagioclase except in its groundmass. The intrusion yields a K-Ar age of 2.60±0.05 Ma. **(3) Sayre Mesa**, a mafic lava-flow remnant (54.2% SiO_2), 50–80 m thick, rich in olivine and plagioclase phenocrysts forms a 1.3-km-long subhorizontal remnant capping a ridge 4 km northwest of Mount Juhle. Its vent is uncertain but could have been Maynard Crag. Shew and Lanphere (1992) measured a K-Ar age of 2.64±0.04 Ma for plagioclase from the lava. **(4) Fenners Saddlehorn**, a basaltic remnant (51.7% SiO_2) only 250-by-400-m wide but more than 200 m high, is the eponymous horn on the north wall of Saddlehorn Creek. The compact mass has horizontal and inclined columns in about 10 tiers, each tier 5–20 m thick. The rock is fine grained, with abundant 1-mm olivine and subordinate plagioclase microphenocrysts; it is probably intrusive, but joint sets perpendicular to sideslope basement rocks are alternatively consistent with a thick lava-flow remnant banked against a paleocanyon wall, though no fragmental facies is recognized. The horn yields an age of 2.27±0.11 Ma. **(5) Folsoms Bluff**, an andesitic (55–60% SiO_2) funnel-shaped vent complex, is a multi-lobate glassy lava mass 600 m long and 200 m high that protrudes from the canyon wall in upper Saddlehorn Creek. Marked by steep flow foliation and several sets of inclined, subhorizontal, or steeply curving glassy columns suggestive of ice-contact emplacement, the lava has a brecciated base that overlies 8–15 m of stratified, poorly sorted proximal fallout, which includes scoria bombs as big as 75 cm and ejected blocks of basement granitoid as big as 30 cm. The basal fallout drapes a steep paleoslope and extends uphill into a mass of agglutinated lithic-rich rubble at least 20 m thick, probably vent fill largely concealed by the overlying lava. All lithologies contain abundant small plagioclase as well as olivine and clinopyroxene phenocrysts in a chilled glassy groundmass. Its canyon-wall setting and eruptive facies relations suggest that, like Fenners Saddlehorn 2 km downstream, this undated glassy unit should be younger than the three ridge-capping members of the cluster. Copious scree shed by the bluff supports a rock glacier

QTri **Rhyolite ignimbrite of Ikagluik Creek (early Quaternary or Pliocene)**—Undated remnants cap Ikagluik Creek-Griggs Fork divide east of Mount Griggs; source vent unknown. As thick as 100 m, the tuff is nonwelded but indurated by silicification, rich in lithic clasts of andesite and basement rocks, and disintegrates into screes of frost-riven slabs and flakes. Contains abundant plagioclase and quartz phenocrysts and sparse biotite, amphibole, and FeTi oxides, but pumice clasts are phenocryst-poor. Pink, white, and pale-gray-green, the tuff typically weathers tan. Rests on basement rocks and locally on a 10-m-thick remnant of andesitic lava (too small to show on map)

Trs **Rhyolite sills of West Mageik Lake (Pliocene)**—Three main sills (72–77% SiO_2), each 5–10 m thick, intrude Naknek Formation (unit bu), strata of which here dip 15°NNE (Lowenstern and Mahood, 1991; Lowenstern and others, 1991). North sill near lake yields K-Ar age of 3.08±0.07 Ma. Associated dikes of the rhyolite, 1–2 m thick, cut the adjacent dacitic Pinnacle Porphyry stock (see unit Ti description). Dikes of the dacite porphyry, 1–3 m thick, in turn cut proximal parts of the rhyolite sills. Such relations suggest contemporaneity

Ti **Tertiary intrusive rocks (Pliocene and Miocene)**—Granodiorite, tonalite, and quartz diorite (mostly 63–67% SiO_2), typically porphyritic. Mount Ikagluik porphyry intrusion (64% SiO_2) yields K-Ar age of 20.2±0.2 Ma. Pinnacle Porphyry (63–65% SiO_2) near West Mageik Lake is inferred to have crystallized about 3 Ma (see unit Trs description). Undated stock just east of Mount Griggs has 67% SiO_2. Large pluton beneath Mount Juhle, also undated, has 64–67% SiO_2; possibly connected to it at depth is the nearby granitoid outlier exposed on northeast wall of the Valley of Ten Thousand Smokes. Several additional plutons near Ikagluik Creek and Rainbow River, not sampled or mapped adequately by us, are shown on the regional map of Riehle and others (1993)

Td **Tertiary porphyritic granitoid dikes (Pliocene? and Miocene)**—Dacitic in composition (63–65% SiO_2), typically near vertical, 5–8 m thick, disintegrating into angular joint blocks. Mapped only at conspicuous sites near the Valley of Ten Thousand Smokes, west and southeast of Mount Griggs and northwest of Mount Mageik; at each location, dikes intrude Late Jurassic Naknek Formation (unit bu) and appear to issue from local Tertiary plutons (unit Ti). Comparable dikes seen near upper Angle Creek, on canyon walls of Rainbow River, and on Mount Katolinat were not mapped

bu **Basement rocks, undivided (Tertiary to Jurassic)**—Main component is Naknek Formation (Late Jurassic), consisting of siltstone, sandstone, and subordinate conglomerate deposited in shallow marine shelf, neritic, and fluvial environments (Oxfordian to Tithonian); described in detail by Detterman and others (1996); gently dipping, broadly warped strata about 2,000 m thick constitute the predominant basement rocks exposed beneath Quaternary volcanic deposits in the map area. A second basement component includes several Tertiary granitoid plutons, 1 to 10 km across and largely porphyritic, that intrude Naknek Formation; in addition to plutons selectively mapped by us as unit Ti, others not shown on our map are distributed principally around upper Ikagluik Creek and upper Rainbow River (see Riehle and others, 1993). A third component of the exposed basement consists of volcanic rocks not related to identified centers; undated but presumed to be mostly Miocene, but some are perhaps as young as early Quaternary; largely andesite-dacite lava flows and their vent complexes, many propylitized or otherwise altered; such rocks form glaciated peaks and ridges between Mount Katmai and Snowy Mountain and around the headwaters of Katmai River, as well as forming much of the Barrier Range (Riehle and others, 1993)

REFERENCES CITED

Abe, K., 1992, Seismicity of the caldera-making eruption of Mount Katmai, Alaska, in 1912: Seismological Society of America Bulletin, v. 82, p. 175–191.

Allen, E.T., and Zies, E.G., 1923, A chemical study of the fumaroles of the Katmai region: National Geographic

Society, Contributed Technical Papers, Katmai Series, no. 2, p. 75–155.

Avery, V.F., 1992, A petrogenetic study of the dacite from the 1912 eruption of Novarupta, Katmai National Park, Alaska: Implications for magma storage locations: University of Alaska, Fairbanks, M.S. thesis, 177 p.

Bacon, C.R., and Druitt, T.H., 1988, Compositional evolution of the zoned calcalkaline magma chamber of Mount Mazama, Crater Lake, Oregon: Contributions to Mineralogy and Petrology, v. 98, p. 224–256.

Baedecker, P.A., ed., 1987, Methods for geochemical analysis: U.S. Geological Survey Bulletin 1770.

Ballard, Sanford, Carrigan, C.R., and McConnell, V.S., 1991, Shallow conductive-component of heat flow near Novarupta dome, Katmai, Alaska: Geophysical Research Letters, v. 18, p. 1529–1532.

Bordet, P., Marinelli, G., Mittempergher, M., and Tazieff, H., 1963, Contribution à l'étude volcanologique du Katmai et de la Vallée des Dix Mille Fumées (Alaska): Mémoires de la Société Belge de Géologie, no. 7, 70 p.

Burk, C.A., 1965, Geology of the Alaska Peninsula-Island arc and continental margin: Geological Society of America Memoir 99, 250 p., 3 plates.

Casadevall, T.J., ed., 1994, Volcanic ash and aviation safety: Proceedings of the First International Symposium on Volcanic Ash and Aviation Safety: U.S. Geological Survey Bulletin 2047, 450 p.

Clocchiatti, R., 1972, Les cristaux de quartz des ponces de la Vallée des Dix Mille Fumées (Katmai, Alaska): Académie des Sciences [Paris], Comptes Rendus, v. 274, p. 3037–3040.

Coombs, M.L., Eichelberger, J.C., and Rutherford, M.J., 2000, Magma storage and mixing conditions for the 1953-1968 eruption of Southwest Trident Volcano, Katmai National Park, Alaska: Contributions to Mineralogy and Petrology, v. 140, p. 99–118.

Coombs, M.L., and Gardner, J.E., 2001, Shallow-storage conditions for the rhyolite of the 1912 eruption at Novarupta, Alaska: Geology, v. 29, p. 775–778.

Curtis, G.H., 1968, The stratigraphy of the ejecta from the 1912 eruption of Mount Katmai and Novarupta, Alaska, *in* Coats, R.R., Hay, R.L., and Anderson, C.A., eds., Studies in Volcanology: Geological Society of America Memoir 116, p. 153–210.

Decker, R.W., 1963, Proposed volcano observatory at Katmai National Monument: A preliminary study: Hanover (New Hampshire), Dartmouth College, unpublished report submitted to and on file with National Park Service, 54 p.

Detterman, R.L., Case, J.E., Miller, J.W., Wilson, F.H., and Yount, M.E., 1996, Stratigraphic framework of the Alaska Peninsula: U.S. Geological Survey Bulletin 1969–A, 74 p.

Fenner, C.N., 1920, The Katmai region, Alaska, and the great eruption of 1912: Journal of Geology, v. 28, p. 569-606.

Fenner, C.N., 1923, The origin and mode of emplacement of the great tuff deposit of the Valley of Ten Thousand Smokes: National Geographic Society, Contributed Technical Papers, Katmai Series, no.1, p. 1–74.

Fenner, C.N., 1925, Earth movements accompanying the Katmai eruption: Journal of Geology, v. 33, p. 116–139, 193–223.

Fenner, C.N., 1926, The Katmai magmatic province: Journal of Geology, v. 34, p. 673–772.

Fenner, C.N., 1930, Mount Katmai and Mount Mageik: Zeitschrift für Vulkanologie, Band 13, p. 1–24.

Fenner, C.N., 1938, The phenomena of Falling Mountain: American Journal of Science, v. 35–A, p. 35–48.

Fenner, C.N., 1950, The chemical kinetics of the Katmai eruption: American Journal of Science, v. 248, p. 593–627, 697–725.

Fierstein, J., and Hildreth, W., 1992, The plinian eruptions of 1912 at Novarupta, Katmai National Park, Alaska: Bulletin of Volcanology, v. 54, p. 646–684.

Fierstein, J., and Hildreth, W., 2000, Preliminary volcano-hazard assessment for Katmai Volcanic Cluster, Alaska: U.S. Geological Survey Open-File Report 00–489, 50 p., 1 plate [available on the World Wide Web at http://geopubs.wr.usgs.gov/open-file/of00489/].

Fierstein, J., and Hildreth, W., in press, Recent explosive eruptive record in the Mount Katmai area, Alaska: Quaternary Research.

Fierstein, J., Hildreth, W., Hendley, J.W., II, and Stauffer, P.H., 1998, Can another great volcanic eruption happen in Alaska?: U.S. Geological Survey Fact Sheet 075–98.

Fierstein, J., Houghton, B.F., Wilson, C.J.N., and Hildreth, W., 1997, Complexities of plinian fall deposition at vent: An example from the 1912 Novarupta eruption (Alaska): Journal of Volcanology and Geothermal Research, v. 76, p. 215–227.

Fliedner, M.M., and Klemperer, S.L., 2000, Crustal structure transition from oceanic arc to continental arc, eastern Aleutian Islands and Alaska Peninsula: Earth and Planetary Science Letters, v. 179, p. 567–579.

Gill, J.B., 1981, Orogenic andesites and plate tectonics: Berlin, Heidelberg, New York, Springer-Verlag, 390 p.

Goodliffe, A.M., Stone, D.B., Kienle, Jürgen, and Kasameyer, Paul, 1991, The vent of the 1912 Katmai eruption: Gravity and magnetic measurements: Geophysical Research Letters, v. 18, p. 1521–1524.

Griggs, R.F., 1918, The great hot mud flow of the Valley of Ten Thousand Smokes: Ohio Journal of Science, v. 19, p. 117–142.

Griggs, R.F., 1920, The great Mageik landslide: Ohio Journal of Science, v. 20, p. 325–354.

Griggs, R.F., 1922, The Valley of Ten Thousand Smokes: Washington, D.C., National Geographic Society, 340 p.

Hammer, J.E., Rutherford, M.J., and Hildreth, W., 2002, Storage conditions of intermediate magmas prior to the

1912 eruption in the Valley of Ten Thousand Smokes, Alaska: Contributions to Mineralogy and Petrology, v. 144, p. 144–162.

Higbie, Ruth Griggs, 1975, The Katmai eruption and the Valley of Ten Thousand Smokes, *in* Oehser, P.H., ed., National Geographic Society Research Reports 1890-1954: Washington, D.C., National Geographic Society, p. 141–170.

Hildreth, W., 1981, Gradients in silicic magma chambers: Implications for lithospheric magmatism: Journal of Geophysical Research, v. 86, p. 10153–10192.

Hildreth, W., 1983, The compositionally zoned eruption of 1912 in the Valley of Ten Thousand Smokes, Katmai National Park, Alaska: Journal of Volcanology and Geothermal Research, v. 18, p. 1–56.

Hildreth, W., 1987, New perspectives on the eruption of 1912 in the Valley of Ten Thousand Smokes, Katmai National Park, Alaska: Bulletin of Volcanology, v. 49, p. 680–693.

Hildreth, W., 1990, Trident, Alaska Peninsula, *in* Wood, C.A., and Kienle, J., eds., Volcanoes of North America: Cambridge University Press, p. 68–69.

Hildreth, W., 1991, The timing of caldera collapse at Mount Katmai in response to magma withdrawal toward Novarupta: Geophysical Research Letters, v. 18, p. 1541–1544.

Hildreth, W., and Fierstein, J., 1987, Valley of Ten Thousand Smokes, Katmai National Park, Alaska: Geological Society of America Centennial Field Guide—Cordilleran Section, p. 425–432.

Hildreth, W., and Fierstein, J., 1992, Hydrothermal explosion breccia emplaced during caldera collapse of Mount Katmai, Alaska, on 6 June 1912: Eos (Transactions, American Geophysical Union), v. 73, p. 635–636.

Hildreth, W., and Fierstein, J., 2000, Katmai volcanic cluster and the great eruption of 1912: Geological Society of America Bulletin, v. 112, p. 1595–1620.

Hildreth, W., Fierstein, J., Lanphere, M.A., and Siems, D.F., 1999, Alagogshak volcano: A Pleistocene andesite-dacite stratovolcano in Katmai National Park, *in* Geologic Studies in Alaska by the U.S. Geological Survey, 1997: U.S. Geological Survey Professional Paper 1614, p. 105–113.

Hildreth, W., Fierstein, J., Lanphere, M.A., and Siems, D.F., 2000, Mount Mageik: A compound stratovolcano in Katmai National Park, *in* Kelly, K.D., and Gough, L.P., eds., Geologic Studies in Alaska by the U.S. Geological Survey, 1998: U.S. Geological Survey Professional Paper 1615, p. 23–41.

Hildreth, W., Fierstein, J., Lanphere, M.A., and Siems, D.F., 2001, Snowy Mountain: A pair of small andesite-dacite stratovolcanoes in Katmai National Park, *in* Geologic Studies in Alaska by the U.S. Geological Survey, 1999, U.S. Geological Survey Professional Paper 1633, p. 13–34.

Hildreth, W., Fierstein, J., Lanphere, M.A., and Siems, D.F., 2002, Mount Griggs: A compositionally distinctive Quaternary stratovolcano behind the main volcanic line in Katmai National Park, *in* Wilson, F.H., and Galloway, J.P., eds., Studies by the U.S. Geological Survey in Alaska, 2000: U.S. Geological Survey Professional Paper 1662.

Hildreth, W., Fierstein, J., Lanphere, M.A., and Siems, D.F., in press, Trident Volcano: Four contiguous stratocones adjacent to Katmai Pass, Alaska Peninsula, *in* Galloway, J.P., ed., Studies by the U.S. Geological Survey in Alaska, 2001, U.S. Geological Survey Professional Paper 1678.

Hildreth, W., and Lanphere, M.A., 1994, Potassium-argon geochronology of a basalt-andesite-dacite arc system: The Mount Adams volcanic field, Cascade Range of southern Washington: Geological Society of America Bulletin, v. 106, p. 1413–1429.

Hildreth, W., and Moorbath, S., 1988, Crustal contributions to arc magmatism in the Andes of central Chile: Contribution to Mineralogy and Petrology, v. 98, p. 455–489.

Houghton, B.F., Wilson, C.J.N., Fierstein, J., and Hildreth, W., 2003, Complex proximal deposition during the Plinian eruptions of 1912 at Novarupta, Alaska: Bulletin of Volcanology, v. 65.

Jaggar, T.A., 1927, Eruption of Mageik in Alaska: The Volcano Letter, no. 147, Hawaiian Volcano Observatory. [Implausible eruption report.]

Jolly, A.D., and McNutt, S.R., 1999, Seismicity at the volcanoes of Katmai National Park, Alaska; July 1995–December 1997: Journal of Volcanology and Geothermal Research, v. 93, p. 173–190.

Kasameyer, Paul, Wilt, Michael, Daily, William, and Felske, Donald, 1991, Time-domain electromagnetic soundings in the vicinity of Novarupta, Katmai National Park, Alaska: Geophysical Research Letters, v. 18, p. 1525–1528.

Keith, T.E.C., 1991a, Argillic alteration in the Novarupta vent region, Katmai National Park, Alaska: Geophysical Research Letters, v. 18, p. 1549–1552.

Keith, T.E.C., 1991b, Fossil and active fumaroles in the 1912 eruptive deposits, Valley of Ten Thousand Smokes, Alaska: Journal of Volcanology and Geothermal Research, v. 45, p. 227–254.

Keith, T.E.C., Thompson, J.N., Hutchinson, R.A., and White, L.D., 1992, Geochemistry of waters in the Valley of Ten Thousand Smokes region, Alaska: Journal of Volcanology and Geothermal Research, v. 49, p. 209–231.

Keller, A.S., and Reiser, H.N., 1959, Geology of the Mount Katmai area, Alaska: U.S. Geological Survey Bulletin 1058–G, p. 261–298.

Kienle, J., 1991, Depth of the ash flow deposit in the Valley of Ten Thousand Smokes, Alaska: Geophysical Research Letters, v. 18, p. 1533–1536.

Kienle, J., Swanson, S.E., and Pulpan, H., 1983, Magmatism and subduction in the eastern Aleutian arc, *in* Shimozuru, D., and Yokoyama, I., eds., Arc volcanism: Physics and Tectonics: Tokyo, Terra Scientific Publishing Company, p. 191–224.

Kimball, H.H., 1913, The effect upon atmospheric transparency of the eruption of Katmai volcano: Monthly Weather Review (Weather Bureau, U.S. Deptartment of Agriculture), v. 41, p. 153–159.

Kleinman, J.W., Iwatsubo, E.Y., Power, J.A., and Endo, E.T., 1997, Geodetic studies in the Novarupta area, Katmai National Park, Alaska, 1990 to 1995, *in* Geologic Studies in Alaska by the U.S. Geological Survey, 1995: U.S. Geological Survey Professional Paper 1574, p. 83–92.

Kodosky, L.G., 1989, Surface mercury geochemistry as a guide to volcanic vent structure and zones of high heat flow in the Valley of Ten Thousand Smokes, Alaska: Journal of Volcanology and Geothermal Research, v. 38, p. 227–242.

Kosco, D.G., 1981, Characteristics of andesitic to dacitic volcanism at Katmai National Park, Alaska: University of California, Berkeley, Ph.D. thesis, 249 p., Part II.

Lanphere, M.A., 2000, Comparison of conventional K-Ar and $^{40}Ar/^{39}Ar$ dating of young mafic volcanic rocks: Quaternary Research, v. 53, p. 294–301.

Lescinsky, D.T., and Fink, J.H., 2000, Lava and ice interaction at stratovolcanoes: Use of characteristic features to determine past glacial extents and future volcanic hazards: Journal of Geophysical Research, v. 105, p. 23711–23726.

Lescinsky, D.T., and Sisson, T.W., 1998, Ridge-forming, ice-bounded lava flows at Mount Rainier, Washington: Geology, v. 26, p. 351–354.

Lovering, T.S., 1957, Halogen-acid alteration of ash at Fumarole No. 1, Valley of Ten Thousand Smokes, Alaska: Geological Society of America Bulletin, v. 68, p. 1585–1604.

Lowell, R.P., and Keith, T.E.C., 1991, Chemical and thermal constraints on models of thermal springs, Valley of Ten Thousand Smokes, Alaska: Geophysical Research Letters, v. 18, p. 1553–1556.

Lowenstern, J.B., 1993, Evidence for a copper-bearing fluid in magma erupted at the Valley of Ten Thousand Smokes, Alaska: Contributions to Mineralogy and Petrology, v. 114, p. 409–421.

Lowenstern, J.B., and Mahood, G.A., 1991, Petrogenesis of high-silica rhyolite on the Alaska Peninsula: Geophysical Research Letters, v. 18, p. 1565–1568.

Lowenstern, J.B., Wallmann, P.C., and Pollard, D.D., 1991, The West Mageik Lake sill complex as an analogue for magma transport during the 1912 eruption at the Valley of Ten Thousand Smokes, Alaska: Geophysical Research Letters, v. 18, p. 1569–1572.

Lu, Z., Fatland, R., Wyss, M., Eichelberger, J., Dean, K., and Freymueller, J., 1997, Deformation of New Trident volcano measured by ERS-1 SAR interferometry, Katmai National Park, Alaska: Geophysical Research Letters, v. 24, p. 695–698.

Lu, Z., and Freymueller, J.T., 1998, Synthetic aperture radar interferometry coherence analysis over Katmai volcano group, Alaska: Journal of Geophysical Research, v. 103, p. 29887–29894.

Martin, G.C., 1913, The recent eruption of Katmai volcano in Alaska: National Geographic Magazine, v. 24, p. 131–181.

Martin, G.C., 1926, The Mesozoic stratigraphy of Alaska: U.S. Geological Survey Bulletin 776, 493 p.

McBirney, A.R., 1979, Effects of assimilation, Chapter 10, *in* Yoder, H.S., Jr., ed., The Evolution of the Igneous Rocks, Fiftieth Anniversary Perspectives: Princeton University Press, p. 307–338.

Miller, T.P., McGimsey, R.G., Richter, D.H., Riehle, J.R., Nye, C.J., Yount, M.E., and Dumoulin, J.A., 1998, Catalog of the historically active volcanoes of Alaska: U.S. Geological Survey Open File Report 98–582, 104 p.

Miller, T.P., and Richter. D.H., 1994, Quaternary volcanism in the Alaska Peninsula and Wrangell Mountains, Alaska, Chapter 24, *in* Plafker, G., and Berg, H.C., eds., The Geology of Alaska: The Geology of North America, v. G–1, Geological Society of America.

Miyashiro, A., 1974, Volcanic rock series in island arcs and active continental margins: American Journal of Science, v. 264, p. 321–355.

Moore, J.C., and 11 others, 1991, EDGE deep seismic reflection transect of the eastern Aleutian arc-trench layered lower crust reveals underplating and continental growth: Geology, v. 19, p. 420–424.

Moran, S.C., 2003, Multiple seismogenic processes for high-frequency earthquakes at Katmai National Park, Alaska: Evidence from stress tensor inversions of fault plane solutions: Bulletin of the Seismological Society of America, v. 93, no. 1, p. 94–108.

Morrison, R., and Kukla, G., 1998, The Pliocene-Pleistocene (Tertiary-Quaternary) boundary should be placed at about 2.6 Ma, not at 1.8 Ma: GSA Today, August 1998, p. 9.

Muller, E.H., 1952, The glacial geology of the Naknek district, the Bristol Bay region, Alaska: Urbana, University of Illinois, Ph.D. thesis, 98 p.

Muller, E.H., 1953, Northern Alaska Peninsula and eastern Kilbuck Mountains, Alaska, *in* Péwé, T.L., and six others, eds., Multiple Glaciation in Alaska, a progress report: U.S. Geological Survey Circular 289, p. 2–3.

Muller, E.H., Juhle, W., and Coulter, H.W., 1954, Current volcanic activity in Katmai National Monument: Science, v. 119, p. 319–321.

Papike, J.J., 1992, The Valley of Ten Thousand Smokes, Katmai, Alaska: A unique geochemistry laboratory: Geochimica et Cosmochimica Acta, v. 56, p. 1429–1449.

Papike, J.J., Keith, T.E.C., Spilde, M.N., Shearer, C.K., Galbreath, K.C., and Laul, J.C., 1991a, Major and trace element mass flux in fumarolic deposits, Valley of Ten

Thousand Smokes, Alaska: Rhyolite-rich protolith: Geophysical Research Letters, v. 18, p. 1545–1548.
Papike, J.J., Keith, T.E.C., Spilde, M.N., Shearer, C.K., Galbreath, K.C., and Laul, J.C., 1991b, Geochemistry and mineralogy of fumarolic deposits, Valley of Ten Thousand Smokes, Alaska: Bulk chemical and mineralogical evolution of dacite-rich protolith: American Mineralogist, v. 76, p. 1662–1673.
Peacock, M.A., 1931, Classification of igneous rock series: Journal of Geology, v. 39, p. 54–67.
Pinney, D.S., and Beget, J.E., 1991, Late Pleistocene volcanic deposits near the Valley of Ten Thousand Smokes, Katmai National Park, Alaska, *in* Reger, R.D., ed., Short Notes on Alaskan Geology, 1991: Alaska Division of Geological & Geophysical Surveys Professional Report 111, p. 45–53.
Plafker, G., Moore, J.C., and Winkler, G.R., 1994, Geology of the southern Alaska margin, Chapter 12, *in* Plafker, G., and Berg, H.C., eds., The Geology of Alaska: The Geology of North America, v. G–1, Geological Society of America.
Poreda, R.J., and Craig, H., 1989, Helium isotope ratios in circum-Pacific volcanic arcs: Nature, v. 338, p. 473–478.
Power, J.A., Moran, S.C., McNutt, S.R., Stihler, S.D., and Sanchez, J.J., 2001, Seismic response of the Katmai volcanoes to the 6 December 1999 magnitude 7.0 Karluk Lake earthquake, Alaska: Bulletin of the Seismological Society of America, v. 91, p. 57–63.
Ramdohr, P., 1962, Erzmikroskopische Untersuchungen an Magnetiten der Exhalationen im Valley of the 10000 Smokes: Neues Jahrbuch für Mineralogie, Monatshefte 3/4, p. 49–59.
Ray, D.K., 1967, Geochemistry and petrology of the Mt. Trident andesites, Katmai National Monument, Alaska: Fairbanks, University of Alaska, Ph.D. thesis, 198 p.
Reger, R.D., Pinney, D.S., Burke, R.M., and Wiltse, M.A., 1996, Catalog and initial analyses of geologic data related to middle to late Quaternary deposits, Cook Inlet region, Alaska: Alaska Division of Geological & Geophysical Surveys Report of Investigations 95–6, 188 p.
Richmond, G.M., and Fullerton, D.S., 1986, Introduction to Quaternary glaciations in the United States of America: Quaternary Science Reviews, v. 5, p. 3–10.
Riehle, J.R., and Detterman, R.L., 1993, Quaternary geologic map of the Mount Katmai quadrangle and adjacent parts of the Naknek and Afognak quadrangles, Alaska: U.S. Geological Survey Map I–2032, scale 1:250,000.
Riehle, J.R., Detterman, R.L., Yount, M.E., and Miller, J.W., 1993, Geologic map of the Mount Katmai quadrangle and adjacent parts of the Naknek and Afognak quadrangles, Alaska: U.S. Geological Survey Map I–2204, scale 1:250,000.
Sayre, J.D., and Hagelbarger, P.R., 1919, A study of temperatures in the Valley of Ten Thousand Smokes: Ohio Journal of Science, v. 19, p. 249–278.
Scott, W.E., Hoblitt, R.P., Torres, R.C., Self, S., Martinez, M.M.L., and Nillos, T., Jr., 1996, Pyroclastic flows of the June 15, 1991, climactic eruption of Mount Pinatubo, *in* Newhall, C.G., and Punongbayan, R.S., eds., Fire and Mud: Eruptions and Lahars of Mount Pinatubo, Philippines: Seattle, University of Washington Press, p. 545–570.
Shearer, C.K., Papike, J.J., Spilde, M.N., and Shimizu, N., 1991, Pyroxene/melt trace element behavior: A study of pyroxenes from the Valley of Ten Thousand Smokes, Alaska: Geophysical Research Letters, v. 18, p. 1557–1560.
Sheppard, D.S., Janik, C.J., and Keith, T.E.C., 1992, A comparison of gas geochemistry of fumaroles in the 1912 ash-flow sheet and on active stratovolcanoes, Katmai National Park, Alaska: Journal of Volcanology and Geothermal Research, v. 53, p. 185–197.
Shew, N., and Lanphere, M.A., 1992, Map showing potassium-argon ages from the Mount Katmai and adjacent parts of the Naknek and Afognak quadrangles, Alaska Peninsula, Alaska: U.S. Geological Survey Miscellaneous Field Studies Map MF–2021–E, scale 1:250,000.
Shipley, J.W., 1920, Some chemical observations on the volcanic emanations and incrustations in the Valley of 10,000 Smokes, Katmai, Alaska: American Journal of Science, v. 50, p. 141–153.
Simkin, T., and Siebert, L., 1994, Volcanoes of the World: Tucson, Geoscience Press, 349 p.
Smith, W.R., 1925, The Cold Bay-Katmai district, *in* Brooks, A.H., and others, eds., Mineral Resources of Alaska, Report on progress of investigations in 1923: U.S. Geological Survey Bulletin 773, p. 183–207.
Snyder, G.L., 1954, Eruption of Trident volcano, Katmai National Monument, Alaska: U.S. Geological Survey Circular 318, 7 p.
Spurr, J.E., 1900, A reconnaissance in southwestern Alaska in 1898, *in* Twentieth Annual report of the U.S. Geological Survey to the Secretary of the Interior, 1898-1899; Part VII, Explorations in Alaska in 1898: Washington, Government Printing Office, p. 31–264.
Volz, F.E., 1975, Distribution of turbidity after the 1912 Katmai eruption in Alaska: Journal of Geophysical Research, v. 80, p. 2643–2648.
Wallmann, P.C., Pollard, D.D., Hildreth, W., and Eichelberger, J.C., 1990, New structural limits on magma chamber locations at the Valley of Ten Thousand Smokes, Katmai National Park, Alaska: Geology, v. 18, p. 1240–1243.
Ward, P.L., and Matumoto, T., 1967, A summary of volcanic and seismic activity in Katmai National Monument, Alaska: Bulletin Volcanologique, v. 31, p. 107–129.
Ward, P.L., Pitt, A.M., and Endo, E., 1991, Seismic evidence for magma in the vicinity of Mt. Katmai, Alaska: Geophysical Research Letters, v. 18, p. 1537–1540.

Westrich, H.R., Eichelberger, J.C., and Hervig, R.L., 1991, Degassing of the 1912 Katmai magmas: Geophysical Research Letters, v. 18, p. 1561–1564.

Wilson, C.J.N., and Hildreth, W., 1997, The Bishop Tuff: New insights from eruptive stratigraphy: Journal of Geology, v. 105, p. 407–439.

Wilson, F.H., 1985, The Meshik arc—An Eocene to earliest Miocene magmatic arc on the Alaska Peninsula: Alaska Division of Geological and Geophysical Surveys, Professional Report 88, 14 p.

Wood, C.A., and Kienle, J., eds., 1990, Volcanoes of North America: Cambridge University Press, 354 p.

Wright, F.E., 1952, Memorial to Clarence Norman Fenner: Proceedings Volume of the Geological Society of America for 1951, p. 103–107.

Zies, E.G., 1924a, Hot springs of the Valley of Ten Thousand Smokes: Journal of Geology, v. 32, p. 303–310.

Zies, E.G., 1924b, The fumarolic incrustations in the Valley of Ten Thousand Smokes: National Geographic Society, Contributed Technical Papers, Katmai Series, v. 1, no. 3, p. 157–179.

Zies, E.G., 1929, The Valley of Ten Thousand Smokes: I. The fumarolic incrustations and their bearing on ore deposition. II. The acid gases contributed to the sea during volcanic activity: National Geographic Society, Contributed Technical Papers, Katmai Series, v. 1, no. 4, p. 1–79.